Characterizing Pleiotropic Effects of Glucocorticoids in Mice Using Heavy Water Labeling and Mass Spectrometry

By

Donald Jason Roohk

A dissertation submitted in partial satisfaction of the requirements for the degree of

Doctor of Philosophy

in

Endocrinology

in the

Graduate Division

of the

University of California, Berkeley

Committee in charge:

Professor Marc Hellerstein, Chair

Professor Jen-Chywan Wang

Professor Joseph Napoli

Spring 2011

Abstract

Characterizing Pleiotropic Effects of Glucocorticoids in Mice Using Heavy Water Labeling and Mass Spectrometry

by

Donald Jason Roohk

Doctor of Philosophy in Endocrinology

University of California, Berkeley

Professor Marc Hellerstein, Chair

Glucocorticoids are widely prescribed to treat autoimmune and inflammatory diseases. While they are extremely potent, their utility in clinical practice is limited by a variety of adverse effects, including osteoporosis, skin thinning and increased susceptibility to bruising, muscle wasting, fat redistribution, cognitive impairments and mood disorders, and insulin resistance and diabetes. Development of compounds that retain the potent immunomodulating and anti-inflammatory properties of classic glucocorticoids while exhibiting reduced adverse actions is therefore a priority. Much attention has been focused on developing selective glucocorticoid receptor modulators (SGRMs) that would dissociate adverse effects from therapeutic immunomodulatory and anti-inflammatory effects.

Here we present several approaches to the field of SGRM development: characterization of a novel putative SGRM (compound L5); characterization of the effects of a glucocorticoid receptor mutant mouse (the $GR^{dim/dim}$ mouse); and comparison of acute vs. chronic effects of glucocorticoids using a model of chronic glucocorticoid excess (the CRH-transgenic mouse). The phenotypic actions of glucocorticoids were measured in these mice by a heavy water labeling strategy combined with mass spectrometry that allows measurement of fluxes through multiple target metabolic pathways concurrently. Pathways monitored included collagen

synthesis in bone and skin, protein synthesis in skeletal muscle, triglyceride dynamics in adipose tissue and liver, and proliferation of cells in spleen, pancreatic islets, and hippocampal neuronal precursors. To quantify accumulation or distribution of bone mass, lean tissue mass, and fat mass, we used DEXA and microCT. To quantify changes in glucose homeostasis, we used the deuterated glucose disposal test, a modified oral glucose tolerance test that also reveals glucose uptake and metabolism by peripheral tissues in addition to the standard measurements of glucose and insulin concentrations.

We demonstrate for the first time that L5, a compound belonging to a novel class of potential SGRMs, exhibits clearly selective actions on disease-relevant pathways compared to prednisolone. Prednisolone reduced bone collagen synthesis, skin collagen synthesis, muscle protein synthesis, and splenic lymphocyte counts, proliferation, and cell death, whereas L5 had none of these actions. In contrast, L5 was a more rapid and potent inhibitor of hippocampal neurogenesis than was prednisolone; and L5 and prednisolone induced insulin resistance equally.

We also demonstrate that, contrary to expectations, some metabolic effects of glucocorticoid treatment are exaggerated in adipose tissue of $GR^{dim/dim}$ mice compared to wildtype mice. The $GR^{dim/dim}$ mouse has a mutation in the dimerization domain of GR, and has been shown to have attenuated transactivation with intact repression. The predominant, current hypothesis is that $GR^{dim/dim}$ mice should experience fewer or less severe effects of glucocorticoids, because the $GR^{dim/dim}$ mutation is a loss of function mutation, from a molecular standpoint. Thus, it would be surprising, *a priori*, if $GR^{dim/dim}$ mice were to show any exaggerated responses to glucocorticoids. Our labeling studies demonstrate that adipose tissue triglyceride synthesis and *de* novo lipogenesis exhibit greater stimulation by glucocorticoid treatment in $GR^{dim/dim}$ mice than in wildtype controls. More concordant with the predominant hypothesis were our findings that glucocorticoid-dependent inhibition of bone and skin collagen synthesis and decreases in insulin sensitivity were diminished in $GR^{dim/dim}$ mice compared to wildtype mice. Wildtype and $GR^{dim/dim}$ mice were equally sensitive to glucocorticoid-dependent decreases in muscle protein synthesis. Thus the consequences of mutation in the dimerization domain of the glucocorticoid receptor vary on a pathway-by-pathway basis, and are not restricted to reduced responses to glucocorticoids.

Finally, we demonstrated that increased futile cycling between triglycerides and free fatty acids occurs in both abdominal and subcutaneous fat depots in a model of chronic glucocorticoid exposure, CRH-transgenic ($CRH\text{-}Tg^{+}$) mice, and in these mice triglyceride accumulation is favored over net lipolysis. In these studies, we characterized multiple pathways in mice exposed to both chronically and acutely-elevated levels of glucocorticoids ($CRH\text{-}Tg^{+}$ mice and wildtype mice administered glucocorticoids, respectively) to explore how glucocorticoids act on these pathways over time. In bone and skin, fractional collagen synthesis rates were dramatically inhibited by acute glucocorticoid exposure, but in $CRH\text{-}Tg^{+}$ mice, which had reduced bone mass and thinner skin compared to controls, fractional collagen synthesis rates were only modestly lower in bone and are similar in skin compared to controls. In muscle, fractional synthesis of total muscle protein was not dramatically inhibited by either acute or chronic exposure to glucocorticoids, although $CRH\text{-}Tg^{+}$ mice had measurably less muscle mass relative to controls. In adipose tissue there were no remarkable changes in triglyceride dynamics in young mice given glucocorticoids acutely, but in $CRH\text{-}Tg^{+}$ mice we observed more triglyceride synthesis in

subcutaneous and abdominal fat depots, more *de novo* lipogenesis in the abdominal depot only, more triglyceride accumulation in both fat depots and no difference in glyceroneogenesis in either depot compared to controls. Fat accumulation had occurred much more slowly than measured triglyceride synthesis in both depots in CRH-Tg^{+} mice, thus while gradual accumulation, rather than reduction, of fat is favored, both triglyceride synthesis and lipolysis occurs simultaneously at a high rate. We conclude that futile cyling between triglycerides and free fatty acids occurs at a high rate, in response to chronic, but not acute, glucocorticoid exposure, and that chronic, endogenous glucocorticoid exposure has different metabolic consequences than acute, exogenous administration.

We draw several conclusions relevant to novel glucocorticoid agents. First, ligands for the glucocorticoid receptor can exhibit phenotypic selectivity. Second, although L5 may not be a therapeutically attractive candidate, it is a SGRM, and further testing on other compounds of the same class is warranted. Third, dose response ranges vary depending on the ligand, the pathway measured, and the tissue in which it is measured, so a variety of pathways need to be measured in different tissues to accurately establish therapeutic index. Fourth, while the expectation is that SGRMs will activate only a subset of glucocorticoid receptor-dependent pathways, it is important to assess the tissue-specific effects of all potential SGRMs on global transcription and GC-dependent metabolic pathways in many different tissues to accurately establish therapeutic indices of compounds. Fifth, targeting the glucocorticoid receptor dimerization domain pharmacologically is not likely to result in simple diminution of glucocorticoid actions due to attenuated transactivation with intact repression, but may result in stimulation of certain processes. Sixth, there are several advantages of this heavy water labeling method combined with mass spectrometry, in particular that small amounts of drug, subjects, and tissues are required relative to the large amount of information gained. Finally, this method can be adapted to characterize ligands for the glucocorticoid receptor and other nuclear hormone receptors, can be applied to disease models and transgenic mice, and can be integrated into existing clinical studies.

This work is dedicated to my wife for her love, patience, and inspiration

Table of Contents

Chapter 1: Introduction…… p. 1

Chapter 2: Differential in vivo effects on target pathways of a novel arylpyrazole glucocorticoid receptor modulator compared to prednisolone……. p. 8

Tables and Figures…….…… p. 20

Chapter 3: Glucocorticoid Mediated Changes in Adipose Triacylglycerol Metabolism Are Exaggerated, Not Diminished, in the Absence of a Functional GR Dimerization Domain…… p. 34

Tables and Figures.……... p. 50

Chapter 4: CRH-trangenic Mice Exhibit Increased Fluxes Through Adipose Tissue Triglyceride Synthesis Pathways…….. p. 57

Tables and Figures.……... p. 72

Chapter 5: Summary…… p. 80

References…… p. 90

Chapter 1: Introduction

Abbreviations

Glucocorticoid: GC; hypothalamic-pituitary-adrenal: HPA; corticotropin-releasing hormone: CRH; adrenocorticotropic hormone: ACTH; glucocorticoid receptor: GR; DNA binding domain: DBD; glucocorticoid response element: GRE; 11- β -hydroxysteroid-dehydrogenase-1: 11-β-HSD1; phosphoenolpyruvate-carboxykinase: PEP-CK; selective glucocorticoid receptor modulators: SGRM; selective glucocorticoid receptor agonists: SEGRA; triglyceride: TG; *de novo* lipogenesis: DNL; dual energy X-ray absorptiometry: DEXA;

Introduction to glucocorticoids

Glucocorticoids (GCs), one of the most potent, pleiotropic, and effective classes of drugs known, are used to treat many common acute and chronic inflammatory and autoimmune diseases, including asthma, rheumatoid arthritis, dermatological conditions, inflammatory bowel disease, and collagen-vascular diseases. However, their use is limited by a long list of severe side effects, including osteoporosis, loss of muscle mass, redistribution of body fat and obesity, skin thinning and increased susceptibility to bruising, insulin resistance or diabetes mellitus, and neuropsychiatric disturbances, including depression, cognitive dysfunction and mood lability (Buttgereit et al., 2005b; Stanbury and Graham, 1998). Whether the source of excessively high GCs is from endogenous production or exogenous administration, the side effects are commonly devastating.

The HPA axis and endogenously-produced glucocorticoids

Endogenous levels of GCs are controlled by the hypothalamic-pituitary-adrenal (HPA) axis. Corticotropin-releasing hormone (CRH) is released from the hypothalamus in response to higher brain stimuli into the hypophyseal portal system where it travels a short distance to the anterior pituitary. CRH signals the corticotrophs in the anterior pituitary to synthesize and release adrenocorticotropic hormone (ACTH) into the circulation. ACTH then signals the adrenal cortex to synthesize and release GCs, primarily cortisol in humans and corticosterone in rodents, into the circulation. Each step in this pathway is under the control of negative feedback inhibition by downstream products. Overstimulation of this axis and/or disruption of negative feedback control systems at any point can result in elevated levels of endogenously-produced circulating GCs. Chronic exposure to elevated levels of GCs, regardless of the source, results in Cushing's syndrome, which is characterized by the aforementioned negative effects of GCs (Besser and Edwards, 1972).

Molecular mechanisms of glucocorticoids and their receptor

GCs mediate their responses via binding the glucocorticoid receptor (GR) (Hollenberg et al., 1985; Schoneveld et al., 2004). GR is a member of the nuclear hormone receptor transcription factor superfamily, and can be mechanistically classified among the androgen receptor, estrogen receptor, and progesterone receptor. GR contains several modular domains including a DNA binding domain (DBD), ligand binding domain, and activation domains 1 and 2 (AF1, AF2) (Giguère et al., 1986; Schoneveld et al., 2004). In the absence of ligand, GR is sequestered in the cytosol bound to a heat shock protein complex (Dittmar et al., 1997). When a ligand binds to and activates GR, the heat shock proteins dissociate from GR, and GR translocates to the nucleus.

Once in the nucleus, activated GR can homodimerize and bind to a sequence of DNA, called a glucocorticoid response element (GRE), located in the proximal promoter, enhancer, or other regions of a gene (Schoneveld et al., 2004). Various transcriptional cofactors are also recruited, and transcription of the target gene is either induced or repressed (Rosen and Miner, 2005; Schoneveld et al., 2004). GR can modulate transcription of target genes by other mechanisms, such as but not limited to binding to DNA as a monomer on a GRE half site (Rosen and Miner, 2005; Schoneveld et al., 2004), binding to DNA and to another transcription factor that is also binding the DNA at a composite element (Rosen and Miner, 2005; Schoneveld et al., 2004), or binding via protein-protein interactions exclusively to another transcription factor (tethering) (Rosen and Miner, 2005; Schoneveld et al., 2004). Many of the well-characterized anti-inflammatory mechanisms of GR involve binding with pro-inflammatory transcription factors, such as NF-κB and AP-1, via tethering or at a composite element, whereby activated GR binds to and inhibits their normal pro-inflammatory actions, such as production and release of pro-inflammatory cytokines, chemokines, and adhesion molecules (Miner and Yamamoto, 1992; Nissen and Yamamoto, 2000; Ray and Prefontaine, 1994; Rosen and Miner, 2005; Scheinman et al., 1995; Vayssiere et al., 1997; Yang-Yen et al., 1990). In addition to the mechanisms for the therapeutically desirable anti-inflammatory and immunomodulatory actions of GR, recent studies have also focused on the mechanisms underlying the undesirable, tissue-specific effects of GR.

Mechanisms of glucocorticoid-induced bone loss

In bone GCs have been shown to cause both decreased bone formation and increased bone resorption in humans and rodents. In humans it has been shown that GC-induced bone loss occurs rapidly during the first few months of therapy, and then more slowly as therapy continues over a period of several years (Manolagas and Weinstein, 1999). In humans and in mice it has been shown that GCs inhibit bone formation by suppressing osteoblast formation, proliferation, and activity, and increasing ostocyte apoptosis (LoCascio et al., 1990; O'Brien et al., 2004; Weinstein et al., 1998). Cell-based studies on osteoblasts have shown that GCs reduce procollagen I mRNA, stabilize collagenase 3 mRNA, and increase the levels of proteases by post-transcriptional mechanisms (Delany et al., 1995; Rydziel et al., 2004). Furthermore, it has been shown that IGF-1 enhances osteoblastic function, induces collagen synthesis in osteoblasts, and suppresses collagenase 3 transcription, and it has been suggested that GCs may oppose, block, or impair the actions of IGF-1 locally in osteoblasts or on matrix proteins by decreasing IGF-1 transcription, signaling, or by their actions on IGF binding proteins (Canalis and Agnusdei, 1996; Chen et al., 1991; McCarthy et al., 1989).

Mechanisms of glucocorticoid-induced skin thinning

Skin is about 70% collagen by weight, and the dermis is comprised of types I and III collagen with type I collagen being the most abundant (Epstein and Munderloh, 1978). It is largely through their effects on collagen synthesis and degradation that GCs are thought to exert their effects on skin. Both acute and chronic administration of GCs has been shown to induce skin thinning (Lubach et al., 1995). Topical and systemic GCs have been shown to dramatically decrease rates of skin collagen synthesis in humans (Autio et al., 1994; Haapasaari et al., 1996). In humans it has been shown that collagen synthesis rates decrease rapidly and dramatically after two or three days of topical GC treatment (Haapasaari et al., 1996). Collagen synthesis rates

rebound partially three days after discontinuation of topical GC treatment, but only return to about 50% of control levels two weeks thereafter, indicating that GCs may exert both long term and short term effects on skin collagen turnover that may operate through distinct mechanisms (Haapasaari et al., 1996).

Glucocorticoid-induced muscle wasting

GCs have been shown to induce muscle wasting through direct effects on muscle protein breakdown and synthesis, as well as through indirect effects on whole body glucose metabolism and insulin and IGF-1-dependent pathways (Long et al., 2001; Louard et al., 1994; Odedra et al., 1983). GCs stimulate muscle protein breakdown directly by inducing genes in the ubiquitin proteasome pathway (Wing and Goldberg, 1993). It has been shown that both acute and chronic administration of GCs inhibits protein synthesis by interfering with translation and via other mechanisms, and that the mechanisms responsible can persist after several days of treatment (Rannels and Jefferson, 1980; Rannels et al., 1978; Shah et al., 2000). Fractional muscle protein synthesis rates of mixed muscle proteins in rat gastrocnemius have been reported to decrease dramatically in response to GC treatment after only 1-3 days (Odedra 1983). It has been shown that GCs antagonize insulin in humans (Louard et al., 1994), and it is widely known that GCs induce insulin resistance. In addition, IGF-1 is known to stimulate protein synthesis and prevent proteolysis in muscle, and GCs may induce muscle wasting at least in part by negatively affecting IGF-1 synthesis and signaling in myocytes (Canalis, 2005).

Glucocorticoid-induced effects on adipose tissue and fat redistribution

In humans with Cushing's disease, characterized by chronically high levels of endogenously-produced GCs, undesirable fat redistribution occurs with loss of fat from subcutaneous depots and accumulation of fat in the abdomen, around the face, and behind the neck (Besser and Edwards, 1972). Hepatic fat accumulation has also been described in humans with Cushing's disease (Taskinen et al., 1983). Patients with Cushing's disease have been shown to have elevated expression of lipoprotein lipase in abdominal fat depots (Rebuffe-Scrive et al., 1988), and five times more intra-abdominal fat than control subjects (Mayo-Smith et al., 1989). In cell-based assays, GCs have been shown to induce hormone-sensitive lipase in adipocytes, induce pre-adipocyte differentiation, induce lipogenic gene expression in adipocytes, and cause cellular hypertrophy in adipocytes isolated from central fat depots (Gaillard et al., 1991; Samra et al., 1998; Seckl et al., 2004; Slavin et al., 1994). In addition, GCs have recently been implicated in obesity and in the metabolic syndrome (Walker, 2006). Transgenic mice overexpressing 11-β-hydroxysteroid-dehydrogenase-1 (11-β-HSD1) in adipocytes accumulate fat in visceral depots, and in peripheral depots to a lesser extent (Seckl et al., 2004). Increased lipogenic capacity and increased VLDL secretion have also been reported in isolated hepatocytes (Martin-Sanz et al., 1990). It has been previously shown that GCs decrease glyceroneogenesis in the white adipose tissue via inhibition of phosphoenolpyruvate-carboxykinase (PEP-CK), and increase glyceroneogenesis in the liver via induction of PEP-CK (Hanson and Reshef, 2003). It has also been shown that glyceroneogenesis plays a crucial role in triglyceride/fatty acid cycling in these tissues (Reshef et al., 2003).

The concept of selective glucocorticoid receptor modulators

Historically, GCs had been thought of as either pure agonists, compounds that activate all target pathways of GCs, or pure antagonists, compounds that block activation of all target pathways of GCs (Stanbury and Graham, 1998). Recently, however, the concept of selective glucocorticoid receptor modulators (SGRMs), also called selective GR agonists (SEGRAs), has emerged (Buttgereit et al., 2005a; De Bosscher; Rosen and Miner, 2005; Schacke et al., 2007). Conceptually, SGRMs are partial GR agonists that may have improved therapeutic index by exhibiting desirable anti-inflammatory and immunomodulating effects to a greater extent than the undesirable effects. SGRMs are conceptually analogous to selective estrogen receptor modulators (Dutertre and Smith, 2000; Webb et al., 2003), selective thyromimetics (Ocasio, 2005; Trost et al., 2000), and selective PPAR-agonists (Pourcet et al., 2006; Seimandi et al., 2005; Sznaidman et al., 2003). The variable actions of known SGRMs on GR-dependent pathways are thought to be due to their ability to induce variations in cofactor recruitment or variable affinity of activated GR for different GRE sequences (De Bosscher; Schacke et al., 2007). The challenge in designing modern GCs as medicines is not in increasing their potency, meaning how well they activate GR, or their specificity, meaning how exclusively they bind GR as opposed to other nuclear hormone receptors, but rather in designing compounds that bind the one putatively active GR subtype (GRα) with high affinity, but evoke its therapeutically desirable actions while limiting its adverse actions (Buttgereit et al., 2005a; Rosen and Miner, 2005; Schacke et al., 2007). Thus, the central challenge for the next generation of GC pharmacologic agents will play out in the realm of metabolic phenotype, rather than GR physical chemistry.

Strategies for designing, screening, and validating SGRMs

The typical discovery strategy for SGRMs is to screen chemical libraries using high throughput strategies followed by medicinal chemistry optimization or to use structure-guided rational drug design approaches (Schacke et al., 2007). Once synthesized, compounds are usually screened for GR affinity in *in vitro* binding assays and for GR activation in *in vitro* reporter assays (Schacke et al., 2007). GR agonists are then screened for tissue and pathway-specific selective actions in cell-based assays (Schacke et al., 2007). Selective actions must then be verified in animals, usually mouse models initially, before lead candidates are selected for subsequent preclinical and clinical testing. Several mechanisms have been proposed for how SGRMs might activate certain GR-dependent pathways and not others, including tissue or cell-specific variability in cofactor recruitment or gene-specific affinity for different GREs (Rosen and Miner, 2005). Because many of the potent anti-inflammatory actions of GR have been attributed to inhibitory events involving tethering of GR with pro-inflammatory transcription factors (Schäcke et al., 2002), a model has emerged depicting the anti-inflammatory actions of GCs as being mediated by GR repression, which are dependent largely on GR tethering with another transcription factor, and the adverse metabolic effects as being mediated by transactivation, which are dependent largely on GR-GR homodimerization and DNA binding at a classic GRE. Based on this model, much attention has been focused on the possibility of developing so called dissociated SGRMs, ligands that "dissociate" activation from repression of GR target genes, that would retain anti-inflammatory properties with reduced metabolic adverse effects (De Bosscher; De Bosscher et al., 2005; Kleiman and Tuckermann, 2007; Miner, 2002; Schacke et al., 2007; Schacke et al., 2004). It should be noted that SGRMs are distinctly different from soft steroids, also called antedrugs,

which are pure GR agonists that act only locally and are metabolized to an inactive form before they can enter the systemic circulation (Rosen and Miner, 2005).

The $GR^{dim/dim}$ mouse

Site directed mutagenesis of the GR dimerization domain (within the DBD) revealed mutants that abrogated GR homodimerization-dependent transactivation of GRE-reporter constructs while leaving tethering-based repression intact (Heck et al., 1994). Homologous recombination has been used to "knock-in" this point mutation in mice (Reichardt et al., 1998). In contrast to $GR^{-/-}$ mice that die at birth, $GR^{dim/dim}$ mice are viable (Reichardt et al., 1998). In addition, many of the GR-dependent anti-inflammatory pathways of $GR^{dim/dim}$ mice have been previously shown to be intact in these mice (Reichardt et al., 2001). $GR^{dim/dim}$ mice have served, not only as a genetic model for a novel class of potential SGRMs (De Bosscher; De Bosscher et al., 2005; Kleiman and Tuckermann, 2007; Miner, 2002; Schacke et al., 2007; Schacke et al., 2004), but also to tease out mechanisms by which GR mediates its effects on target genes and metabolic pathways, in particular in pathways associated with the therapeutically undesirable effects of GR activation (Frijters et al.; Rauch et al.; Reichardt et al., 1998; Waddell et al., 2008). In our studies involving $GR^{dim/dim}$ mice we directly tested the hypothesis that $GR^{dim/dim}$ mice experience fewer undesirable effects of and are less sensitive to dexamethasone than wildtype mice. We also characterized multiple GC-dependent phenotypic outcomes as being GR dimerization dependent or independent.

The CRH-Tg^{+} mouse

In order to study multiple effects of chronic GC exposure concurrently, we obtained CRH-Tg^{+} mice. CRH-Tg^{+} mice carry a transgene of rat CRH genomic sequence driven by the mMT-1 metallothionein promoter (Stenzel-Poore et al., 1992). CRH-Tg^{+} mice exhibit centrally-derived overstimulation of the HPA axis, and have 5-fold elevated baseline levels of ACTH and 10-fold elevated baseline levels of corticosterone (Stenzel-Poore et al., 1992; Stenzel-Poore et al., 1996). Adrenalectomy largely results in reversal of the CRH phenotype (Shinahara et al., 2009), which gives further evidence that this phenotype is centrally-derived and dependent on HPA axis activation rather than a direct endocrine or paracrine effect of CRH itself on target peripheral tissues. Despite that fact that the metallothionein promoter is normally active in tissues outside the central nervous system, such as liver and kidney, plasma CRH is not elevated in these mice (Stenzel-Poore et al., 1992). Furthermore, expression of the mMT-CRH transgene is limited to numerous regions of the brain, testes, heart, adrenal, and lung; and no expression was detected in the liver or kidney (Stenzel-Poore et al., 1992). Mice carrying a CRH transgene have been used extensively to study the effects of CRH on the immune response and psychological and neurological disorders (Stenzel-Poore et al., 1992; Stenzel-Poore et al., 1996; Stenzel-Poore et al., 1994; van Gaalen et al., 2002). In addition, there are several similarities between CRH-Tg^{+} mice and humans exposed to chronically high levels of GCs, such as patients affected by Cushing's disease. Like humans with Cushing's disease, CRH-Tg^{+} mice have chronically high levels of endogenously-produced GCs (Stenzel-Poore et al., 1992; Stenzel-Poore et al., 1996), primarily cortisol in humans, and corticosterone in mice. They have noticeably thin skin and exhibit alopecia, muscle atrophy, and fat accumulation (Stenzel-Poore et al., 1992; Stenzel-Poore et al., 1996). We note that CRH-Tg^{+} mice also accumulate fat behind the neck and high on the

back, analogous to the characteristic "buffalo hump" commonly reported in Cushing's patients. In summary, the CRH-Tg^{+} mouse has a phenotype that closely mimics that of chronic stress, and is considered to be an apt model for Cushing's disease in humans, and thus of chronic, endogenous GC exposure. This model allows us to study multiple effects of chronic GC exposure concurrently, without having to administer GCs in the diet or via mini osmotic pump implantation and with minimal stressors to the animal which could confound our results.

Heavy water labeling and mass spectrometry

This work focuses mainly, but not exclusively, on the undesirable metabolic effects of GCs described in detail above. Here we systematically characterized and compared the effects of GCs in wildtype mice, $GR^{dim/dim}$ mice, and CRH-Tg^{+} mice on a number of disease-relevant pathways that are targets of GR ligands, using a heavy water ($^{2}H_2O$) labeling approach with mass spectrometric analysis (Busch et al., 2006; Busch et al., 2007; Gardner et al., 2007; Shankaran et al., 2006; Turner et al., 2007). The target pathways were selected based on their believed role as "disease-modifying" processes (Buttgereit et al., 2005b; Canalis, 2003; Stanbury and Graham, 1998), i.e., driving forces underlying pathogenic or therapeutic actions of GR ligands. This heavy water labeling approach allows concurrent measurement of flux rates through numerous disease-relevant pathways, including bone collagen synthesis rates (relevant to osteoporosis-related actions); skin collagen synthesis rates (skin thinning and bruisability); insulin-mediated glucose utilization and pancreatic beta cell compensation to insulin resistance (diabetes mellitus and metabolic syndrome); pancreatic beta cell proliferation rates (diabetes); skeletal muscle protein synthesis rates (muscle wasting); TG synthesis, lipolysis and DNL rates in adipose tissue (fat redistribution); hippocampal neurogenesis rate (disorders of cognition and mood); and lymphocyte proliferation and death rates (immunosuppressive actions). In addition, we were also able to quantify the source of TG-glycerol as percentage derived from glyceroneogenesis, as opposed to glycolysis, using this method. These measurements were able to be performed in relatively few numbers of living mice with a relatively small amount of drug because of the high sensitivity and reproducibility of *in vivo* heavy water labeling (Chen et al., 2007; Gardner et al., 2007; Kim et al., 2005; Neese et al., 2002). For some studies, we also performed body composition analysis using dual energy X-ray absorptiometry (DEXA) and microCT. Using DEXA, we quantified lean and fatty tissue mass, as well as bone area, bone mass, and bone mineral density. Using MicroCT, we were able to image sections of long bone and quantify differences in bone mass. Using these methods, we characterized and compared the effects of a putative SGRM to prednisolone, tested the hypothesis that $GR^{dim/dim}$ mice experience fewer or less severe negative effects of dexamethasone, characterized GC-dependent metabolic pathways as being GR homodimerization dependent or independent using $GR^{dim/dim}$ mice, and characterized the chronic effects of GCs on GC-dependent metabolic pathways in CRH-Tg^{+} mice and compared the results to those of other studies in which GCs were administered acutely in wildtype mice.

Chapter 2: Differential *in vivo* effects on target pathways of a novel arylpyrazole glucocorticoid receptor modulator compared to prednisolone

Abstract

Glucocorticoids are widely prescribed to treat autoimmune and inflammatory diseases. While they are extremely potent, their utility in clinical practice is limited by a variety of adverse side effects. Development of compounds that retain the potent immunomodulating and anti-inflammatory properties of classic glucocorticoids while exhibiting reduced adverse actions is therefore a priority. Using heavy water labeling and mass-spectrometry to measure fluxes through multiple glucocorticoid-responsive, disease-relevant target pathways in vivo in mice, we compared the effects of a classic glucocorticoid receptor ligand, prednisolone, to those of a novel arylpyrazole-based compound, L5. We show for the first time that L5 exhibits clearly selective actions on disease-relevant pathways compared to prednisolone. Prednisolone reduced bone collagen synthesis, skin collagen synthesis, muscle protein synthesis, and splenic lymphocyte counts, proliferation, and cell death, whereas L5 had none of these actions. In contrast, L5 was a more rapid and potent inhibitor of hippocampal neurogenesis than was prednisolone; and L5 and prednisolone induced insulin resistance equally. Administration of prednisolone or L5 increased expression comparably for one GR-regulated gene involved in protein degradation in skeletal muscle (Murf1) and one GR-regulated gluconeogenic gene in liver (PEPCK). In summary, L5 dissociates the pleiotropic effects of the GR ligand prednisolone in intact animals in ways that neither gene expression nor cell-based models were able to fully capture or predict. Because multiple actions can be measured concurrently in a single animal, this method is a powerful systems approach for characterizing and differentiating the effects of ligands that bind nuclear receptors.

Abbreviations

GR, glucocorticoid receptor; SGRM, selective glucocorticoid receptor modulator; TG, triglyceride; DNL, de novo lipogenesis; ^{2}H-GDT, ^{2}H-glucose disposal test; IRIS, isotope ratio infrared spectrometry; GC-MS, gas chromatography-mass spectrometry; PFB, pentafluorobenzyl; MS, mass spectrometry; NCI, negative chemical ionization; m/z, mass to charge; SIM, selected ion monitoring; dR, deoxyribose; GC, gas chromatography; FA, fatty acid; MIDA, mass isotopomer distribution analysis; RT-PCR, reverse transcription polymerase chain reaction.

Introduction

Glucocorticoids act as ligands for the glucocorticoid receptor (GR) and are among the most widely prescribed drugs in contemporary medicine. Glucocorticoids are used for the treatment of many common acute and chronic inflammatory and autoimmune diseases, including asthma, rheumatoid arthritis, dermatological conditions, inflammatory bowel disease, and collagen-vascular diseases. An important limitation of glucocorticoid therapy, however, is that the desired anti-inflammatory and immunomodulating effects are frequently accompanied by undesirable effects, such as osteoporosis, loss of muscle mass, redistribution of body fat, skin thinning and bruisability, insulin resistance or diabetes mellitus and neuropsychiatric disturbances, including depression, cognitive dysfunction and mood lability (Buttgereit et al., 2005b; Stanbury and Graham, 1998).

Until recently, the classic teaching had been that adverse effects of glucocorticoid treatment cannot be pharmacologically dissociated from beneficial effects (Stanbury and Graham, 1998). A new therapeutic concept has emerged, however, in the past few years: namely, different ligands for nuclear receptors can in principle exhibit selectivity for phenotypic actions due to receptor subtype specificity or variations in co-factor recruitment (Coghlan et al., 2003; Webb et al., 2003). Selective glucocorticoid receptor modulators (SGRM), for example, might exhibit desirable anti-inflammatory and immunomodulating effects to a greater extent than the undesirable biologic actions. The typical discovery strategy for SGRMs is to screen chemical libraries using high throughput screening strategies followed by medicinal chemistry optimization or to use structure-guided rational drug design approaches (Schacke et al., 2007). Subsequent investigations of phenotypic selectivity of SGRMs have generally been based on *in vitro* ligand-receptor binding assays or selective activation or repression of gene transcription in cell-based assays (Schacke et al., 2007).

A group of novel arylpyrazole compounds have recently been identified as potential SGRMs (Shah and Scanlan, 2004), Each of the compounds carries a different substituent at a single position in a common arylpyrazole backbone, and all 15 compounds (named L1-L15) have binding affinities for the GR similar to potent synthetic glucocorticoid agonists, such as dexamethasone and prednisolone, and to endogenous glucocorticoid agonists, such as cortisol. Figure 1 shows chemical structures and GR binding affinities of L5, prednisolone, and dexamethasone for comparison (Wang et al., 2006). The pleiotropic effects of these arylpyrazole agents have been characterized in cell culture-based systems (Wang et al., 2006). Among the arylpyrazole SGRMs studied, compound L5 {[1-(4-fluorophenyl)-4a-methyl-5,6,7,8-tetrahydro-4H-benzo[f]indazol-5-yl]-[4-(trifluoromethyl)phenyl]methanol} exhibited a pattern of favorable anti-inflammatory effects and a reduced side effect profile in glucocorticoid-responsive cell types. Similar to dexamethasone, although to a lesser extent, L5 inhibited gene expression of the pro-inflammatory cytokine genes IL-8, RANTES, GRO1, MCP1, GM-CSF, and IL-6 in A549 human lung epithelial cells induced with TNF-α (Wang et al., 2006). In contrast to dexamethasone, which potently inhibits differentiation of MC3T3-L1 preosteoblasts to osteoblasts and potently induces differentiation of 3T3-L1 preadipocytes to adipocytes - characteristics that may reflect the negative side effects of glucocorticoid agonists on bone and adipose tissue, respectively - L5 did not inhibit differentiation of MC3T3-L1 preosteoblasts and only modestly induced differentiation of 3T3-L1 preadipocytes.

Here, we systematically characterized and compared the effects of the compound L5 and prednisolone on a number of disease-relevant pathways that are targets of GR ligands, using a heavy water (^2H_2O) labeling approach with mass spectrometric analysis (Busch et al., 2006; Busch et al., 2007; Gardner et al., 2007; Shankaran et al., 2006; Turner et al., 2007). The target pathways were selected based on their hypothesized role as "disease-modifying" processes (Buttgereit et al., 2005b; Canalis, 2003; Stanbury and Graham, 1998), i.e., driving forces underlying pathogenic or therapeutic actions of GR ligands. The heavy water labeling approach allows concurrent measurement of flux rates through numerous disease-relevant pathways, including bone collagen synthesis (relevant to osteoporosis-related actions); skin collagen synthesis (skin thinning and bruisability); insulin-mediated glucose utilization and pancreatic beta cell compensation to insulin resistance (diabetes mellitus and metabolic syndrome); pancreatic islet cell proliferation (diabetes); skeletal muscle protein synthesis (muscle wasting); triglyceride (TG) synthesis, lipolysis and de novo lipogenesis (DNL) rates in adipose tissue (fat redistribution); hippocampal neurogenesis rate (disorders of cognition and mood); and lymphocyte proliferation and death (immunosuppressive actions). These measurements were able to be performed in living mice with a relatively small amount of L5 material (<50 mg), because of the high sensitivity and reproducibility of *in vivo* heavy water labeling (Chen et al., 2007; Gardner et al., 2007; Kim et al., 2005; Neese et al., 2002). We also analyzed the expression of genes known to be regulated by glucocorticoids, including Murf1 in skeletal muscle and PEPCK in liver, to confirm that L5 was demonstrating glucocorticoid-like effects on gene expression in tissues of living mice.

Methods

Animals

Forty-two C57BL/6J mice (male, 7-8 weeks old, Charles River Breeding Laboratories, Wilmington, MA) were housed in groups of no more than 5 under temperature-controlled conditions with a 12 h light/12 h dark cycle. Mice were fed a semi-purified AIN-93M (Bio-Serv, Frenchtown, NJ) diet ad libitum. All studies received prior approval from the Animal Care and Use Committee at UC Berkeley.

Heavy water (^2H_2O) labeling protocol

Thirty C57Bl/6 mice were labeled with ^2H_2O throughout the study as described elsewhere (Neese et al., 2002). Briefly, mice were given two priming intraperitoneal bolus injections of isotonic 99.9% ^2H_2O (Cambridge Isotope Lab, Andover, MA) to raise the ^2H_2O concentration in body water to ca. 5%. Body ^2H_2O enrichments of ca. 5% were then maintained by *ad libitum* administration of 8% ^2H_2O drinking water throughout the 7 day labeling period, as described previously (Busch et al., 2007).

GR-ligand treatment protocol

Mice labeled with ^2H_2O were randomized into 5 groups (n = 6 per group). Mice were administered either vehicle (0.5% w/v carboxymethylcellulose in water), 5 or 30 mg/kg/d prednisolone succinate dissolved in vehicle, or 5 or 30 mg/kg/d L5 dissolved in vehicle, for seven days. Half of the daily dose of each drug was administered by twice a day (b.i.d.) oral gavage. Vehicle-treated animals were administered vehicle by twice a day oral gavage. Compound L5 was provided by Thomas S. Scanlan, Oregon Health & Science University, Portland, OR.

Tissue collection

Mice labeled with ^2H_2O were anesthetized using isofluorane. Blood was collected by cardiac puncture and stored on ice. Water distillate was collected from plasma, and ^2H enrichment was measured using gas chromatography-mass spectrometry (GC-MS) after conversion to tetrabromoethane, as described in detail elsewhere (Collins et al., 2003; Turner et al., 2003). Mice were killed by cervical dislocation and were immediately decapitated, with all four limbs removed. The brain was removed; and the hippocampus was dissected, minced, and placed in Hibernate A medium (BrainBits LLC, Springfield, IL) on ice. Hippocampal neural progenitor stem cells were isolated as previously described (Shankaran et al., 2006). The spleen was dissected, minced with scissors, and strained through 35 µm nylon mesh. CD4+ and non-CD4+ T-cells, B-cells, and non B/T-cells from spleen were counted and isolated by flow cytometry and cell sorting. Bone Marrow was isolated from dissected femurs by perfusing the central cavity with ice cold PBS. Pancreatic islet cells were isolated from pancreati perfused with HBSS containing collagenase, as previously described (Chen et al., 1994). DNA was isolated from several cell types (hippocampal progenitor cells, splenic T-cells, splenic B-cells, remaining spleen cells, bone marrow cells, and pancreatic islet cells), using Qiagen kits (Qiagen, Valencia, CA). Purified DNA was then was hydrolyzed to free deoxyribonucleosides and the deoxyribose (dR) moiety of purine deoxyribonucleosides was derivatized to pentane tetra-acetate, and

analyzed by GC-MS to quantify DNA synthesis rates (cell proliferation rates) as described elsewhere (Neese et al., 2002; Neese et al., 2001; Varady et al., 2007a). TG-glycerol and fatty acids (FA) were isolated from dissected epididymal and inguinal adipose tissue depots and prepared for GC-MS analysis as described previously (Turner et al., 2003; Turner et al., 2007). L-4-(O-tert-butyldimethylsilyl)-hydroxyproline pentafluorobenzyl ester was prepared from dissected femur and dorsal skin flap and analyzed by GC-MS to quantify collagen synthesis rates as previously described (Gardner et al., 2007). Pentafluorobenzyl-*N*,*N*-di(pentafluorobenzyl)-alanine (PFB-Ala) was prepared from acid hydrolysates (6N HCl, 110^{o}C, 12h) of mixed muscle proteins from dissected quadriceps, and analyzed by GC-MS to quantify protein synthesis rates as previously described (Busch et al., 2006).

^{2}H-glucose disposal test (^{2}H-GDT)

The ^{2}H-glucose disposal test (^{2}H-GDT) was used in a separate subset of mice to measure insulin mediated glucose utilization (insulin resistance) and pancreatic beta-cell compensation as previously described (Beysen et al., 2007). Twelve animals were randomized to three groups (n = 4 per group). Each group was administered vehicle, 30 mg/kg/day prednisolone, or 30 mg/kg/day compound L5 for seven days.

Mass Spectrometry

GC-MS was performed using a 5890 gas chromatograph attached to either a 5971 or 5973 mass spectrometer. Unlabeled compounds of interest, along with their singly and doubly-labeled mass isotopomers (M_0, M_1, and M_2 for each compound of interest) were analyzed by selected ion monitoring (SIM). For pentane tetra-acetate derivatives from DNA (m/z ratios 435-436), Gas chromatography (GC) was performed using a DB-17 GC column, and mass spectrometry (MS) was performed in negative chemical ionization (NCI) mode. For glycerol-triacetate (m/z ratios 159-161), GC was performed using a DB-225 GC column, and MS was performed in positive chemical ionization (PCI) mode. For FA-methyl esters (m/z ratios 270-272), GC was performed using a DB-225 GC column, and MS was performed in electron impact ionization (EI) mode. For L-4-(O-tert-butyldimethylsilyl)-hydroxyproline pentafluorobenzyl ester (derivatized hydroxyproline) and PFB-Alanine (m/z ratios 424-426 and 448-450, respectively) GC was performed using a DB-225 GC column, and MS was performed in NCI mode.

Statistical analyses

Statistical analyses were performed using SigmaStat 3.0 (SPSS Inc., Chicago IL). One-way ANOVA was performed within groups administered L5 or vehicle or prednisolone or vehicle to assess statistically significant differences between group means. If a significant difference between groups was found ($P < 0.001$, all levels), a Bonferroni t-test was used to compare test groups to controls. $P < 0.05$ was considered to be significant for the post-hoc test.

Results

Effect of L5 vs prednisolone on bone and skin collagen synthesis

Reductions in bone collagen synthesis represent a primary mechanism underlying reduced bone mass during glucocorticoid treatment (Canalis, 2003). The binding affinity of L5 to the GR is similar to that of prednisolone (Shah and Scanlan, 2004; Wang et al., 2006) but the absorption and pharmacokinetics of L5 have not been established. Accordingly, we gave identical doses (mg:mg) of L5 and prednisolone, two doses were tested (5 mg/kg/d and 30 mg/kg/d), to cover a range of potential activity and administration was twice a day, to increase tissue exposure in case the half-life of L5 is shorter than that of prednisolone. The doses of each compound were by intent high, to increase the likelihood of observing robust changes in multiple tissues over a one week dosing period.

Prednisolone had a dose-dependent inhibitory effect on collagen synthesis in the femur, whereas L5 had no effect (Figure 2). The group that received 30 mg/kg/day of prednisolone for 7 days showed a significantly lower rate of bone collagen synthesis compared to controls ($P < 0.05$). In contrast, groups administered L5 at either dose showed rates of bone collagen synthesis that were not significantly different from controls.

Skin collagen synthesis was also measured in a subset of animals from each group (data not shown). Groups that received 5 and 30 mg/kg/day of prednisolone showed approximately 50% and 75% reductions, respectively, in the rate of skin collagen synthesis compared to controls. Rates of skin collagen synthesis in groups administered either dose of L5 were similar to controls.

Thus, L5 demonstrated no significant effect on bone collagen and skin collagen synthesis rates whereas prednisolone reduced both.

Effect of L5 vs prednisolone on skeletal muscle protein synthesis

Stimulation of proteolysis is likely the primary mechanism by which glucocorticoids reduce skeletal muscle mass, but reductions in muscle protein synthesis are also observed (Long et al., 2001; Louard et al., 1994; Odedra et al., 1983). Prednisolone exhibited modest effects on skeletal muscle protein synthesis (Figure 3), with significant reductions observed in the group administered 5 mg/kg/day for 7 days, compared to controls ($P < 0.05$). In contrast, L5 did not decrease skeletal muscle protein synthesis at either dose.

Effect of L5 vs prednisolone on insulin sensitivity

Measurement of peripheral tissue insulin sensitivity by the ^{2}H-GDT (Beysen et al., 2007) involved a separate set of animals than the heavy water protocol used for the other target pathways (see Methods). To conserve L5 compound, only one dose of the agents was given. Administration of L5 or prednisolone at 30 mg/kg/day in divided doses for 7 days resulted in a significantly lower insulin sensitivity index [(% glucose load metabolized/AUC insulin) (Figure 4A)]. Administration of L5 at 30 mg/kg/day also resulted in significantly higher insulin AUC levels than in controls (Figure 4B). No significant differences in fasting insulin levels, fasting blood glucose levels, total glucose utilized (representing pancreatic compensation to insulin

resistance), or blood glucose AUC (integrated over time points 0-10 min) were observed between groups. Thus, both L5 and prednisolone induced peripheral tissue insulin resistance at 30 mg/kg/day in the intact mouse.

Effects on hippocampal progenitor cell proliferation in the brain

The proliferation rate of hippocampal progenitor cells is a sensitive measure of neurogenesis in adult rodents (Shankaran et al., 2006). Neurogenesis is altered in models of depression, stress and cognitive dysfunction and is a drug target for anti-depressant and cognition-enhancing agents. Interestingly, L5 was a potent inhibitor of hippocampal progenitor cell proliferation in the hippocampus, whereas prednisolone had no effect (Figure 5). Hippocampal neurogenesis was significantly lower ($P < 0.05$) in groups administered either 5 or 30 mg/kg/day of L5 for 7 days, compared to controls. The groups administered prednisolone at 5 or 30 mg/kg/day showed no statistically significant reduction in hippocampal progenitor cell proliferation compared to controls. We have previously reported that treatment with prednisolone for 4 weeks at 40 mg/kg/day but not 5 mg/kg/d significantly reduced hippocampal progenitor cell proliferation, while treatment for 1 week had no effect (Shankaran et al., 2006). Accordingly, L5 is a more potent and faster-onset inhibitor of hippocamapal neurogenesis than prednisolone has been shown to be.

Effect of L5 vs prednisolone on splenic lymphocyte counts, proliferation rates and death rates

Prednisolone reduced numbers of, T-cells, B-cells, and total cells in spleen, whereas L5 had no effect on cell counts (Figure 6). The effects of prednisolone on cell counts were dose-dependent for all types of cells analyzed. Counts were significantly lower at the 30 mg/kg/d prednisolone dose compared to controls for total spleen cells and non-CD4+ T-cells, and at the 5 mg/kg/d prednisolone dose for B-cells and CD4+ T-cells.

Prednisolone decreased both fractional and absolute proliferation rates of splenic T- and B-cell subpopulations dose-dependently, with no significant reduction in proliferation rates of total spleen cells (Figure 7 and Figure 8). The effects of prednisolone on splenic T-cell proliferation were statistically significant at the 30 mg/kg/d dose for both fractional and absolute proliferation rates ($P < 0.05$ and $P < 0.01$, respectively). The effects of prednisolone on splenic B-cell proliferation were statistically significant at the 5 mg/kg/d dose for both fractional and absolute proliferation rates ($P < 0.001$ and $P < 0.01$, respectively). In contrast, L5 treatment had no effect on the fractional or absolute proliferation rates of any cell type analyzed in spleen.

Cell death rates in the total, B- and T-cell subpopulations in spleen increased in a dose-dependent manner in response to prednisolone administration. Cell death rates for splenic T-cells, splenic B-cells, and total spleen cells were more than 5-fold, 4-fold, and 3-fold greater, respectively, in the high-dose prednisolone group than in the control group. L5 had no effect on cell death rates in spleen (Figure 9).

In summary, prednisolone potently reduced numbers, reduced proliferation rates and increased death rates of lymphocytes in the spleen, whereas L5 exhibited none of these effects.

Effect of L5 vs prednisolone on pancreatic islet cell proliferation

Pancreatic islet cell proliferation rates are stimulated in several rodent models of chronic insulin resistance (Bonner-Weir et al., 1989; Bruning et al., 1997; Paris et al., 2003). We measured pancreatic islet cell proliferation rates in control animals (Chen et al., 2007) and animals given 30 mg/kg/day of either prednisolone or L5 (Figure 10). No significant differences in islet cell proliferation were observed, however, after 7 days of treatment with prednisolone or L5.

Effect of L5 vs prednisolone on TG metabolism in adipose tissue

Because glucocorticoids are widely known to alter adipose tissue fat metabolism, we measured fat pad weights, fractional TG turnover, absolute TG synthesis rates, net lipolysis rates, DNL, and glyceroneogenesis in the abdominal epididymal fat depot (Table 1) and the subcutaneous inguinal fat depot (Table 2). Fractional TG turnover in the high-dose prednisolone group was slightly lower ($P < 0.05$) compared to controls in the epididymal depot (32% vs. 36% for the high-dose prednisolone vs. control group, respectively). Animals administered 30 mg/kg/day of L5 had on average significantly more inguinal fat ($P < 0.05$) than controls (283 vs. 200 mg). All other groups administered either L5 or prednisolone showed values similar to those for the control group for all other metrics (Tables 1 and 2). Thus, short-term treatment with neither prednisolone nor L5 induced major changes in adipose tissue lipid dynamics, although long-term exposure to elevated endogenous glucocorticoids markedly increases adipose TG turnover (Harris C, Roohk DJ, Farese R, Hellerstein MK, unpublished).

Effect of L5 vs prednisolone on gene expression in liver and skeletal muscle

Expression of the gluconeogenic gene PEPCK in liver was induced more than 2-fold and 3-fold on average, in mice administered either dose of prednisolone or L5, respectively, compared to controls (Figure 11). Expression of the gene Murf1 in muscle, a gene involved in ubiquitin-based protein degradation pathways, was also elevated relative to control in animals administered either dose of prednisolone or L5. Murf1 was induced on average between 2- and 3.5-fold over controls in response to either dose of prednisolone or L5. These results are consistent with comparable absorption and systemic tissue exposure for both L5 and prednisolone, at least with regard to genes expressed in liver and muscle.

Body weights

No group gained weight over the course of the 7 day treatment period. The groups given vehicle and 30 mg/kg/d prednisolone had significantly lower body weights ($P < 0.01$ and $P < 0.001$, respectively) on day 7 compared to day 0. Rodents have previously been maintained on chronic ^2H_2O intake at up to 30% enrichment in drinking water without effects on growth, food intake, behavior, activity or fertility (Koletzko et al., 1997) and we have studied hundreds of mice on 8% ^2H_2O in drinking water without any effect on body weight gain. It is therefore very unlikely that the absence of weight gain here is due to heavy water administration but may relate to the daily gavage procedure.

Discussion

In this study, we systematically characterized *in vivo* the pleotropic effects of a putative SGRM, compound L5, in comparison to a classic GR ligand, prednisolone. The actions of these GR ligands were measured by a heavy water labeling strategy that allows measurement of fluxes through multiple target metabolic pathways concurrently, including the dynamics of lipids, proteins and cells, in the whole organism (Busch et al., 2006; Busch et al., 2007; Chen et al., 2007; Gardner et al., 2007; Kim et al., 2005; Neese et al., 2002; Shankaran et al., 2006; Turner et al., 2007). Target pathways were selected based on their hypothesized relevance to the pathophysiology of major adverse effects of glucocorticoids. By measuring flux rates through these disease-modifying pathways that may underlie the initiation or progression of undesired outcomes, we were able to demonstrate convincing evidence of side-effect relevant metabolic selectivity for a putative SGRM. Importantly, because multiple pathway fluxes could be measured concurrently in the same animal and with great sensitivity by the heavy water labeling approach (Busch et al., 2006; Busch et al., 2007; Chen et al., 2007; Gardner et al., 2007; Kim et al., 2005; Neese et al., 2002; Shankaran et al., 2006; Turner et al., 2003; Turner et al., 2007), this systematic characterization was possible in whole animals with only a limited amount of compound L5 (less than 50 mg).

The data clearly demonstrate that prednisolone and L5 exert different patterns of activity on these disease-modifying pathways (Table 3). Prednisolone potently inhibited bone and skin collagen synthesis, reduced splenic lymphocyte proliferation rates, increased splenic lymphocyte death rates, and modestly reduced muscle protein synthesis and TG turnover in abdominal fat, while L5 had no effects on any of these processes. On the other hand, L5 treatment for 7 days significantly reduced hippocampal progenitor cell proliferation, whereas prednisolone treatment had no significant effect (but has previously been shown to have significant effects on hippocampal progenitor cell proliferation after 4 weeks, at a higher dose) and prednisolone and L5 induced insulin resistance equally. Finally, L5 and prednisolone treatment resulted in similar induction of the expression of GR-target genes PEPCK in liver and Murf1 in muscle, and neither exhibited significant effects on pancreatic islet cell proliferation after 7 days of treatment.

These results answer several key issues regarding selectivity of the SGRM, compound L5. First, L5 clearly has glucocorticoid agonist effects *in vivo* in mice, based on the observed glucocorticoid-like effects on insulin resistance (Figure 4), hippocampal neurogenesis (Figure 5), and gene expression in muscle and liver (Figure 11). Accordingly, the compound was absorbed and got to at least some target tissues. Although we did not measure uptake or volume of distribution, these results make it unlikely that pharmacokinetic differences can explain the absence of effect of L5 on other pathways altered by prednisolone.

Second, L5 has some apparent advantages over prednisolone, particularly its lack of inhibition of bone and skin collagen synthesis or muscle protein synthesis. L5 also has potential disadvantages compared to prednisolone, including an apparent lack of immunosuppressive actions (as evidenced by absence of effects on lymphocyte counts, proliferation or death rates) and its increased potency toward suppression of hippocampal neurogenesis. An important class of actions of GR ligands that we did not evaluate here was anti-inflammatory effects (Buttgereit et al., 2005a; Rosen and Miner, 2005; Schacke et al., 2007) , because an animal model of

inflammation is required, whereas all the parameters that were studied here could be performed in animals in their baseline health status.

Third, *in vitro* comparisons of actions of L5 and the potent glucocorticoid receptor agonist dexamethasone in cell-based models (Wang et al., 2006) correlated well, but not perfectly, with *in vivo* actions on target pathways. Differential effects of dexamethasone and L5 on differentiation of MC3T3-E1 preosteoblasts to osteoblasts (Wang et al., 2006) parallel our observation of differential effects of prednisolone and L5 on bone collagen synthesis (Figure 2). Similar inhibitory effects of L5 and dexamethasone on insulin-stimulated glucose uptake were also observed in OP9 adipocytes (Wang JC, unpublished results), consistent with our finding that both L5 and prednisolone reduce whole-body insulin-mediated glucose disposal (Figure 4). In contrast, dexamethasone and L5 both repressed transcription of several pro-inflammatory genes including RANTES, MCP1, and IL-6 in TNF-α-induced A549 cells (Wang et al., 2006), with L5 doing so to a lesser degree, but these cytokine-inhibitory effects did not predict the different effects of prednisolone and L5 on lymphocyte proliferation, and death rates or counts *in vivo* (Figures 6-9). Nor was the finding of increased lipolysis by dexamethasone but not L5 in OP9 cells (Wang JC, unpublished results) supported *in vivo* by our data, at least after 7 days of treatment (Tables 1 and 2).

The use of *ex vivo* cell-based models for predicting *in vivo* phenotypic selectivity in the whole organism is therefore potentially informative, but results have to be interpreted cautiously. The differentiation of MC3T3-E1 preosteoblasts to osteoblasts appears to predict effects of GR-ligands on bone collagen synthesis in mice, for example, suggesting that this cell model may be useful in screening for SGRMs that do not reduce bone mass. As a general principle, however, intact organisms must be used to establish definitively whether GR ligands induce differential actions *in vivo.*

Moreover, different metabolic pathways exhibit ligand-specific dose-response relationships. For prednisolone, dose-response effects on T-cell dynamics (Figure 6A-B, Figure 7A, Figure 8A, and Figure 9A) and muscle protein synthesis (Figure 3) are quite different, for example. Studies to establish therapeutic index should therefore include a number of target pathways.

An important practical feature of the strategy used here is that a broad array of physiological effects could be quantified simultaneously in a relatively small number of animals. This feature is enabled by the sensitivity and reproducibility of mass spectrometric flux measurements after heavy water administration (Hellerstein, 2004; Hellerstein and Murphy, 2004). Our results here show that some metabolic pathways are rapidly affected by administration of GR ligands, while others may require more prolonged exposure. Insulin-mediated glucose disposal, lymphocyte proliferation and death rates, bone collagen synthesis, and skin collagen synthesis responded to 7 days of prednisolone treatment. In contrast, inhibition of hippocampal neurogenesis requires longer administration of prednisolone (Shankaran et al., 2006) though not of L5 (Figure 5), and we have observed marked changes in adipose tissue lipid dynamics in transgenic mice overproducing endogenous GCs from birth (Harris C, Roohk DJ, Farese R, Hellerstein MK, unpublished observations), but not in response to 7 days of prednisolone treatment. Similarly, increased pancreatic islet cell proliferation associated with insulin resistance is observed after 4

weeks of prednisolone treatment (Chen S, Hellerstein M, unpublished observations) but not after 7 days of treatment.

In a general sense, our results demonstrate that *in vivo* phenotypic selectivity on disease-modifying target pathways can be achieved for GR ligands. Compound L5 is undeniably selective in its effects on GR-mediated pathways, whether or not L5 represents an attractive drug candidate. These findings are encouraging for other putative SGRMs. When incorporated into existing clinical and pre-clinical screening strategies, this approach can also inform upstream selection of models and assays.

There are a number of future directions that may help to optimize the use of *in vivo* pathway measurements for evaluating selectivity of GR ligands. Testing the effects of SGRMs in animal models of inflammation and including pathways related to inflammation.may extend the findings generated here in healthy animals. Many of the parameters described here can also be translated directly into clinical studies in humans using the heavy water labeling approach (Beysen et al., 2007; Hellerstein, 2004; Hellerstein and Murphy, 2004). Data generated in this manner may also allow quantitative comparison of dose-response effects of leads, rapid evaluation of different doses and regimens, and the capacity to evaluate the relevance of pre-clinical models to actions in humans. It will be also instructive to correlate gene expression, pharmacokinetics of tissue drug exposure and *in vivo* phenotypic outcomes in detail. Target pathways interrogated by flux measurements can also be expanded

In summary, we show here for the first time that a novel arylpyrazole compound, L5, exhibits selective actions on disease-modifying target pathways of GR ligands *in vivo* in intact animals. The net pattern of activities for L5 exhibits both disadvantages and advantages compared to prednisolone. The capacity to decouple inhibition of bone collagen synthesis, skin collagen synthesis, and muscle protein synthesis from induction of insulin resistance and suppression of neurogenesis, however, is encouraging for the long-term goal of creating SGRM ligands for targeted disease indications. Neither gene expression nor cell-based models fully captured the phenotypic selectivity of L5 compared to prednisolone. *In vivo* measurement of dynamic fluxes in a wide array of target pathways represents an efficient and powerful systems approach for interrogating the phenotypic selectivity of ligands that bind nuclear transcription factors.

Tables

	Fat Pad Weight (mg)	Fractional Replace-ment of TG (%/wk)	Absolute TG synthesis (mg/wk)	Absolute Lipolysis (mg/wk)	DNL – Fractional Replace-ment of Palmitate (%/wk)	DNL – Absolute palmitate synthesis (mg/wk)	% gly-cero-neo-gen-esis
Vehicle	313 (32)	36 (3)	101 (13)	118 (16)	20 (8)	10.4 (4.8)	21 (8)
Pred 5 mg/kg	293 (112)	36 (2)	93 (37)	106 (39)	29 (20)	10.9 (3.7)	16 (6)
Pred 30 mg/kg	308 (49)	32 (1)*	89 (14)	109 (17)	15 (2)	7.2 (1.6)	11 (8)
L5 5 mg/kg	358 (74)	35 (2)	113 (27)	119 (29)	22 (4)	12.9 (4.6)	13 (9)
L5 30 mg/kg	402 (69)	35 (2)	127 (21)	131 (20)	23 (3)	14.7 (2.9)	16 (9)

Table 1. Effect of L5 vs. prednisolone on TG metabolism in adipose tissue - abdominal fat pad. Data shown are mean (SD), n = 6 per group. * $P < 0.05$ compared to vehicle control.

	Fat Pad Weight (mg)	Fractional Replace-ment of TG (%/wk)	Absolute TG synthesis (mg/wk)	Absolute Lipolysis (mg/wk)	DNL - Fractional Replace-ment of Palmitate (%/wk)	DNL - Absolute palmitate synthesis (mg/wk)	% gly-cero-neo-gen-esis
Vehicle	200 (60)	46 (4)	83 (30)	94 (33)	47 (10)	15.5 (7.7)	24 (8)
Pred 5 mg/kg	228 (48)	46 (4)	97 (33)	107 (32)	55 (10)	19.7 (5.7)	17 (6)
Pred 30 mg/kg	202 (53)	42 (4)	76 (23)	91 (30)	45 (10)	11.4 (7.2)	12 (8)
L5 5 mg/kg	223 (50)	46 (4)	92 (24)	96 (23)	50 (5)	17.7 (4.5)	16 (10)
L5 30 mg/kg	283 (48)*	44 (2)	112 (20)	115 (19)	50 (6)	22.5 (3.9)	16 (8)

Table 2. Effect of L5 vs. prednisolone on TG metabolism in adipose tissue – subcutaneous fat pad. Data shown are mean (SD), n = 6 per group. * $P < 0.05$ compared to vehicle control.Table 2.

Pathway	**Prednisolone**	**L5**
Immunosuppression (lymphocyte birth and death)	+ +	No effect
Muscle protein synthesis	-	No effect
Bone and skin collagen synthesis	- -	No effect
Insulin resistance (insulin-mediated glucose utilization)	+ +	+ +
Hippocampal neurogenesis	No effect	- -
Lipolysis (abdominal fat pad)	No effect	No effect
TG turnover (abdominal fat pad)	-	No effect

Table 3. Summary of prednisolone and L5 actions on flux through several disease-relevant glucocorticoid-responsive pathways.

Figures

Figure 1

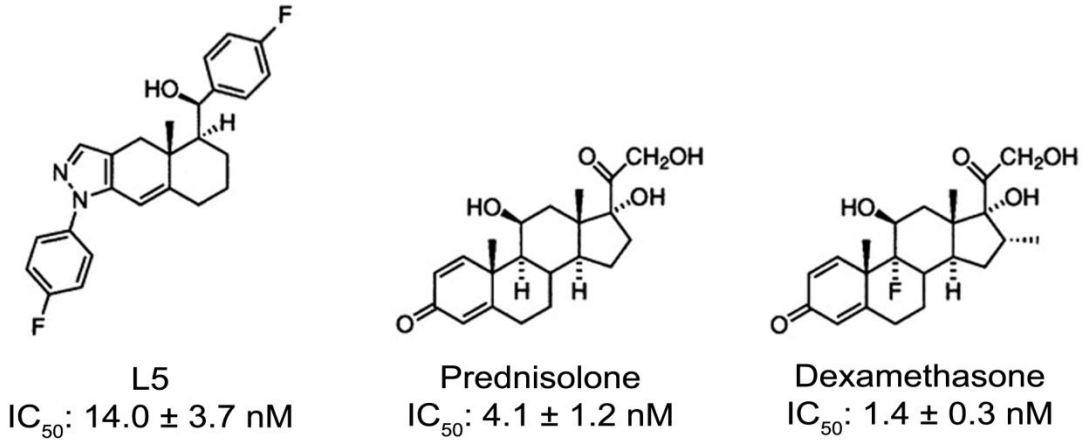

Figure 1. Structures and GR binding affinities of L5, prednisolone, and dexamethasone (from Wang et al., 2006).

Figure 2

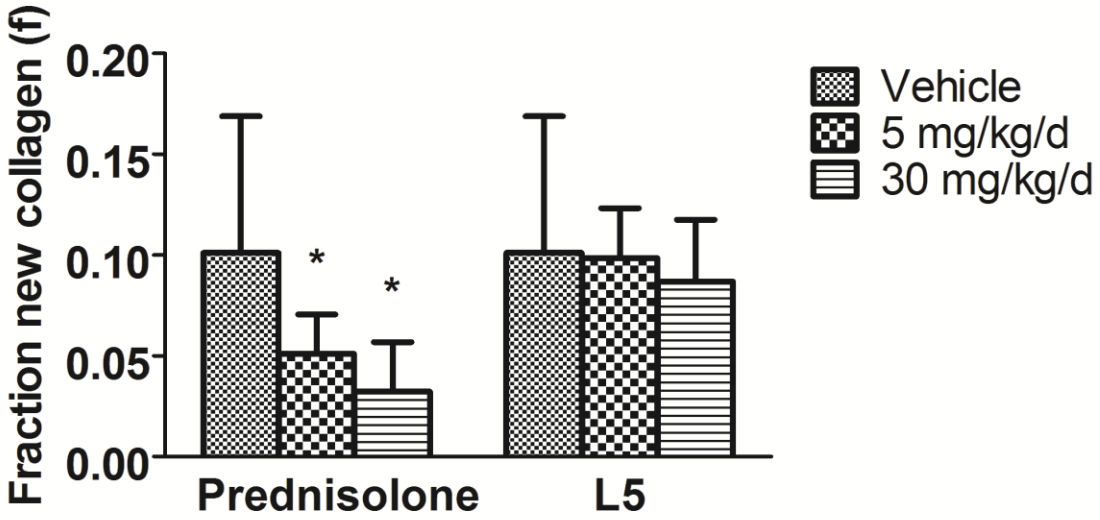

Figure 2. Fraction (f) of new bone collagen (hydroxyproline) synthesized and retained over the course of one week in femur. Data are shown as mean ± SD, n = 6 per group.* $P < 0.05$ compared to vehicle control.

Figure 3

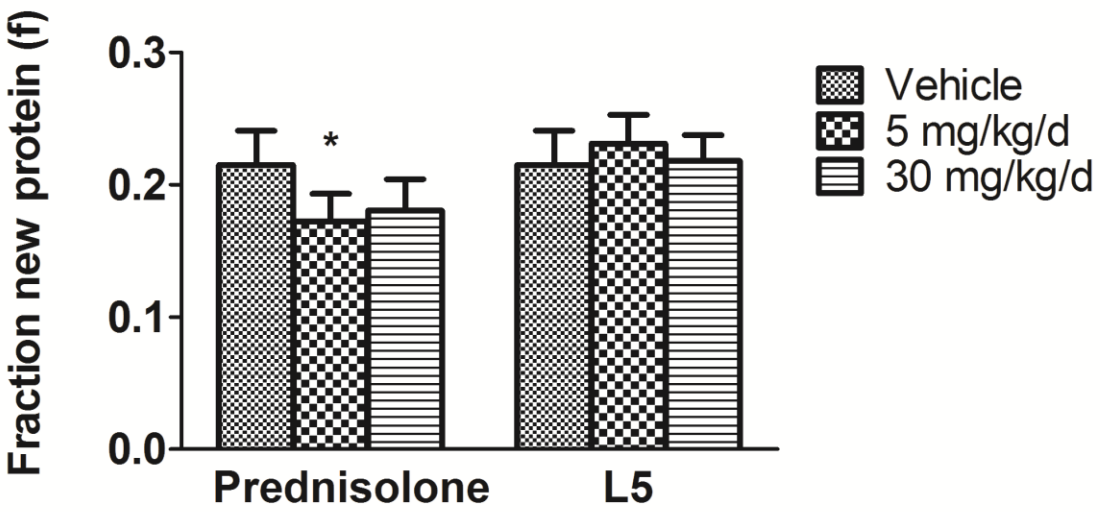

Figure 3. Fraction (f) of new protein (alanine) synthesized and retained over the course of one week in quadriceps muscle. Data are shown as mean ± SD, n = 6 per group. * $P < 0.05$ compared to vehicle control.

Figure 4

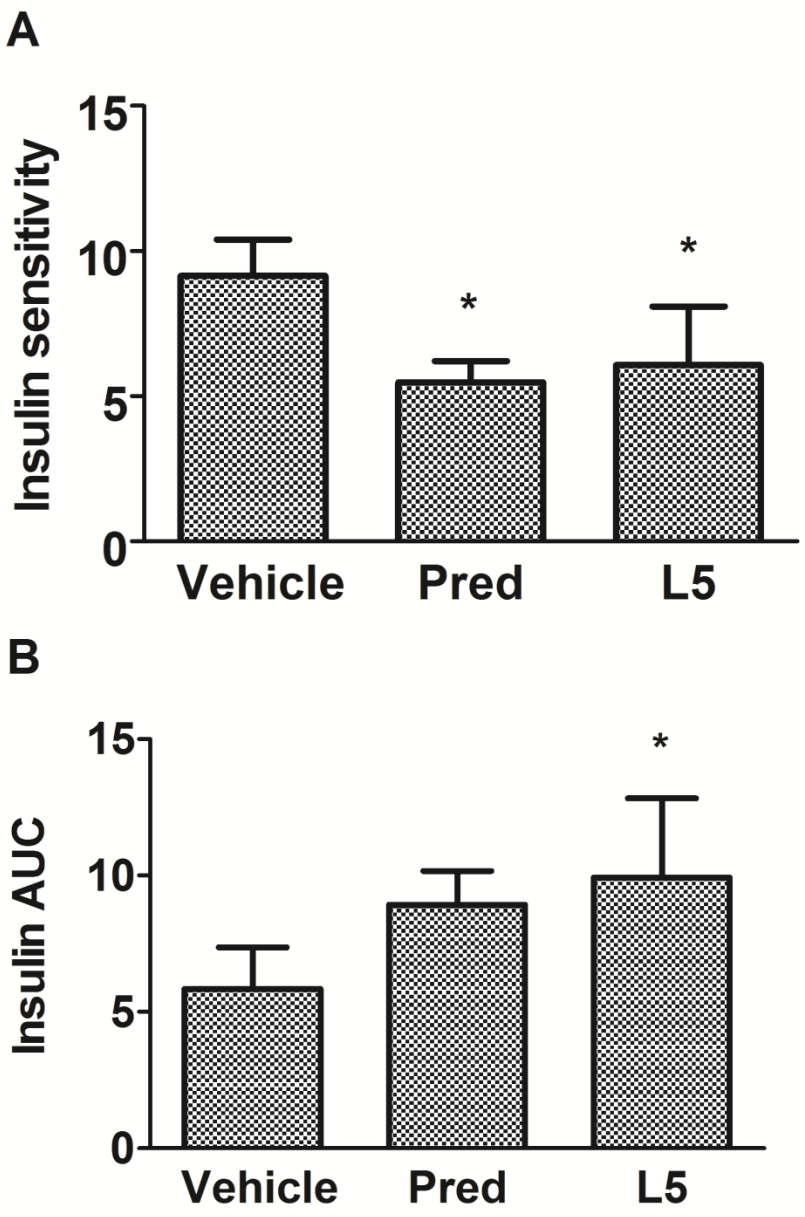

Figure 4. (A) Insulin Sensitivity Index, calculated as percent glucose load metabolized divided by insulin AUC (Beysen et al., 2007)**.** (B) Insulin AUC, measured by the trapezoidal method, as average insulin concentration in µg/mL at time 0 and time 10 min multiplied by 10 min. Vehicle: vehicle control group; Pred: group treated with 30 mg/kg/d of prednisolone; L5: group treated with 30 mg/kg/d of compound L5. Data are shown as mean ± SD, n = 4 per group. * $P < 0.05$ compared to vehicle control.

Figure 5

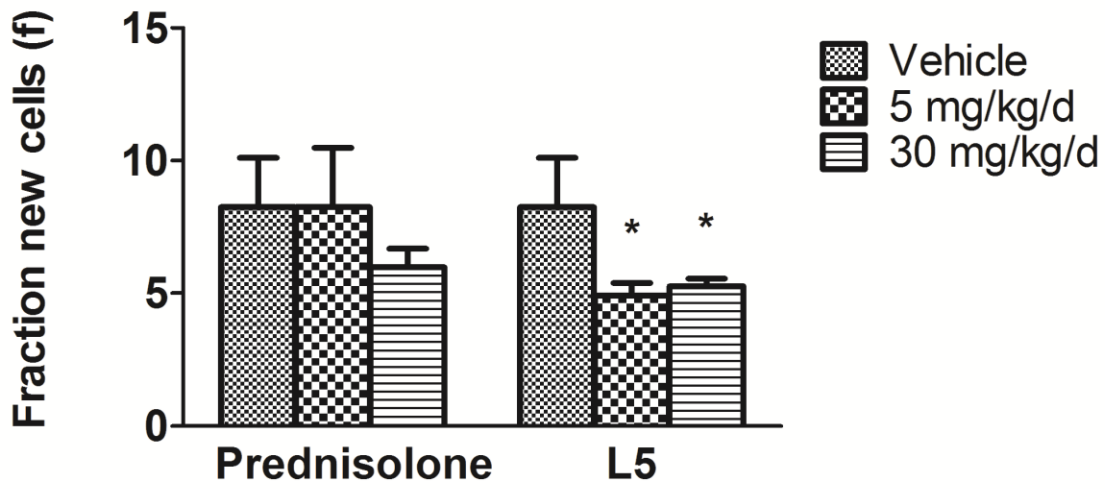

Figure 5. Fraction (f) of newly-formed neural progenitor stem cells in the hippocampus. Data are shown as mean ± SD, n = 6 per group. * $P < 0.05$ compared to vehicle control.

Figure 6

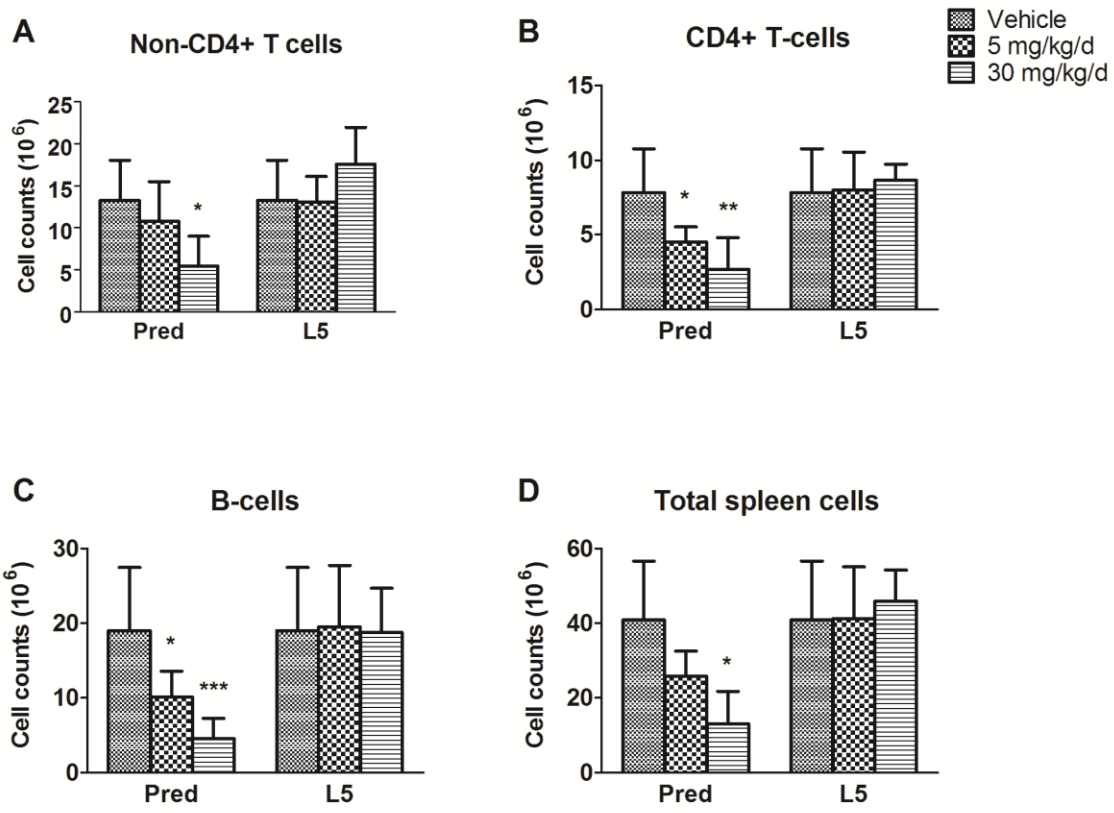

Figure 6. A-D: Cell counts (millions) after one week of treatment with either vehicle, 5 mg/kg/d or 30 mg/kg/d of prednisolone or compound L5,for splenic non-CD4+ T-cells (A), CD4+ T-cells (B), B-cells (C), and total spleen cells (D). Data are shown as mean ± SD, n = 6 per group. * $P < 0.05$ compared to vehicle control. ** $P < 0.01$ compared to vehicle control. *** $P < 0.001$ compared to vehicle control.

Figure 7

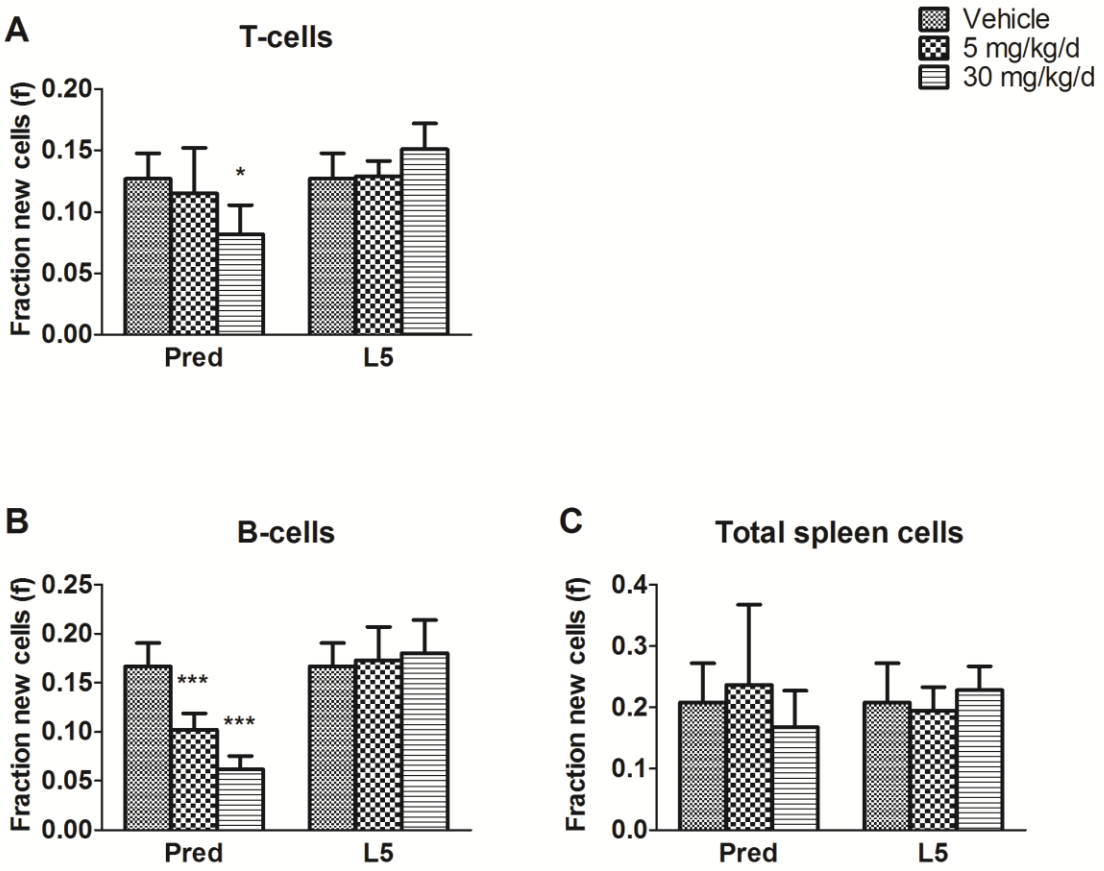

Figure 7. A-C: Fraction of newly-formed splenic T-cells (A), B-cells (B), and total spleen cells (C) throughout the course of one week of treatment with either vehicle, 5 mg/kg/d or 30 mg/kg/d of prednisolone or compound L5. Data are shown as mean ± SD, n = 6 per group. * $P < 0.05$ compared to vehicle control. *** $P < 0.001$ compared to vehicle control.

Figure 8

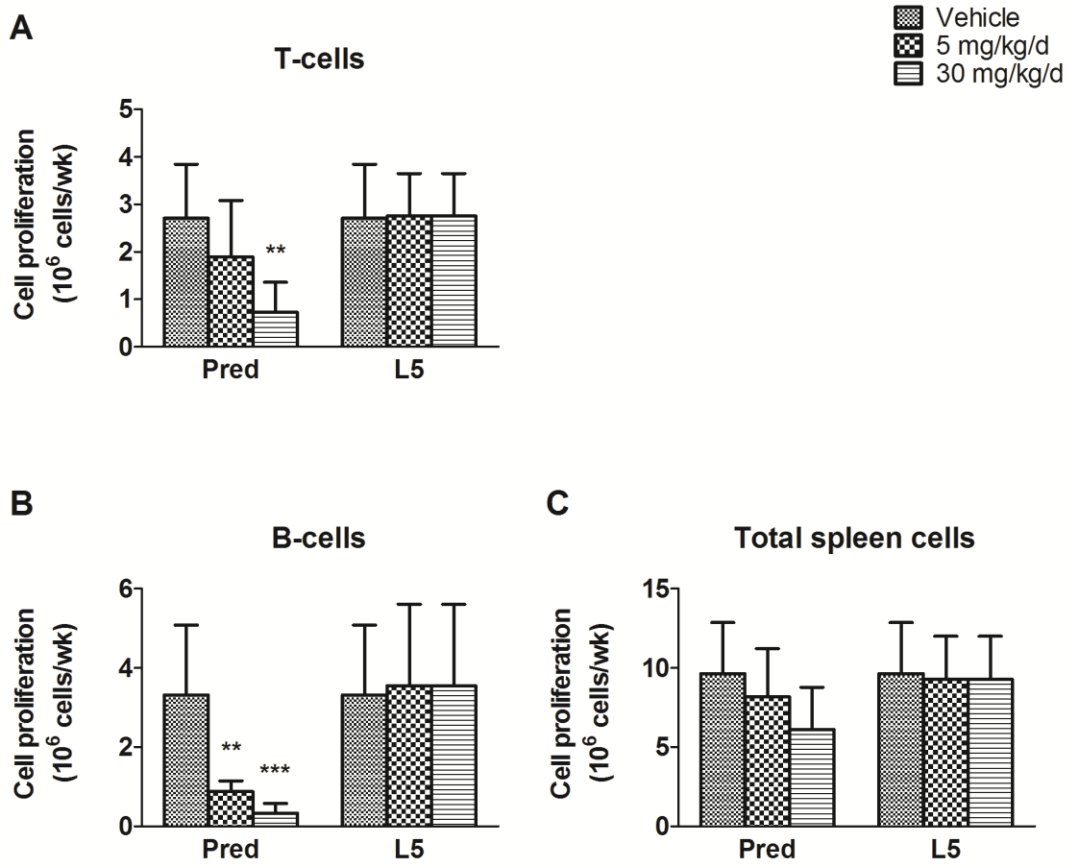

Figure 8. A-C: Proliferation (millions of cells) of splenic T-cells (A), B-cells (B), and total spleen cells (C) throughout the course of one week of treatment with either vehicle, 5 mg/kg/d or 30 mg/kg/d of prednisolone or compound L5. Data are shown as mean ± SD, n = 6 per group. ** $P < 0.01$ compared to vehicle control. *** $P < 0.001$ compared to vehicle control.

Figure 9

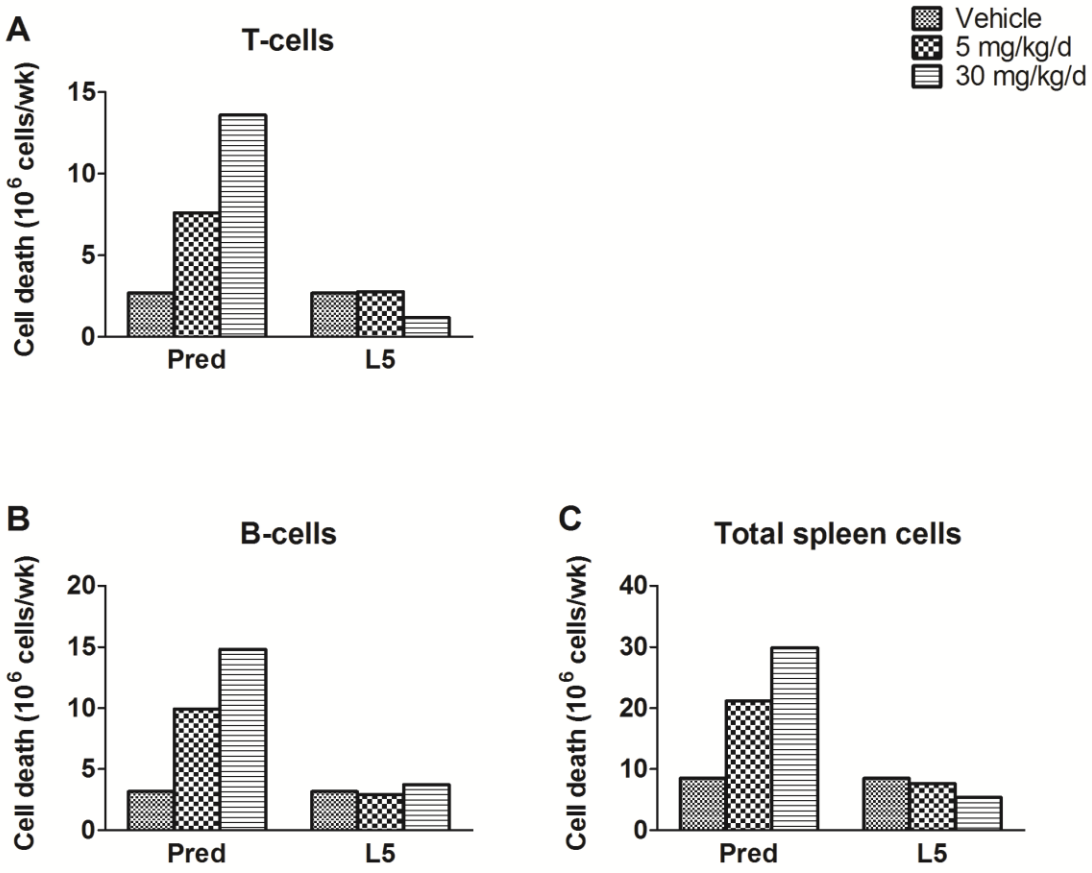

Figure 9. A-C: Calculated group average cell death in millions of cells of splenic T-cells (A), B-cells (B), and total spleen cells (C) throughout the course of one week of treatment with either vehicle, 5 mg/kg/d or 30 mg/kg/d of prednisolone or compound L5. Data are shown as calculated group means only.

Figure 10

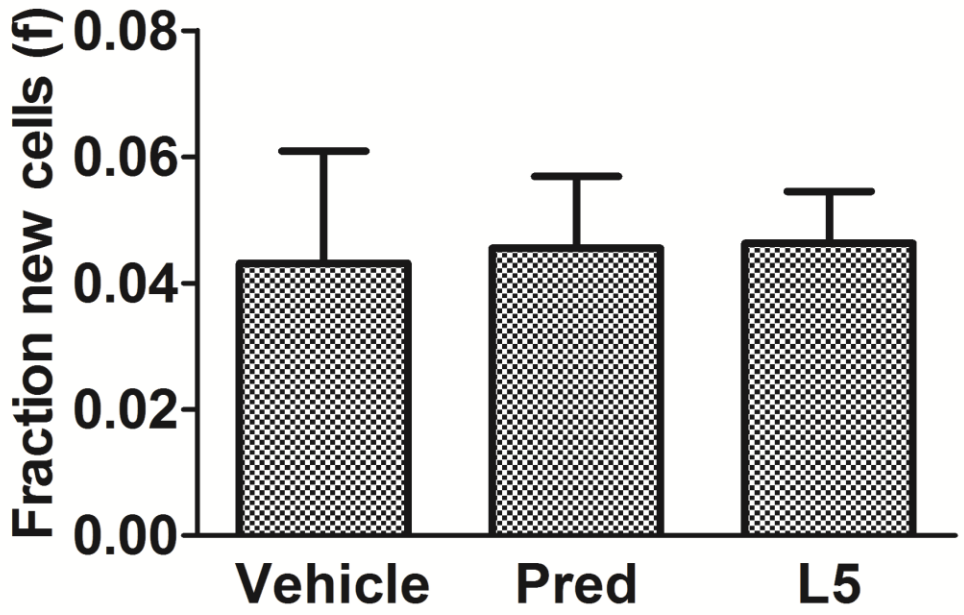

Figure 10. Fraction (f) of newly-formed cells in islets isolated from pancreas. Data are shown as mean ± SD, n = 6 per group.

Figure 11

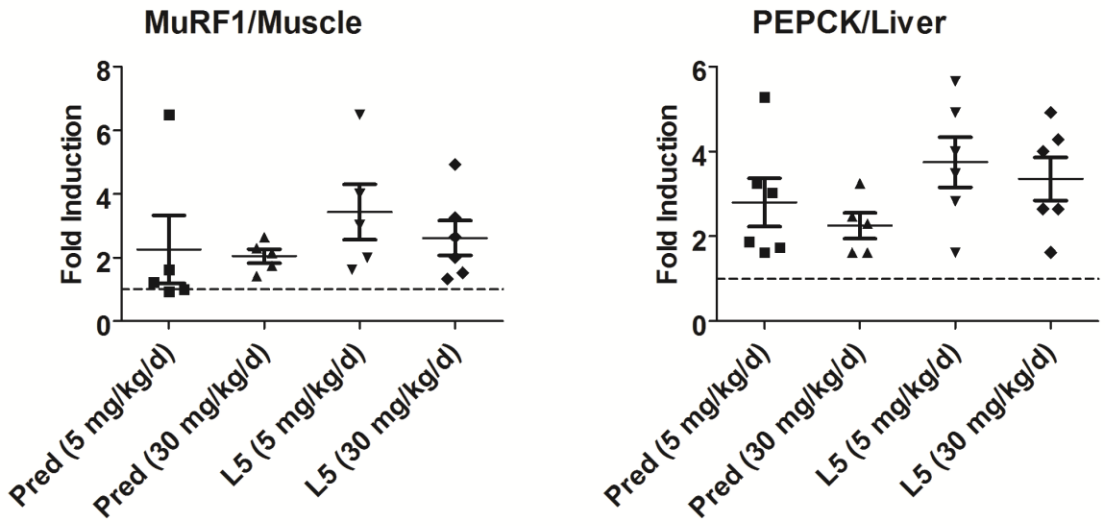

Figure 11. Induction of selective glucocorticoid target genes by prednisolone and L5 *in vivo*. Mice were treated with either vehicle, prednisolone or L5 (5 or 30 mg/kg/day) for 7 days. At the end of treatment, liver and skeletal muscle were harvested. Total RNA was prepared and subjected to cDNA synthesis. The cDNA was then analyzed by qPCR to measure the relative mRNA levels of two glucocorticoid target genes using gene-specific primers. Data represent the standard error mean (SEM) of the fold induction over that of the vehicle control group (prednisolone- or L5-treated samples divided by vehicle-treated samples) from at least 5 mice in each group.

Chapter 3: Glucocorticoid Mediated Changes in Adipose Triacylglycerol Metabolism Are Exaggerated, Not Diminished, in the Absence of a Functional GR Dimerization Domain

Abstract

The glucocorticoid receptor (GR) has multiple effector mechanisms, including dimerization-mediated transactivation of target genes via DNA binding and transcriptional repression mediated by protein-protein interactions. Much attention has been focused on developing selective GR modulators (SGRMs) that would dissociate adverse effects from therapeutic anti-inflammatory effects. The $GR^{dim/dim}$ mouse has a mutation in the dimerization domain of GR, and has been shown to have attenuated transactivation with intact repression. To understand the role of GR dimerization-dependent targets in multiple tissues, we measured metabolic fluxes through several disease-relevant glucocorticoid target pathways using heavy water labeling and mass spectrometry in wildtype and $GR^{dim/dim}$ mice administered the potent glucocorticoid, dexamethasone. Absolute triglyceride synthesis was increased in both wildtype and $GR^{dim/dim}$ mice by dexamethasone in the inguinal and epididymal fat depots. $GR^{dim/dim}$ mice showed an exaggerated response to dexamethasone in both depots. *De novo* lipogenesis was also greatly increased in both depots in response to dexamethasone in $GR^{dim/dim}$, but not wildtype mice. In contrast, the inhibitory effect of dexamethasone on bone and skin collagen synthesis rates was greater in wildtype compared to $GR^{dim/dim}$ mice. Wildtype mice were more sensitive to dexamethasone-dependent decreases in insulin sensitivity than $GR^{dim/dim}$ mice. Wildtype and $GR^{dim/dim}$ mice were equally sensitive to dexamethasone-dependent decreases in muscle protein synthesis. Chronic elevation of glucocorticoids in $GR^{dim/dim}$ mice results in severe runting and lethality. In conclusion, some metabolic effects of glucocorticoid treatment are exaggerated in adipose tissue of $GR^{dim/dim}$ mice, suggesting that SGRMs based on dissociating GR transactivation from repression should be evaluated carefully.

Abbreviations

Glucocorticoid: GC; glucocorticoid receptor: GR; DNA binding domain: DBD; glucocorticoid response element: GRE; selective glucocorticoid receptor modulator: SGRM; gas chromatography-mass spectrometry: GC-MS; wildtype: WT; dexamethasone: DEX; dual energy X-ray absorptiometry: DEXA; triglyceride: TG; fatty acid: FA; excess M_1 isotopomer: EM_1; *de novo* lipogenesis: DNL; ^{2}H-glucose disposal test or deuterated glucose disposal test: ^{2}H-GDT; insulin sensitivity index (SI)

Introduction

Glucocorticoids (GCs) are potent therapies for a wide range of inflammatory disorders. However, their use is limited by adverse metabolic effects including osteoporosis, weight gain, insulin resistance, altered body fat distribution, hypertension, muscle atrophy, and skin atrophy, a constellation known as Cushing's syndrome (Besser and Edwards, 1972; Stanbury and Graham, 1998). GCs mediate these responses via binding the glucocorticoid receptor (GR) (Hollenberg et al., 1985; Schoneveld et al., 2004). The challenge in designing modern GCs as medicines is not in increasing their potency or specificity for GR, but rather in designing compounds that evoke therapeutically desirable actions of GR, while limiting adverse actions of GR, thus increasing therapeutic index (Buttgereit et al., 2005a; Rosen and Miner, 2005; Schacke et al., 2007).

GR is a member of the nuclear hormone receptor transcription factor superfamily and contains several modular domains, including a DNA binding domain (DBD), ligand binding domain, and activation domains 1 and 2 (AF1, AF2) (Giguère et al., 1986; Schoneveld et al., 2004). When a ligand binds to and activates GR, GR translocates to the nucleus. Once in the nucleus, activated GR can homodimerize and bind to a sequence of DNA, a classical glucocorticoid response element (GRE), located in the proximal promoter, enhancer, or other regions of a gene (Schoneveld et al., 2004). In addition, various transcriptional cofactors are recruited, and transcription of the target gene is either induced or repressed (Rosen and Miner, 2005; Schoneveld et al., 2004). GR can modulate transcription of target genes by other mechanisms, such as binding to DNA as a monomer on a GRE half site (Rosen and Miner, 2005; Schoneveld et al., 2004), binding to DNA and to another transcription factor that is also binding the DNA at a composite element (Rosen and Miner, 2005; Schoneveld et al., 2004), or binding via protein-protein interactions exclusively to another transcription factor (tethering) (Rosen and Miner, 2005; Schoneveld et al., 2004). Many of the well-characterized anti-inflammatory mechanisms of GR, for example, involve binding with pro-inflammatory transcription factors, such as NF-κB and AP-1, via tethering or at a composite element, whereby activated GR binds to and inhibits their normal pro-inflammatory actions (Miner and Yamamoto, 1992; Nissen and Yamamoto, 2000; Ray and Prefontaine, 1994; Rosen and Miner, 2005; Scheinman et al., 1995; Vayssiere et al., 1997; Yang-Yen et al., 1990).

Historically, GCs have been thought of as either pure agonists or pure antagonists (Stanbury and Graham, 1998). Recently, however, the concept of selective GR agonists or selective glucocorticoid receptor modulators (SGRMs) has emerged (Buttgereit et al., 2005a; De Bosscher; Rosen and Miner, 2005; Schacke et al., 2007). The variable actions of known SGRMs on GR-dependent pathways are thought to be due to their ability to induce variations in cofactor recruitment or variable affinity of activated GR for different GRE sequences (De Bosscher; Schacke et al., 2007). Because many of the potent anti-inflammatory actions of GR have been attributed to inhibitory events involving tethering of GR with pro-inflammatory transcription factors (Schäcke et al., 2002), a model has emerged depicting the anti-inflammatory actions of GCs as being mediated by GR repression, which are dependent largely on GR tethering with another transcription factor, and the adverse metabolic effects as being mediated by transactivation, which are dependent largely on GR-GR homodimerization and DNA binding at a classic GRE. Based on this model, much attention has been focused on the possibility of developing SGRMs that would retain anti-inflammatory properties with reduced metabolic

adverse effects (De Bosscher; De Bosscher et al., 2005; Kleiman and Tuckermann, 2007; Miner, 2002; Schacke et al., 2007; Schacke et al., 2004). Site-directed mutagenesis of the GR dimerization domain (within the DBD) revealed mutants that abrogated GR-GR homodimerization-dependent transactivation of GRE-reporter constructs while leaving tethering-based repression intact (Heck et al., 1994). Homologous recombination has been used to "knock-in" this point mutation in mice (Reichardt et al., 1998). In contrast to $GR^{-/-}$ mice that die at birth, $GR^{dim/dim}$ mice are viable (Reichardt et al., 1998). In addition, many of the GR-dependent anti-inflammatory pathways of $GR^{dim/dim}$ mice have been previously shown to be intact in these mice (Reichardt et al., 2001). $GR^{dim/dim}$ mice have served, not only as a genetic model for a novel class of potential SGRMs (De Bosscher; De Bosscher et al., 2005; Kleiman and Tuckermann, 2007; Miner, 2002; Schacke et al., 2007; Schacke et al., 2004), but also to tease out mechanisms by which GR mediates its effects on target genes and metabolic pathways, in particular in pathways associated with the therapeutically undesirable effects of GR activation (Frijters et al.; Rauch et al.; Reichardt et al., 1998; Waddell et al., 2008).

In this study we sought to determine the requirements for an intact GR dimerization domain in mediating the effects of GCs in multiple target pathways of GCs. We directly assessed the roles of GR dimerization-dependent targets in mediating several therapeutically undesirable metabolic effects of GCs by use of stable isotope labeling with gas chromatographic-mass spectrometric (GC-MS) methods. Kinetic measurements included bone and skin collagen synthesis, muscle protein synthesis, adipose tissue lipid dynamics and insulin sensitivity in wildtype (WT) and $GR^{dim/dim}$ mice administered vehicle or dexamethasone (DEX). Our goal was not only to understand molecular requirements for GR effects on GC-dependent pathways, but also to further explore the $GR^{dim/dim}$ mutation as a potential genetic model for SGRMs.

Materials and Methods

Animal Husbandry and Breeding

$GR^{dim/+}$ (GR-A458T back-crossed onto a C57Bl/6 background) mice were a gift of Günther Schütz (German Cancer Research Center, Heidelberg, Germany). $GR^{dim/+}$ mice were rederived at UCSF by embryo transfer. $GR^{dim/dim}$ mice and $GR^{+/+}$ (WT) mice were housed in groups of no more than 5 under temperature-controlled conditions with a 12 h light/12 h dark cycle. Mice were fed a PicoLab® Rodent Diet 20 (5053, PMI Nutrition International, St. Louis, MO; 13% of calories from fat) *ad libitum*. All studies received prior approval from the Animal Care and Use Committee at UCSF, and were performed in conformity with the Public Health Service (PHS) Policy on Humane Care and Use of Laboratory Animals. $GR^{dim/dim}$ mice did not survive to weaning at the expected Mendelian frequency. Intercrosses of $GR^{dim/+}$ mice resulted in approximately 5% $GR^{dim/dim}$ mice with a ratio of $GR^{+/+}$ to $GR^{dim/+}$ that suggested dropout of $GR^{dim/dim}$ mice. In addition, many dead pups were found at birth that were genotyped as $GR^{dim/dim}$. We therefore used $GR^{dim/dim}$ male x $GR^{dim/+}$ female crosses to generate $GR^{dim/dim}$ mice. Here too decreased viability of $GR^{dim/dim}$ mice was seen with only 10% of progeny surviving to weaning from these crosses being $GR^{dim/dim}$. WT littermate controls were bred in parallel from our colony.

Dual Energy X-Ray Absorptiometry (DEXA)

Body composition analysis was performed using DEXA (GE Lunar Piximus). Mice were anesthetized with isoflurane during DEXA scanning. The head region was excluded from analysis using the region of interest feature of Piximus software.

Heavy Water (^2H_2O) Labeling Protocol

WT and $GR^{dim/dim}$ mice (male, 7 weeks or 4 months old) were labeled with ^2H_2O to body water enrichments of approximately 5% for 7 days as described elsewhere (Neese et al., 2002).

DEX Treatment Protocol for ^2H_2O-labeled Mice

Mice were injected intraperitoneally with vehicle or 10 mg/kg DEX every other day for one week. Specifically, DEX injections were performed on days 1, 3, and 5 of ^2H_2O labeling.

Measurement of body ^2H_2O, Hydroxyproline, Alanine, Triglyceride (TG)-glycerol, and TG-palmitate Enrichments by GC-MS in Heavy Water Labeling Studies

GC-MS was performed using a 5890 gas chromatograph attached to either a 5971 or 5973 mass spectrometer (Hewlett Packard, Palo Alto, CA; Agilent Technologies, Santa Clara, CA). Water was distilled from plasma, and ^2H enrichment was measured using GC-MS after conversion to tetrabromoethane, as described in detail elsewhere (Collins et al., 2003; Roohk et al.; Turner et al., 2003). L-4-(O-tert-butyldimethylsilyl)-hydroxyproline pentafluorobenzyl ester was prepared from bone and skin and analyzed by GC-MS as previously described (Gardner et al., 2007; Roohk et al.). Pentafluorobenzyl-*N*,*N*-di(pentafluorobenzyl)-alanine was prepared from skeletal muscle (quadriceps) and analyzed by GC-MS as previously described (Busch et al., 2006; Roohk et al.). TG-glycerol and fatty acids (FA) were isolated from adipose tissue and liver, TG-glycerol was derivatized to glycerol-triacetate, and glycerol-triacetate and separated FA-methyl esters were analyzed by GC-MS as described previously (Bruss et al.; Hellerstein et al., 1991;

Hellerstein et al., 1993; Roohk et al.; Turner et al., 2003; Turner et al., 2007). All compounds were resolved on a DB-225 gas chromatograph column (Agilent Technologies, Santa Clara, CA). Mass spectrometry was performed in negative chemical ionization mode for derivatized hydroxyproline and alanine, positive chemical ionization mode for glycerol-triacetate, and electron impact ionization mode for FA-methyl esters with helium as the carrier gas for all analytes. Mass-to-charge ratios corresponding to unlabeled, singly-labeled, and doubly-labeled (M_0, M_1, and M_2) mass isotopomers of each derivatized compound were analyzed by selected ion monitoring.

Calculation of Fractional Synthesis Rates of Tissue Collagen, Muscle Proteins, TG-glycerol, and TG-palmitate

Fractional synthesis (f), or fraction newly synthesized during the 7-day labeling period was calculated for collagen (hydroxyproline), total protein (alanine), TG-palmitate, and total TG (TG-glycerol). For each analyte, the ratio of the measured excess M_1 isotopomer (EM_1) to the asymptotic value of EM_1 ($EM_{1,max}$) was calculated as previously described (Bruss et al.; Busch et al., 2006; Gardner et al., 2007; Hellerstein and Neese, 1999; Neese et al., 2001; Roohk et al.; Turner et al., 2003) using the following formula:

$$f = EM_{1(sample)} / EM_{1,max}$$

$EM_{1(sample)}$ is the enrichment of M_1 isotopomers in excess of that which occurs in nature, calculated for each analyte using the abundances of the M_0, M_1, and M_2 mass isotopomers measured in the sample and in an unenriched standard:

$$EM_{1(sample)} = [M_1 / (M_0 + M_1 + M_2)]_{sample} - [M_1 / (M_0 + M_1 + M_2)]_{standard}$$

$EM_{1,max}$ is calculated for each analyte in each animal based on the measured body ^2H_2O enrichment, as described previously (Bruss et al.; Busch et al., 2006; Gardner et al., 2007; Hellerstein and Neese, 1999; Neese et al., 2001; Roohk et al.; Turner et al., 2003), and represents the calculated EM_1 of the fully-turned-over analyte at the body ^2H_2O enrichment measured in the animal.

Calculation of Absolute TG-glycerol Synthesis Rates

Absolute TG synthesis rates in inguinal and epididymal fat depots were calculated as previously described (Roohk et al.; Turner et al., 2003; Varady et al., 2007a). Briefly, absolute synthesis rates of adipose TG were calculated from fractional TG synthesis (f_{TG}) multiplied by adipose TG mass multiplied by the fraction of TG in adipose tissue by weight:

$$\text{Absolute synthesis (g/wk)} = f_{TG} \times \text{adipose TG mass (g)} \times (0.9).$$

Calculation of Absolute Rates of *de novo* lipogenesis (DNL)

Absolute rate of DNL in inguinal and epididymal fat depots was calculated as previously described (Roohk et al.; Varady et al., 2007b) from fractional TG-palmitate synthesis (f_{DNL}), adipose TG mass, and the fraction of palmitate relative to other FAs in TG using the following formula:

Absolute DNL (g/wk) = f_{DNL} × adipose TG mass (g) x fraction TG-palmitate,

The fraction of TG-palmitate present in adipose TG was taken to be 20% (Jung et al., 1999; Pouteau et al., 2008).

Ex-vivo Lipolysis

WT and $GR^{dim/dim}$ mice were treated with vehicle or 10 mg/kg DEX every day for 4 days, Mice were sacrificed, inguinal and epididymal adipose tissue collected, and lipolysis measured as previously described (Yu et al.). We also measured lipolysis in adipose tissue explants incubated in 1 μM isoproterenol as a control.

^{2}H-glucose Disposal Test

The ^{2}H-glucose disposal test (^{2}H-GDT), a modified oral glucose tolerance test, was used to measure insulin-mediated glucose utilization (insulin resistance) and pancreatic beta-cell compensation, as previously described (Beysen et al., 2007; Roohk et al.). At age 4 months, mice were subjected to the ^{2}H-GDT to assess baseline (vehicle-treated) values. All mice were allowed to recover for one month, treated with DEX as above, and then again subjected to the ^{2}H-GDT. Blood was taken at regular time points for blood glucose and plasma insulin concentrations, as well as for analysis by isotope ratio infrared spectrometry to quantify $^{2}H_2O$ and $H_2{}^{18}O$ enrichments. Insulin sensitivity index (SI) was calculated as the percent of glucose load metabolized to H_2O divided by the product of insulin AUC and glucose AUC, thus whole body glycolytic utilization of a glucose load per unit of ambient insulin exposure per unit of ambient glucose level.

Statistical Analyses

Statistical analyses were performed using GraphPad Prism 5 (Graphpad Software Inc, La Jolla, CA). In heavy water labeling, *ex-vivo* lipolysis, and ^{2}H-GDT studies, two-way ANOVA was performed to assess statistically significant main effects of DEX treatment and genotype, as well as interaction effect of the two main variables of genotype and DEX treatment, on parameters measured. Bonferroni posttests were performed to assess statistically significant differences between vehicle-treated and DEX-treated groups for each genotype. $P < 0.05$ was considered to be significant. For DEXA analyses t tests were used.

Results

$GR^{dim/dim}$ Mice Are Not Protected from GC-induced Suppression of Collagen Synthesis in Skin and Bone.

We measured collagen synthesis rates in bone and skin in vehicle and DEX-treated WT and $GR^{dim/dim}$ mice in the femurs of 4-month-old mice. DEX treatment did not result in significantly lower rates of collagen synthesis in either WT or $GR^{dim/dim}$ mice compared to their respective vehicle controls (Figure 1A).

Because reductions in bone collagen synthesis rates were comparatively modest in 4-month-old mice, we measured bone collagen synthesis rates in a separate cohort of 8-week-old WT and $GR^{dim/dim}$ mice, an age at which we have previously observed significant effects (Roohk et al.). In the femurs of 8-week-old mice, DEX treatment resulted in significantly lower rates of collagen synthesis in both WT ($P < 0.001$) and $GR^{dim/dim}$ ($P < 0.05$) mice relative to their respective vehicle controls (Figure 1B). The inhibitory effect of DEX treatment on bone collagen synthesis rates was significantly greater ($P < 0.01$) in WT mice compared to $GR^{dim/dim}$ mice.

In the dorsal skin of 4-month-old mice, DEX treatment resulted in significantly lower ($P < 0.001$) rates of collagen synthesis in both WT and $GR^{dim/dim}$ mice compared to their respective vehicle controls (Figure 1C). The inhibitory effect of DEX on fractional skin collagen synthesis rates, specifically the absolute difference between vehicle and DEX-treated values, was greater ($P < 0.01$) in WT mice compared to $GR^{dim/dim}$ mice. However, within both WT and $GR^{dim/dim}$ groups, DEX- treated mice had approximately 90% lower rates of skin collagen synthesis relative to their respective vehicle controls.

In summary, one week of DEX treatment significantly inhibits rates of bone collagen synthesis in 8-week-old, but not 4-month-old, WT and $GR^{dim/dim}$ mice. DEX also significantly inhibits rates of skin collagen synthesis in both WT and $GR^{dim/dim}$ mice. $GR^{dim/dim}$ mice exhibited less inhibition of collagen synthesis than WT in response to DEX, in both bone and skin.

$GR^{dim/dim}$ Mice Are Not Protected from GC-induced Suppression of Skeletal Muscle Protein Synthesis

Because GCs are known to decrease lean tissue mass in part by inhibiting muscle protein synthesis (Long et al., 2001; Louard et al., 1994; Odedra et al., 1983; Roohk et al.), we measured rates of total protein synthesis in quadriceps muscle of vehicle and DEX-treated $GR^{dim/dim}$ and WT mice. DEX treatment resulted in significantly lower ($P < 0.001$) rates of muscle protein synthesis in both WT and $GR^{dim/dim}$ mice compared to their respective vehicle controls (Figure 2). Synthesis rates were 17% lower in WT and 26% lower in $GR^{dim/dim}$ mice. Differences in sensitivity to DEX between genotypes were not significant ($P > 0.05$).

Body Weight and Body Composition

We examined body composition of 8-week-old and 4-month-old WT and $GR^{dim/dim}$ mice. Eight-week-old $GR^{dim/dim}$ mice did not differ from WT mice with respect to total mass or lean mass, but had higher fat mass (Table 1, 3.4 ± 0.7 vs 2.7 ± 0.2, $P < 0.05$) and percent fat mass than WT mice (Table 1, 15.7 ± 3.0 vs. 13.3 ± 1.0, $P < 0.05$). Four-month-old $GR^{dim/dim}$ mice had the same

pattern, with no difference in total mass compared to WT mice, but with increased fat mass and percent fat mass (Table 1, 5.8 ± 1.4 vs 4.3 ± 1.1 and 20.2 ± 3.3 vs 15.7 ± 3.8 , $P < 0.05$ respectively).

$GR^{dim/dim}$ mice exhibit exaggerated lipid metabolic responses to GC administration

Fat Pad Mass

In the inguinal depot DEX treatment resulted in significantly larger ($P < 0.01$) fat pads in $GR^{dim/dim}$ mice, but not in WT mice, relative to their respective vehicle controls (Table 2). In the epididymal depot, DEX treatment did not significantly affect fat pad mass in either WT or $GR^{dim/dim}$ mice relative to their respective vehicle controls (Table 2). Differences in sensitivity to DEX between the two genotypes were not significant for fat pad mass ($P > 0.05$) in either depot.

Adipose Tissue TG Fractional Synthesis Rates

In the inguinal depot DEX treatment did not significantly affect synthesis rates of TG in either WT or $GR^{dim/dim}$ mice relative to their respective vehicle controls (Table 2). In the epididymal depot, DEX treatment resulted in significantly higher rates of TG synthesis in WT ($P < 0.05$) and $GR^{dim/dim}$ ($P < 0.001$) mice relative to their respective vehicle controls (Table 2). Differences in sensitivity to DEX between genotypes were not significant ($P > 0.05$) in either depot.

Adipose Tissue Absolute TG Synthesis Rates

By combining fat pad mass with fractional TG synthesis rates, we calculated absolute TG synthesized over the week-long labeling period in inguinal and epididymal fat depots (Figure 3A and Figure 3B). In both the inguinal and epididymal depots DEX treatment resulted in significantly more TG synthesized in both WT ($P < 0.05$) and $GR^{dim/dim}$ ($P < 0.001$) mice compared to their respective vehicle controls. Furthermore, in both the inguinal and epididymal depots $GR^{dim/dim}$ mice were significantly more sensitive to DEX-dependent increases in absolute TG synthesis compared to WT mice ($P < 0.001$ and $P < 0.01$ in inguinal and epididymal depots, respectively).

Fractional Rates of DNL

DEX treatment resulted in significantly higher fractional rates of palmitate DNL in both depots of $GR^{dim/dim}$ mice ($P < 0.01$ and $P < 0.001$ in the inguinal and epididymal depot, respectively), but not in WT mice, compared to their respective vehicle controls (Table 2). While significant differences between genotypes in sensitivity to DEX were not found in the inguinal depot, in the epididymal depot $GR^{dim/dim}$ mice were found to be significantly more sensitive ($P < 0.01$) to DEX-dependent increases in rates of DNL compared to WT.

Absolute DNL

By combining fat pad mass with fractional rates of DNL, we calculated absolute palmitate synthesized by DNL over the week-long labeling period (Figure 4C and Figure 4D). In both the inguinal and epididymal fat depots DEX treatment resulted in significantly more ($P < 0.001$) absolute DNL in $GR^{dim/dim}$ mice, but not in WT mice, compared to their respective vehicle

controls. Furthermore, in both fat depots $GR^{dim/dim}$ mice were significantly more ($P < 0.001$) sensitive to DEX-dependent increases in absolute DNL compared to WT.

Summary of Adipose Tissue Lipid Dynamics in Vivo

In summary, $GR^{dim/dim}$ mice have slightly larger inguinal and epididymal fat pads than WT mice. In the absence of DEX, $GR^{dim/dim}$ and WT mice synthesize similar amounts of TG and synthesize similar amounts of FA via DNL in both fat depots. While both $GR^{dim/dim}$ and WT mice synthesize more TG in response to DEX treatment, $GR^{dim/dim}$ mice are much more sensitive to a DEX-dependent increase in TG synthesis, and only $GR^{dim/dim}$ mice synthesize more FA via DNL.

Ex-vivo Lipolysis

We measured glycerol release as a surrogate for lipolysis in inguinal and epididymal adipose tissue explants (Figure 4). Rates of lipolysis were significantly lower ($P < 0.05$) by 40% in inguinal adipose tissue from $GR^{dim/dim}$ mice treated with DEX. $GR^{dim/dim}$ mice were also significantly more ($P < 0.05$) sensitive to DEX-dependent decreases in rates of lipolysis compared to WT in the inguinal depot. No other significant differences in rates of lipolysis or sensitivity to DEX were found in adipose tissue from either depot.

Insulin Sensitivity

GCs are widely known to decrease insulin sensitivity. Accordingly, we measured peripheral tissue insulin sensitivity using the ^{2}H-GDT. DEX treatment did not significantly affect blood glucose AUC in WT ($15 \pm 3.8 \times 10^3$ mg min/dL for vehicle vs. $15 \pm 2.7 \times 10^3$ mg min/dL for DEX) or $GR^{dim/dim}$ mice ($13 \pm 2.7 \times 10^3$ mg min/dL for vehicle vs. $12 \pm 2.5 \times 10^3$ mg min/dL for DEX) compared to their respective vehicle controls (Figure 5A). Average blood glucose AUC of all $GR^{dim/dim}$ mice was significantly lower ($12 \pm 2.5 \times 10^3$ mg min/dL for DIM vs. $15 \pm 3.2 \times 10^3$ mg min/dL for WT, $P < 0.05$, main effect of genotype, two-way ANOVA) compared to all WT mice.

DEX treatment resulted in significantly higher insulin levels in both $GR^{dim/dim}$ (65 ± 17 ng min/mL for vehicle vs. 180 ± 50 ng min/mL for DEX, $P < 0.001$) and WT (32 ± 8.4 ng min/mL for vehicle vs. 150 ± 77 ng min/mL for DEX, $P < 0.01$) mice compared to their respective vehicle controls (Figure 5B). $GR^{dim/dim}$ mice were not significantly more sensitive to DEX-dependent increases in insulin AUC compared to WT ($P > 0.05$).

Percent glucose load metabolized to water was used as a metric of uptake and metabolism of an oral glucose load to water by peripheral tissues. No significant differences between groups were found (Figure 5C).

By combining glucose AUC, insulin AUC, and percent glucose load metabolized to water we calculated SI (Figure 5D). Treatment with DEX resulted in significantly lower ($P < 0.001$) SI in WT mice, but not in $GR^{dim/dim}$ mice, compared to their respective vehicle controls. Furthermore, WT mice were significantly more ($P < 0.05$) responsive to DEX-dependent decreases in SI compared to $GR^{dim/dim}$ mice.

In summary, $GR^{dim/dim}$ mice had lower blood glucose levels than WT, and DEX increased plasma insulin levels similarly in both $GR^{dim/dim}$ and WT mice. Absorption of blood glucose and metabolism to water by peripheral tissues was similar in both $GR^{dim/dim}$ and WT mice, and was unaffected by DEX administration. DEX treatment resulted in decreased SI in WT mice, but SI was not significantly decreased by DEX in $GR^{dim/dim}$ mice. Lastly, WT mice were more responsive to DEX-dependent decreases in insulin sensitivity, than were $GR^{dim/dim}$ mice.

Chronically Elevated GCs in $GR^{dim/dim}$ Mice Results in Runting and Lethality

Given the profound abnormalities in the response of $GR^{dim/dim}$ mice to acute GCs, we wanted to know what their response to chronically elevated GCs would be. In order to answer this question, we bred $GR^{dim/dim}$ mice to CRH-Tg^{+}, a transgenic line with a constitutively active CRH transgene resulting in chronically elevated ACTH and corticosterone (Stenzel-Poore et al., 1992). CRH-Tg^{+} mice have increased fat mass, decreased lean mass and decreased bone content (C. Harris, unpublished observations). Of 148 pups born from crosses of CRH-Tg^{+}, $GR^{dim/+}$ males to $GR^{dim/dim}$ females, 15 were $GR^{dim/dim}$. Of these only 3 were $GR^{dim/dim}$, CRH-Tg^{+}. $GR^{dim/dim}$, CRH-Tg^{+} mice were severely runted, and all 3 mice generated died before 6 weeks of age, weighing approximately 5 grams. We were therefore unable to further study metabolic parameters in these mice.

Discussion

An Intact GR Dimerization Domain Is Not Required for Suppression of Collagen Synthesis in Skin or Bone or Suppression of Protein Synthesis in Skeletal Muscle

Previous studies have shown that the effects of GCs on bone as assessed by calcein-guided bone formation rates, histomorphometry, and collagen mRNA expression did not require an intact GR dimerization domain (Rauch et al.). However, our study is the first study to examine directly the effects of GCs on skin and bone collagen synthesis *in vivo* in $GR^{dim/dim}$ mice. We were unable to detect significant DEX-dependent decreases in bone collagen synthesis rates in 4-month-old WT or $GR^{dim/dim}$ mice (Figure 1A). We believe that this is due to the fact that the rate of bone collagen turnover decreases as mice get older, so one week of treatment and labeling was likely not sufficient to observe reductions in bone collagen synthesis.

Previously we had observed significant differences in 8-week-old mice treated with prednisolone for one week (Roohk et al.). We repeated the experiment here in a cohort of 8-week-old WT and $GR^{dim/dim}$ mice, and observed significant DEX-dependent decreases in bone collagen synthesis rates in both genotypes (Figure 1B). Interestingly, we found that the difference between vehicle-treated and DEX-treated groups was significantly greater in WT mice compared to $GR^{dim/dim}$ mice. While the effect was greater in WT mice, vehicle-treated (baseline) bone collagen synthesis rates appeared to be slightly lower in $GR^{dim/dim}$ mice. As expected, baseline bone collagen synthesis rates were lower in 4-month-old mice than in 8-week-old mice, and the 4-month-old $GR^{dim/dim}$ mice did not have lower baseline rates of bone collagen synthesis compared to WT.

It is not clear from these studies whether the 8-week-old $GR^{dim/dim}$ mice are less sensitive to DEX-dependent decreases in bone collagen synthesis rates or if they have a slower baseline rate of bone turnover at this age. But because WT and $GR^{dim/dim}$ mice have similar bone mass and bone mineral density (C. Harris, unpublished observations), we hypothesize that there is no consequential difference in baseline bone collagen synthesis rates up to 4 months of age. Furthermore, we conclude that key pathways responsible for GC-dependent decreases in bone collagen synthesis rates in WT mice are mostly intact in $GR^{dim/dim}$ mice.

We observed DEX-dependent decreases in skin collagen synthesis rates in WT and $GR^{dim/dim}$ mice (Figure 1C). There was a significant difference in sensitivity to DEX between genotypes, and baseline skin collagen synthesis rates appeared lower by approximately half in $GR^{dim/dim}$ mice compared to WT. Because no differences in skin thickness were observed (data not shown), we assume that turnover of skin collagen is also lower in $GR^{dim/dim}$ mice. Despite differences in baseline skin collagen synthesis rates, there was approximately a 90% percent reduction in rates of skin collagen synthesis in both genotypes treated with DEX. Thus, we conclude that key pathways responsible for GC-dependent decreases in skin collagen synthesis rates in WT mice are mostly intact in $GR^{dim/dim}$ mice.

In both WT and $GR^{dim/dim}$ mice, we saw modest, but significant, suppression of protein synthesis rates in skeletal muscle (Figure 2). This modest decrease is in line with our previous observations in 8-week-old WT mice (Roohk et al.), with the observations of other groups studying $GR^{dim/dim}$ mice (Waddell et al., 2008), and with GCs causing muscle wasting predominantly by inducing

protein degradation rather than suppressing synthesis (May et al., 1986; Price et al., 2001; Schacke et al., 2007; Schäcke et al., 2002; Tiao et al., 1996; Wing and Goldberg, 1993). Thus, we conclude that key pathways responsible for GC-induced decreases in muscle protein synthesis in WT mice are intact in $GR^{dim/dim}$ mice, however we cannot rule out the possibility that pathways responsible for muscle protein degradation are not.

GC Mediated Changes in Adipose Lipid Dynamics Are Exaggerated in the Absence of a GR Dimerization Domain

We found that GC-induced increases in both TG synthesis and DNL were greatly exaggerated in $GR^{dim/dim}$ mice compared to WT mice (Figure 3). Based on body compositions and fat pad masses (Tables 1 and 2), we conclude that $GR^{dim/dim}$ mice accrue fat faster than WT in response to DEX. We also observed that the difference in the amount of TG synthesized is roughly the same as the difference in fat pad masses between vehicle-treated and DEX-treated WT and $GR^{dim/dim}$ animals. Thus, TG accrued was roughly similar to the amount of TG synthesized in response to DEX in these depots, and DEX had much more of an effect on TG synthesis compared to lipolysis. Furthermore, when we directly measured lipolysis in dissected adipose tissue from WT and $GR^{dim/dim}$ mice treated with vehicle or DEX for 4 days, we found no significant change in rates of lipolysis in adipose tissue from either depot in WT mice and a decrease and no change in rates of lipolysis in adipose tissue from the inguinal and epididymal depot, respectively, of $GR^{dim/dim}$ mice (Figure 4). In summary, we conclude, first, that DEX increases TG synthesis to a much greater extent in $GR^{dim/dim}$ mice than in WT mice, and second, net increases in synthesis are proportionally much greater than net changes in lipolysis.

Even more striking were genotypic differences in DEX-dependent changes in DNL. DEX did not significantly increase DNL in either depot of WT mice, but dramatically increased DNL in both depots of $GR^{dim/dim}$ mice (Figure 3). One limitation of our *in vivo* studies is that because of the prolonged time required for labeling adipose TG, we cannot determine the site of action of the effects of GCs on DNL, such that the increased rate of appearance could be due to increased adipose DNL or increased hepatic DNL with subsequent VLDL export to adipose tissue. In summary, DEX-treated $GR^{dim/dim}$ mice, but not WT mice, retain several-fold more FAs derived from DNL in TG in both inguinal and epididymal adipose depots compared to vehicle-treated $GR^{dim/dim}$ mice.

In the Absence of DEX, $GR^{dim/dim}$ Mice Are Less Insulin Sensitive than WT Mice

The decrease in SI in response to DEX was statistically significant in WT mice, but not in $GR^{dim/dim}$ mice (Figure 5D). However, both WT and $GR^{dim/dim}$ mice had approximately the same SI when treated with DEX. DEX treatment mainly affected insulin levels (Figure 5B), and didn't affect glucose levels (Figure 5A) or the percentage of the oral glucose load metabolized to water (Figure 5C). $GR^{dim/dim}$ mice had significantly lower glucose levels compared to WT, independent of DEX treatment (Figure 5A). Because baseline insulin levels were slightly higher in $GR^{dim/dim}$ mice relative to WT (Figure 5B), vehicle-treated SI was lower in $GR^{dim/dim}$ mice than in WT. Thus, DEX treatment resulted in increases in insulin levels in both genotypes, without changes in glucose levels, and similar SI values in both genotypes. While one interpretation could be that $GR^{dim/dim}$ mice are protected from GC-induced decreases in SI, the results are also consistent

with the conclusion that $GR^{dim/dim}$ mice are less insulin sensitive than WT mice at baseline, and both genotypes are rendered equally insulin resistant when treated with DEX.

It has been previously demonstrated that physiological concentrations of corticosterone inhibit glucose-stimulated insulin secretion in isolated islets from mice (Lambillotte et al., 1997). Based on this previous work and our observations that plasma insulin levels are slightly higher and blood glucose levels are slightly lower at baseline in $GR^{dim/dim}$ mice compared to WT mice, we speculate that GC-dependent inhibition of glucose-stimulated insulin secretion may be dependent on GR homodimerization. When DEX is administered, however, peripheral insulin resistance dominates, the pancreas secretes approximately equal amounts of insulin to compensate, and SI is similar in both genotypes.

Chronically Elevated GCs in $GR^{dim/dim}$ Mice Results in Runting

The severe runting and lethality of CRH-Tg^{+}, $GR^{dim/dim}$ mice suggests a gain of function property of the $GR^{dim/dim}$ mutation, given that this phenotype is not seen in either $GR^{dim/dim}$ mice with normal corticosterone levels or $GR^{+/+}$ mice that are CRH-Tg^{+}. This may be due to the mixed gain and loss of function of the $GR^{dim/dim}$ mutation. The mutation was originally described as being pure loss of function for transactivation of reporter constructs (Reichardt et al., 1998). However, careful analysis of several target genes has revealed potential gain of function properties of the $GR^{dim/dim}$ mutation, as a subset of genes were hyperactivated in U2OS cells overexpressing GR-dim vs. WT GR (Rogatsky et al., 2003). This does not appear to be an overexpression artifact, as the same phenomenon has been observed with endogenous levels of GR (Frijters et al.). Microarray analysis of liver from WT and $GR^{dim/dim}$ mice revealed that in addition to genes that were activated by glucocorticoids in WT but not $GR^{dim/dim}$ mice (GR dimerization-dependent) there was a subset of genes that were induced equally by DEX in both genotypes (GR dimerization-independent), and also a set of genes that were activated in the livers of $GR^{dim/dim}$ mice but not WT mice by DEX ((Frijters et al.) and C. Harris, unpublished observations). We propose the term, "rogue" targets for genes that are up-regulated by DEX in $GR^{dim/dim}$, but not in $GR^{+/+}$. These genes cannot be definitely labeled as GR primary targets without first performing chromatin precipitation experiments, but the early timepoints used favor detection of primary GR targets. Furthermore, the runting of CRH-Tg^{+}, $GR^{dim/dim}$ mice may be due to "rogue" gene activation, because it did not occur in $GR^{dim/dim}$ mice with normal corticosterone levels. We suspect that "rogue" gene activation occurs in a tissue-specific manner, but do not know which tissue or "rogue" genes are responsible for the runting of CRH-Tg^{+}, $GR^{dim/dim}$ mice. Whether the mixed function of the $GR^{dim/dim}$ allele applies to repression as well as transactivation is an open question.

Implications for SGRMs

Much attention has been focused on the search for SGRMs that would dissociate the therapeutic anti-inflammatory effects from the adverse metabolic effects. The $GR^{dim/dim}$ mouse has the promise of being a useful model for dissociating GC action at the level of GR instead of the ligand. The fact that the $GR^{dim/dim}$ mutation can result in gain of function gene expression as well as in mediating GC-induced physiological effects to a greater or lesser extent than WT GR is instructional in the search for SGRMs. In addition to having the beneficial properties of not activating certain subsets of GR targets that mediate adverse effects, it is possible that SGRMs

might activate genes not normally activated by non-dissociated GCs, such as the physiological ligand, cortisol (corticosterone in mice). Therefore, it will be important to assess the tissue-specific effects of all potential SGRMs on global transcription and GC-dependent metabolic pathways.

Acknowledgements: We thank Günther Schütz for $GR^{dim/dim}$ mice and Mary Stenzel-Poore for $CRH\text{-}Tg^{+}$ mice. We thank members of the laboratories of Marc Hellerstein, Robert V Farese Jr and Keith Yamamoto for helpful suggestions. This work was supported bythe UCSF Diabetes, Endocrinology and Metabolism Training Grant NIDDK DK07418-27, an NIH career physician-scientist award (KO8-DK081680 to CH), animal facilities grant NIH/NCRR CO6 RR018928, and the J. David Gladstone Institutes.

Tables

	n	Mass	Lean	Fat	Percent Fat
WT, young-Pre	11	21.6 ± 1.2	17.7 ± 0.9	2.7 ± 0.2	13.3 ± 1.0
WT, young-Veh	6	24.6 ± 1.9	19.3 ± 2.2	2.7 ± 0.3	12.1 ± 1.6
WT, young-Dex	5	21.1 ± 1.1	16.1 ± 1.2	2.8 ± 0.4	15.1 ± 1.8
DIM, young-Pre	10	22.1 ± 1.8	18.1 ± 1.6	3.4 ± 0.7*	15.7 ± 3.0*
DIM, young-Veh	5	24.3 ± 1.8	19.1 ± 2.0	3.2 ± 0.3	15.0 ± 1.3
DIM,young-Dex	5	22.7 ± 1.5	17.4 ± 1.3	3.6 ± 0.5**	16.5 ± 1.8**
WT, older	12	29.2 ± 2.0	23.1 ± 1.9	4.3 ± 1.1	15.7 ± 3.8
DIM, older	13	30 ± 2.6	22.8 ± 1.5	5.8 ± 1.4*	20.2 ± 3.3*

Table 1: Body composition in 8-week-old (young) and 4-month-old (older) WT and $GR^{dim/dim}$ mice. WT, wildtype; DIM, $GR^{dim/dim}$; Pre, before treatment; Veh, after one week of treatment with vehicle; Dex, after one week of treatment with dexamethasone. Data are shown as mean ± S.D. *, $P < 0.05$ from WT. **, $P < 0.05$ from Vehicle by t test.

		Inguinal depot			Epididymal depot		
Group	n	Fat pad mass (mg)	Fraction new TG/week (f)	Fraction new palmitate/ wk (f)	Fat pad mass (mg)	Fraction new TG/week (f)	Fraction new palmitate /wk (f)
WT, Veh	13	248 ± 78	0.35 ± 0.14	0.21 ± 0.12	421 ± 167	0.19 ± 0.06	0.08 ± 0.05
WT, Dex	14	372 ± 221	0.40 ± 0.16	0.24 ± 0.13	638 ± 400	0.25 ± 0.07*	0.12 ± 0.07
DIM, Veh	13	353 ± 116	0.29 ± 0.16	0.16 ± 0.14	728 ± 253	0.15 ± 0.09	0.07 ± 0.10
DIM, Dex	14	534 ± 95**	0.40 ± 0.09	0.33 ± 0.10**	964 ± 311	0.29 ± 0.05***	0.24 ± 0.07***

Table 2: Fat pad mass and fractional synthesis in 4-month-old wildtype (WT) and $GR^{dim/dim}$ (DIM) mice treated with vehicle (Veh) or dexamethasone (Dex) and labeled with heavy water. Data are shown as mean ± S.D. *, $P < 0.05$; **, $P < 0.01$; ***, $P < 0.001$ compared to vehicle of same genotype by 2-way ANOVA followed by Bonferroni posttests.

Figures

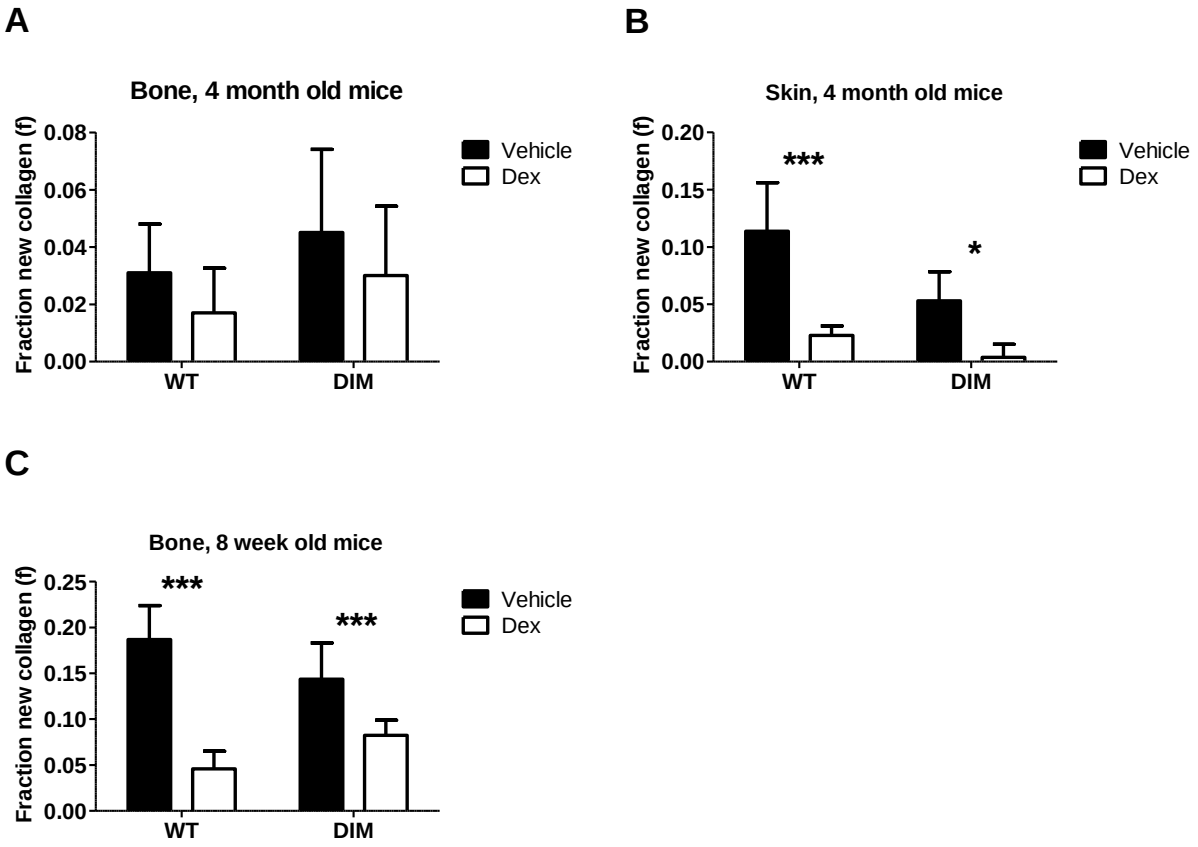

Figure 1: Fractional synthesis rates (f) of collagen (hydroxyproline) in bone in 4-month-old and 8-week-old cohorts and in skin in a 4-month-old cohort of wildtype (WT) and $GR^{dim/dim}$ (DIM) mice. n = 13 for each vehicle-treated 4 month old group, n = 14 for each dexamethasone (DEX)-treated 4 month old group, n = 6 for the vehicle-treated WT 8 week old group, and n = 5 for the other three 8 week old groups. Data are shown as mean ± S.D. *, $P < 0.05$; **, $P < 0.01$; ***, $P < 0.001$ between vehicle and DEX-treated groups within genotypes by two-way ANOVA followed by Bonferroni posttests. A. Bone collagen fractional synthesis in 4 month old mice. Interaction effect was not significant ($P > 0.05$, two-way ANOVA). B. Bone collagen fractional synthesis in 8 week old mice. WT mice were significantly more sensitive to DEX (Interaction $P < 0.01$, two-way ANOVA). C. Skin collagen fractional synthesis in 4 month old mice. WT mice were significantly more sensitive to DEX (Interaction $P < 0.01$, two-way ANOVA).

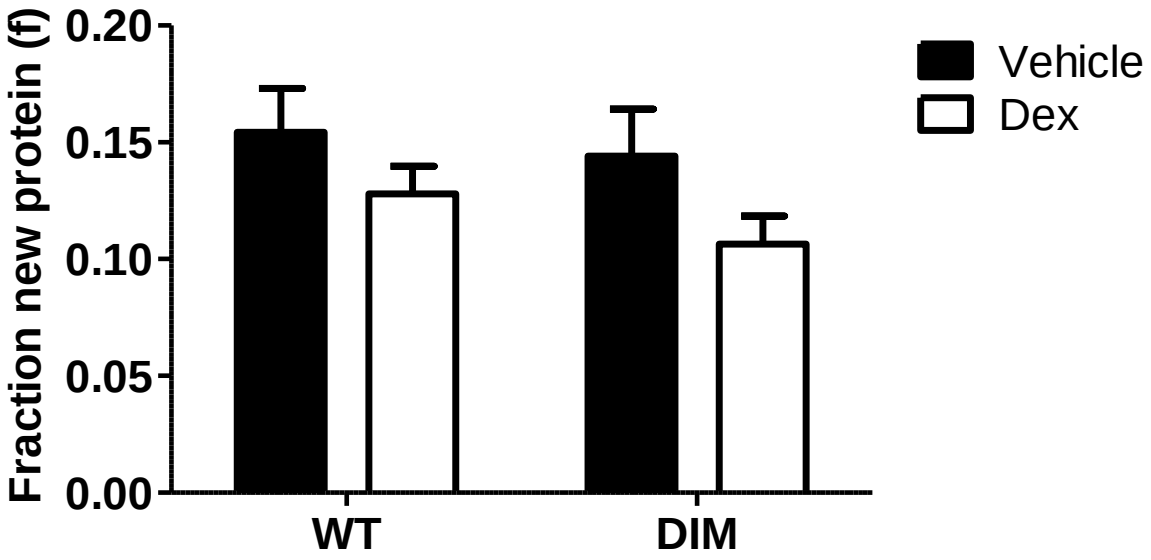

Figure 2: Fractional synthesis rates (f) of muscle protein (alanine) in skeletal muscle (quadriceps) of wildtype (WT) and $GR^{dim/dim}$ (DIM) mice. n = 13 for each vehicle-treated 4 month old group, n = 14 for each dexamethasone (DEX)-treated 4 month old group, n = 6 for the vehicle-treated WT 8-week-old group, and n = 5 for the other three 8-week-old groups. Data are shown as mean ± S.D. *, $P < 0.05$; **, $P < 0.01$; ***, $P < 0.001$ between vehicle and DEX-treated groups within genotypes by two-way ANOVA followed by Bonferroni posttests. Interaction effect was not significant ($P > 0.05$, two-way ANOVA).

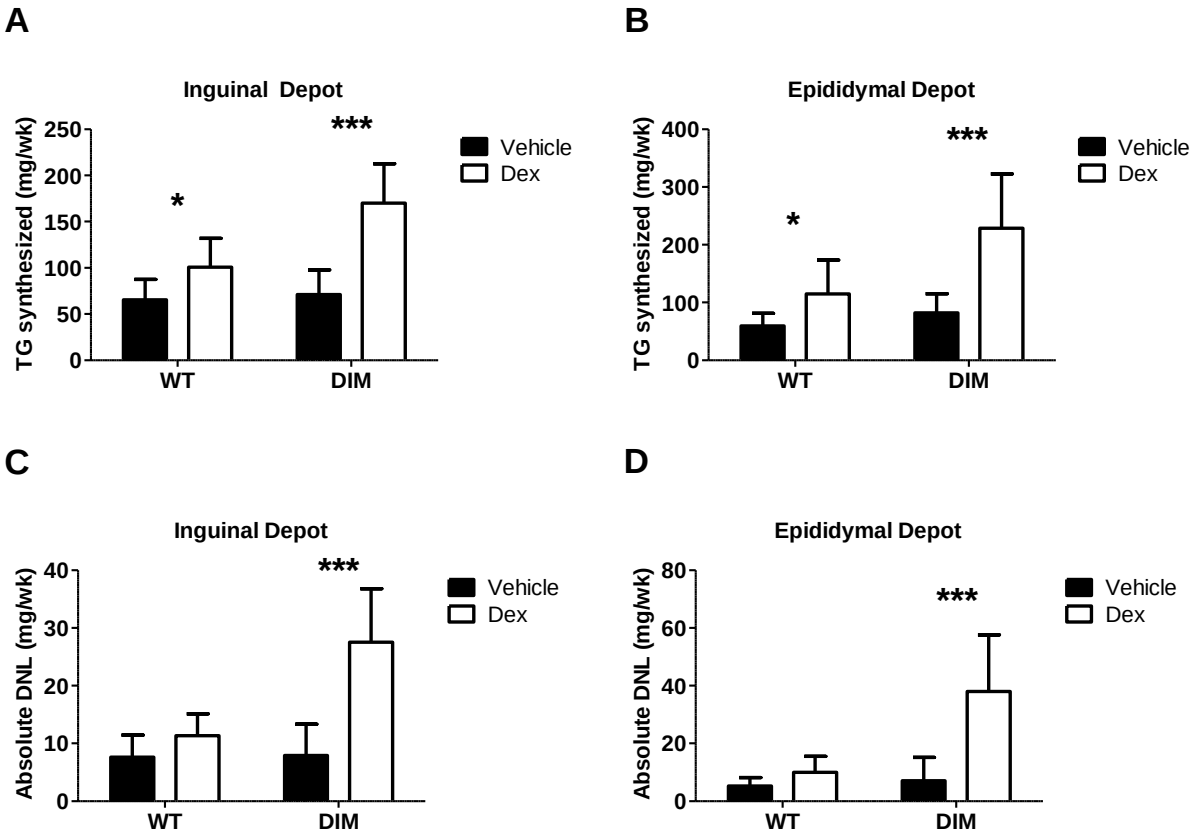

Figure 3: Absolute triglyceride (TG) synthesis and de novo lipogenesis (DNL) in inguinal and epididymal fat pads of 4 month old wildtype (WT) and $GR^{dim/dim}$ (DIM) mice. n = 13 for each vehicle-treated group, n = 14 for each dexamethasone (DEX)-treated group. Data are shown as mean ± S.D. *, $P < 0.05$; ***, $P < 0.001$ between vehicle and DEX-treated groups within genotypes by two-way ANOVA followed by Bonferroni posttests. A. Absolute TG synthesis in the inguinal depot. $GR^{dim/dim}$ mice were significantly more sensitive to DEX (Interaction $P < 0.001$, two-way ANOVA). B. Absolute TG synthesis in the epididymal depot. $GR^{dim/dim}$ mice were significantly more sensitive to DEX (Interaction $P < 0.01$, two-way ANOVA). C. Absolute DNL in the inguinal depot. $GR^{dim/dim}$ mice were significantly more sensitive to DEX (Interaction $P < 0.001$, two-way ANOVA). D. Absolute DNL in the epididymal depot. $GR^{dim/dim}$ mice were significantly more sensitive to DEX (Interaction $P < 0.001$, two-way ANOVA).

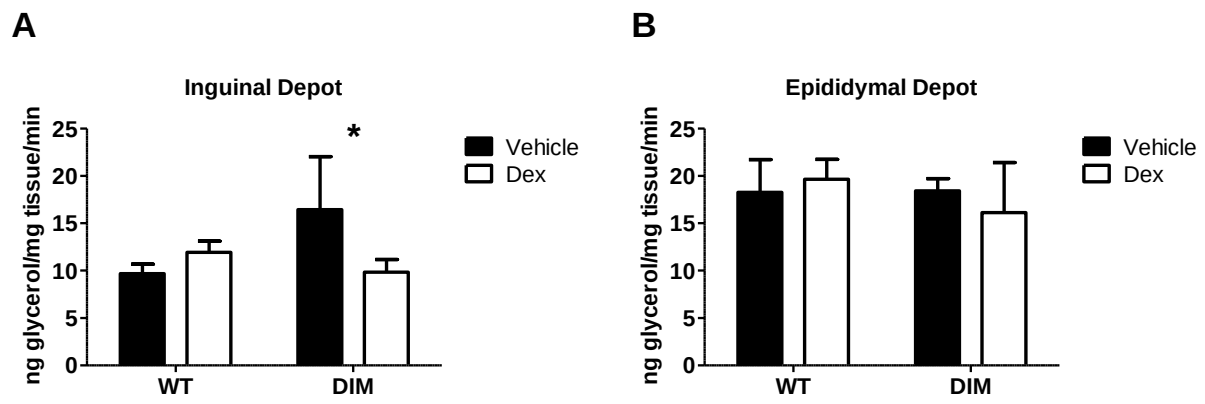

Figure 4: Ex vivo rates of lipolysis in inguinal (A) and epididymal (B) fat depots of wildtype (WT) and $GR^{dim/dim}$ (DIM) mice. Rates of lipolysis were measured in dissected fat as mass (ng) of glycerol released into the surrounding media per mg of adipose tissue per minute. n = 4 per group. *, $P < 0.05$ between vehicle and dexamethasone (DEX)-treated groups within genotypes by two-way ANOVA followed by Bonferroni posttests. $GR^{dim/dim}$ mice were significantly more sensitive to DEX in the inguinal depot only (Interaction $P < 0.05$, two-way ANOVA).

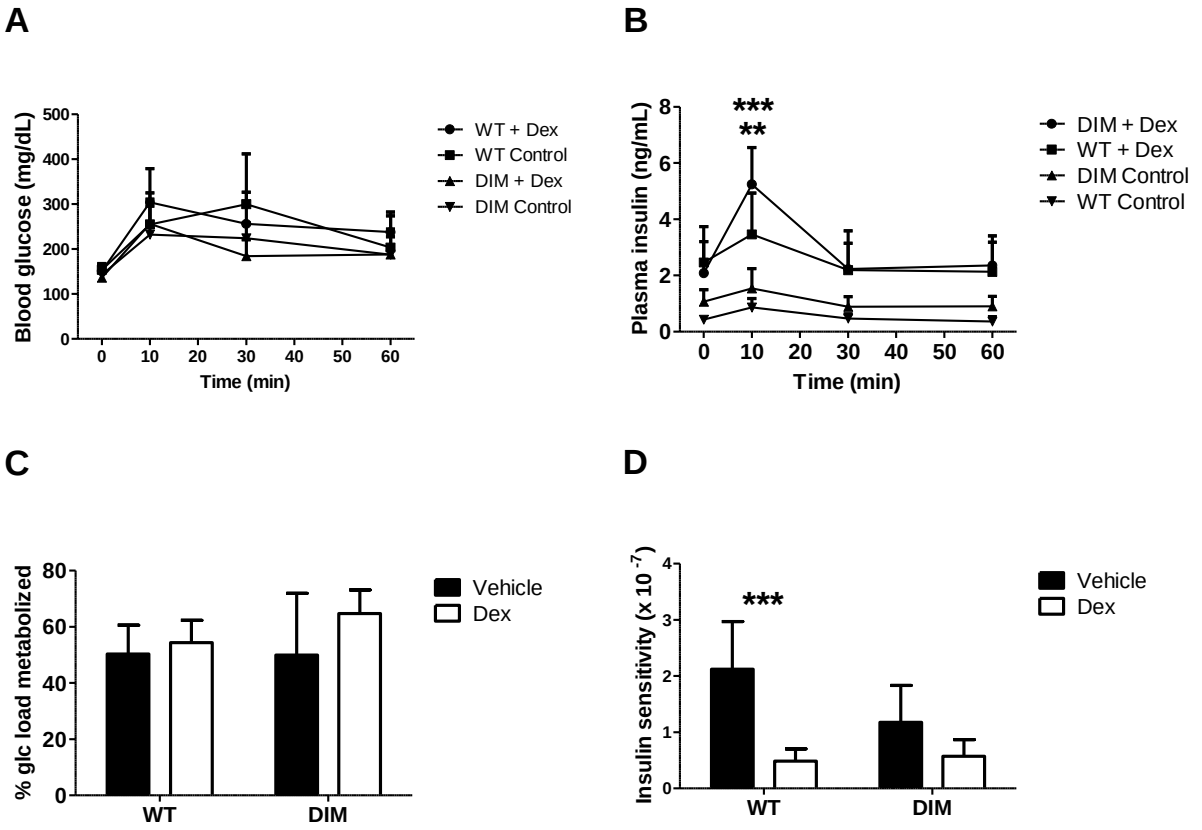

Figure 5: Glucose disposal test, a modified oral glucose tolerance test. Blood glucose concentrations, plasma insulin concentrations, percentage of orally-administered glucose load absorbed by peripheral tissues and metabolized to water (% glc load metabolized), and insulin sensitivity index, calculated % glc load metabolized divided by the product of plasma insulin AUC and blood glucose AUC. n = 7 per group. Data are shown as mean ± S.D. **, $P < 0.01$; ***, $P < 0.001$ between vehicle and dexamethasone (DEX)-treated groups within genotypes by two-way ANOVA followed by Bonferroni posttests. A. Blood glucose concentrations throughout the test. $GR^{dim/dim}$ groups had on average significantly lower blood glucose than WT groups (main effect of genotype $P < 0.05$, two-way ANOVA). Interaction effect was not significant ($P > 0.05$, two-way ANOVA). B. Plasma insulin concentrations throughout the test. Interaction effect was not significant ($P > 0.05$, two-way ANOVA). C. Percent glucose load metabolized to water. Interaction effect was not significant ($P > 0.05$, two-way ANOVA). D. Insulin sensitivity index. WT mice were significantly more sensitive to DEX (Interaction $P < 0.05$, two-way ANOVA).

Chapter 4: CRH-trangenic Mice Exhibit Increased Fluxes Through Adipose Tissue Triglyceride Synthesis Pathways

Abstract

Glucocorticoids are extremely potent anti-inflammatory and immunomodulatory therapies, but their clinical use is limited due to their severe side effects, including osteoporosis, muscle wasting, fat redistribution, and skin thinning and increased susceptibility to bruising. While these endpoint phenotypic changes associated with chronically-elevated exposure to glucocorticoids are widely known, the relative time of onset and persistence of glucocorticoid-induced alterations in key regulatory pathways responsible for these phenotypic changes remain poorly characterized. In chapters 2 and 3, we reported on the acute effects of prednisolone on bone and skin collagen synthesis, muscle protein synthesis, and adipose tissue triglyceride dynamics in young mice using a method that combines heavy water labeling with mass spectrometry to measure fluxes through these glucocorticoid-responsive pathways. In this study we combine this method for measuring kinetics with methods for measuring body composition, and we apply these techniques to characterize these pathways in CRH-Tg^{+} mice. CRH-Tg^{+} mice are exposed to chronically-elevated, endogenously-produced corticosterone, and have a phenotype that closely mimics Cushing's disease in humans. We then compared the results of this study to those of our previous studies to draw conclusions about how glucocorticoids act on these pathways over time. In bone and skin fractional collagen synthesis rates were dramatically inhibited by acute administration of prednisolone in young mice, but in CRH-Tg^{+} mice, which had reduced bone mass and thinner skin compared to controls, fractional collagen synthesis rates were only modestly lower in bone and are similar in skin compared to controls. In muscle, fractional synthesis of total muscle protein was not dramatically inhibited by either acute or chronic exposure to glucocorticoids, although CRH-Tg^{+} mice had measurably less muscle mass relative to controls. In adipose tissue we previously observed no remarkable changes in TG dynamics in young mice given an acute dose of prednisolone, but in CRH-Tg^{+} mice we observed more TG synthesis in subcutaneous and abdominal fat depots, more DNL in the abdominal depot only, more TG accumulation in both fat depots and no difference in glyceroneogenesis in either depot compared to controls. We conclude that degradation, rather than synthesis, pathways are mostly responsible for glucocorticoid-induced decreases in muscle mass, that increased futile cycling between triglycerides and free fatty acids occurs in both abdominal and subcutaneous fat depots in CRH-Tg^{+} mice, and in these mice triglyceride accumulation is favored over net lipolysis. Moreover, the metabolic consequences of chronic, endogenous glucocorticoid excess are different from the effects of acute, exogenous glucocorticoid administration.

Abbreviations

Glucocorticoid: GC; phosphoenolpyruvate-carboxykinase: PEP-CK; triglycerides: TG; free fatty acids: FFA; *de novo* lipogenesis: DNL; selective glucocorticoid receptor modulator: SGRM; corticotropin-releasing hormone: CRH; hypothalamic-pituitary-adrenal: HPA; adrenocorticotropic hormone: ACTH; dual energy X-ray absorptiometry: DEXA; gas chromatography-mass spectrometry: GC-MS; mass spectrometry: MS; negative chemical ionization: NCI; mass-to-charge: m/z; selected ion monitoring: SIM; fatty acids: FA; excess M_1 isotopomer: EM_1

Introduction

Glucocorticoids (GCs) are among the most potent therapies known to treat inflammatory and autoimmune diseases, but their clinical utility is limited by a myriad of undesirable side effects. Negative effects associated with long term use of GCs include osteoporosis, skin thinning and increased bruisability, muscle wasting, fat redistribution, hypertension and insulin resistance (Stanbury and Graham, 1998). GCs have been shown to cause both decreased bone formation and increased bone resorption in humans and rodents (LoCascio et al., 1990; O'Brien et al., 2004; Weinstein et al., 1998). Reduction in bone collagen synthesis is a primary mechanism by which GCs decrease bone mass (Canalis, 2003). Topical GCs have been shown to rapidly and dramatically decrease rates of skin collagen synthesis in humans (Autio et al., 1994; Haapasaari et al., 1996). GCs have been shown to induce muscle wasting through direct effects on muscle protein breakdown and synthesis, as well as through indirect effects on whole body glucose metabolism and insulin and IGF-1-dependent pathways (Long et al., 2001; Louard et al., 1994; Odedra et al., 1983). In humans with Cushing's disease, characterized by chronically high levels of endogenously-produced GCs, undesirable fat redistribution occurs with loss of adipose from subcutaneous depots and accumulation in the abdomen, around the face, and behind the neck (Besser and Edwards, 1972). It has been previously shown that GCs decrease glyceroneogenesis in the white adipose tissue via inhibition of phosphoenolpyruvate-carboxykinase (PEP-CK), and increase glyceroneogenesis in the liver via induction of PEP-CK (Hanson and Reshef, 2003). It has also been shown that glyceroneogenesis plays a crucial role in cycling between triglycerides (TG) and free fatty acids (FFA) in these tissues (Reshef et al., 2003). In addition, GCs have recently been implicated in obesity and in the metabolic syndrome (Walker, 2006). While the many effects of GCs have been studied for over 50 years, rarely have they been studied in an animal model that simultaneously mimics several effects of chronic GC exposure as they manifest in a human.

While the endpoint phenotypic changes in response to chronically-elevated exposure to GCs are widely known, the relative time of onset and persistence of GC-induced alterations in key regulatory pathways responsible for the different phenotypic changes remain poorly characterized. Previously, we characterized multiple effects of short-term treatment with prednisolone concurrently in 8-week-old mice using an approach that combined heavy water labeling with mass spectrometry (Roohk et al.). We reported that prednisolone dramatically reduced bone and skin collagen synthesis, markedly increased insulin resistance, slightly reduced muscle protein synthesis, and had little or no effects on adipose tissue TG dynamics, including TG synthesis, lipolysis, *de novo* lipogenesis (DNL), and glyceroneogenesis after one week of treatment. While our previous study revealed relatively rapid-onset changes in specific key pathways affected by GCs, it was unclear whether or not these effects observed throughout the first week of exposure to GCs would persist after chronic exposure (weeks to months) to GCs. Also unclear was whether or not chronic GC exposure would affect tissues in which we saw little or no effects after one week of GC exposure, but in which we would expect to see marked changes in response to GC exposure, such as adipose and muscle tissue. These are important issues to address given that mice are used as preclinical model for the effects of GCs in man. Although GCs have been used to treat inflammatory conditions for more than 60 years (Hench et al., 1949), newer, improved selective glucocorticoid receptor modulators (SGRMs) with safer adverse effect profiles continue to be tested.

In order to study the effects of chronic GC exposure, we obtained CRH-Tg^{+} mice as a model of chronic GC excess that closely parallels Cushing's disease in humans. CRH-Tg^{+} mice carry a transgene of rat corticotropin-releasing hormone (CRH) genomic sequence driven by the mMT-1 metallothionein promoter (Stenzel-Poore et al., 1992). CRH-Tg^{+} mice exhibit centrally-derived overstimulation of the hypothalamic-pituitary-adrenal (HPA) axis, and have 5-fold elevated adrenocorticotropic hormone (ACTH) compared to baseline levels, and 10-fold elevated corticosterone compared to baseline levels (Stenzel-Poore et al., 1992; Stenzel-Poore et al., 1996). The obesity of CRH-Tg^{+} mice is caused by elevated plasma corticosterone, rather than the effects of elevated CRH or ACTH on peripheral tissues, as the obese phenotype is reversed with adrenalectomy (Shinahara et al., 2009).

In the present study, we characterized multiple effects of chronic, lifetime exposure to elevated endogenous GCs using a heavy water labeling approach combined with mass spectrometry (Busch et al., 2006; Gardner et al., 2007; Roohk et al.; Turner et al., 2007). We used this heavy water labeling approach to quantify rates of retained collagen synthesis in bone and skin; as well as the rate of mixed muscle protein synthesis in skeletal muscle; and TG synthesis, DNL, and glyceroneogenesis in subcutaneous and abdominal fat depots and in liver. We also performed body composition analysis using dual energy X-ray absorptiometry (DEXA) and microCT. Using DEXA, we quantified lean and fatty tissue mass, as well as bone area, bone mass, and bone mineral density. Using microCT, we imaged sections of long bone and quantitatively compared differences in cortical bone mass in CRH-Tg^{+} and wildtype mice.

Methods

Animals

All mice were bred from CRH-Tg^{+} males donated by Mary-Stenzel Poore (OHSU, Portland, OR). CRH-Tg^{+} mice were C57Bl/6 mice back-crossed for several generations onto a C57Bl/6 background. Since CRH-Tg^{+} females are not fertile, male CRH-Tg^{+} males were mated to wildtype C57BL/6 mice. CRH-Tg^{+} and wildtype littermates were housed in groups of no more than 5 under temperature-controlled conditions with a 12 h light/12 h dark cycle. Mice were fed PicoLab Rodent Diet 20, 5053 (LabDiet, 3.41 kCal/gm, percent calories from protein, fat, and carbohydrate is 24.7, 13.2, and 62.1 respectively) diet *ad libitum*. All studies received prior approval from the Animal Care and Use Committee at UCSF.

Body composition analysis

Body composition analysis was performed using DEXA (Lunar Piximus). Mice were anesthetized with isoflurane during DEXA scanning. The head region was excluded from analysis using the region of interest feature of Piximus software.

MicroCT

The distal femur was scanned in vivo and analyzed using a Scanco VivaCT 40 (Scanco Medical) microCT as previously described (Halloran et al.).

Ear skin thickness

Ear skin thickness in adult wildtype and CRH-Tg^{+} mice was measured using a Mitutoyo micrometer.

Heavy water ($^{2}H_2O$) labeling protocol

Eight CRH-Tg^{+} mice and 6 wildtype littermates (all male, 14 weeks old) were labeled with $^{2}H_2O$ throughout the study as described elsewhere (Neese et al., 2002). Briefly, mice were given a priming intraperitoneal bolus injection of 99.9% $^{2}H_2O$ (Cambridge Isotope Lab, Andover, MA) containing 0.9% w/v sodium chloride to raise the $^{2}H_2O$ concentration in body water to approximately 5%. Body $^{2}H_2O$ enrichments of approximately 5% were then maintained by *ad libitum* administration of 8% $^{2}H_2O$ drinking water throughout the 7 day labeling period, as described previously (Busch et al., 2007; Roohk et al.).

Tissue Collection

Mice were anesthetized using isofluorane. Blood was collected for $^{2}H_2O$ analysis by cardiac puncture and stored in heparin-coated tubes on ice until plasma could be isolated by centrifugation. Once isolated, plasma was stored at -80^{o}C until further use. Epididymal and inguinal adipose tissue depots and the liver were completely removed and weighed. A piece of the left and right quadriceps muscles, a dorsal skin flap, and both femurs were dissected. Tissues to be used for stable isotope studies were flash frozen in liquid nitrogen, and stored in tubes on dry ice then subsequently at -80^{o}C until further use.

Measurement of body ^2H_2O enrichment in heavy water labeling studies

Aliquots of plasma (50-100 µL) in the cap of an inverted vial were placed in a 70^{o}C glass bead bath to collect water distillate. ^{2}H enrichment was measured in water distillate using gas chromatography-mass spectrometry (GC-MS) after conversion to tetrabromoethane, as described in detail elsewhere (Collins et al., 2003; Roohk et al.; Turner et al., 2003).

Measurement of hydroxyproline enrichments in bone and skin by GC-MS

L-4-(O-tert-butyldimethylsilyl)-hydroxyproline pentafluorobenzyl ester was prepared from bone and skin and analyzed by GC-MS as previously described (Gardner et al., 2007; Roohk et al.). Briefly, femurs were perfused with PBS as previously described (Macallan et al., 1998). Total protein was isolated from homogenized whole femur or dorsal skin flaps. Total protein was then hydrolyzed, and amino acids were derivatized. Compounds were resolved on a DB-225 column. Mass spectrometry (MS) was performed in negative chemical ionization (NCI) mode with helium as the carrier gas, and mass-to-charge (m/z) ratios 424-426 corresponding to the M_0, M_1, and M_2 mass isotopomers of derivatized hydroxyproline were analyzed by selected ion monitoring (SIM).

Measurement of alanine enrichments from quadriceps mixed muscle proteins by GC-MS

Pentafluorobenzyl-*N*,*N*-di(pentafluorobenzyl)-alanine (PFB-Ala) was prepared from skeletal muscle and analyzed by GC-MS as previously described (Busch et al., 2006; Roohk et al.). Briefly, total protein was isolated from homogenized quadriceps. Total protein was then hydrolyzed, and amino acids were derivatized. Compounds were resolved on a DB-225 column. MS was performed in NCI mode with helium as the carrier gas, and m/z ratios 448-450 corresponding to the M_0, M_1, and M_2 mass isotopomers were analyzed by SIM.

Measurement of glycerol and palmitate enrichments in triglycerides by GC-MS

TG-glycerol and fatty acids (FA) were isolated from adipose tissue and liver and analyzed by GC-MS as described previously (Bruss et al.; Roohk et al.; Turner et al., 2003; Turner et al., 2007). Briefly, lipids were extracted in chloroform-methanol (2:1) by the Folch technique and trans-esterified by incubation with 3 N methanolic HCl (Sigma-Aldrich, St-Louis, MO). Separated TG-glycerol was converted to glycerol-triacetate, and was analyzed under chemical ionization conditions by SIM of m/z ratios 159-161 (representing M_0-M_2). Separated FA-methyl esters were analyzed under electron impact ionization conditions with SIM of m/z ratios 270-272 (representing M_0-M_2) of palmitate-methyl ester.

Calculation of fractional synthesis of tissue collagen, muscle proteins, glycerol, and palmitate

Fractional synthesis (f), or fraction new collagen, protein, palmitate, or triglycerides synthesized during the labeling period, was calculated for each analyte as the ratio of the measured excess M_1 isotopomer (EM_1) to the asymptotic value of EM_1 ($EM_{1,max}$) as previously described (Busch et al., 2006; Neese et al., 2001; Roohk et al.). This calculation for f can be summarized using the following formula:

$$f = EM_{1(sample)} / EM_{1,max}$$

$EM_{1(sample)}$, meaning enrichment of M_1 isotopomers in excess of that which occurs in nature, is calculated for each analyte using the abundances of the M_0, M_1, and M_2 mass isotopomers as measured in the sample and in an unenriched standard by GC-MS using the following formula:

$$EM_{1(sample)} = [M_1 / (M_0 + M_1 + M_2)]_{sample} - [M_1 / (M_0 + M_1 + M_2)]_{standard}$$

$EM_{1,max}$ was calculated for each analyte in each animal from the measured body ^2H_2O enrichment, as described previously (Busch et al., 2006; Hellerstein and Neese, 1999), and represents the calculated EM_1 of the fully-turned-over analyte at the body ^2H_2O enrichment measured in the animal.

Calculation of TG synthesis rates

Absolute TG synthesis rates in inguinal and epididymal fat depots were calculated as previously described (Roohk et al.; Turner et al., 2003; Varady et al., 2007b). Briefly, absolute synthesis rates of adipose TG were calculated from fractional TG synthesis (f) multiplied by adipose TG mass multiplied by a correction factor (0.9) for the fractional mass of TG in adipose tissue:

Absolute synthesis (g/wk) = f_{TG} x adipose TG mass (g) x (0.9).

Calculation of absolute rates of *de novo* lipogenesis

Absolute rates of DNL in inguinal and epididymal fat depots was calculated as previously described (Bruss et al.; Roohk et al.). Briefly, absolute rates of DNL were calculated from fractional palmitate synthesis (f), adipose TG mass, the fraction of TG mass in adipose tissue (0.9), and the fraction of palmitate relative to other fatty acids in TG using the following formula:

Absolute DNL (g/wk) = f_{DNL} x adipose TG mass (g) x fraction TG x fraction TG-palmitate,

The fraction of TG-palmitate present in adipose TG was taken to be 20% (Jung et al., 1999; Pouteau et al., 2008).

Measurement of glyceroneogenesis in adipose tissue and liver

The relative contribution of glyceroneogenesis versus glycolysis to TG-glycerol (% glyceroneogenesis) was calculated using MIDA algorithms and M_0, M_1, and M_2 isotopomer data from derivatized TG-glycerol as measured by GC-MS as previously described (Chen et al., 2005; Hellerstein and Neese, 1999; Roohk et al.; Turner et al., 2003).

Statistical Analyses

Statistical analyses were performed using GraphPad Prism 5 (Graphpad Software Inc, La Jolla, CA). Unpaired t tests were performed for each parameter to assess statistically significant differences between wildtype and CRH-Tg^+ groups. To assess statistically significant differences between more than two groups for a single parameter, specifically for percent glyceroneogenesis

in inguinal fat, epididymal fat, and liver for both genotypes, one-way ANOVA was performed followed by Tukey's posttests. $P < 0.05$ was considered to be significant for all tests.

Results

Body weights and body composition

CRH-Tg$^+$ mice weighed the same as their wildtype littermates (Figure 1A). However, CRH-Tg$^+$ mice had significantly less lean tissue (23.7 ± 1.5 g for wildtype vs. 18.6 ± 2.1 g for CRH-Tg$^+$, $P < 0.001$) and significantly more fat mass (4.8 ± 0.7 g for wildtype vs. 9.6 ± 1.9 g for CRH-Tg$^+$, $P < 0.001$) (Figure 1B), and had approximately twice the percentage of body fat by weight (16.9 ± 1.8% for wildtype vs. 33.8 ± 2.6%, $P < 0.001$, Figure 1B) as measured by DEXA. In summary, CRH-Tg$^+$ mice weighed the same as their wildtype littermates, but had significantly less lean tissue and significantly more fat mass.

Bone parameters

Using microCT we saw that CRH-Tg$^+$ mice had less bone mass in the femur (Figure 2), and using DEXA we found that CRH-Tg$^+$ mice had significantly less bone mineral content (0.450 ± 0.021 g for wildtype vs. 0.320 ± 0.032 g for CRH-Tg$^+$, $P < 0.001$), less bone area (8.67 ± 0.31 cm^2 for wildtype vs. 6.81 ± 0.47 cm^2 for CRH-Tg$^+$, $P < 0.001$), and lower bone mineral density (0.512 ± 0.018 g/cm^2 for wildtype vs. 0.470 ± 0.017 g/cm^2 for CRH-Tg$^+$, $P < 0.001$) than their wildtype littermates (Figure 3A-C). Using our heavy water labeling approach combined with mass spectrometry we found that CRH-Tg$^+$ mice had fractional rates of bone collagen synthesis that were significantly lower (5.9 ± 2.0% for wildtype vs. 3.8 ± 1.4% for CRH-Tg$^+$, $P < 0.05$) by approximately one third compared to their wildtype littermates (Figure 3D). Thus, CRH-Tg$^+$ mice had less bone mass and synthesized bone collagen at a slower fractional rate compared to wildtype mice.

Skin parameters

We used ear skin thickness as a marker for the effects of GCs on total body skin thickness (Halloran et al.). The ear skin of CRH-Tg$^+$ mice was 19% thinner than that of wildtype mice (188+/-15 microns for wildtype vs. 153+/-14 microns for CRH-Tg$^+$, $P < 0.0001$, Figure 4A). Using our heavy water labeling approach combined with mass spectrometry, we found that CRH-Tg$^+$ mice had similar fractional rates of skin collagen synthesis in a dorsal skin flap as their wildtype littermates (10.3 ± 2.1% for wildtype vs. 11.0 ±1.8% for CRH-Tg$^+$, Figure 4B). Thus, while CRH-Tg$^+$ mice had thinner skin, they synthesized skin collagen at a similar replacement rate compared to wildtype mice.

Muscle protein synthesis

CRH-Tg$^+$ mice had significantly less lean tissue than wildtype mice (Figure 1). To investigate kinetic differences in muscle proteins after GC-induced differences in lean tissue mass were apparent, we measured rates of protein synthesis of mixed proteins in quadriceps muscle of CRH-Tg$^+$ mice and their wildtype littermates. We did not observe any significant difference in fractional synthetic rates between the two groups (14.4 ± 0.1% for wildtype vs. 13.6 ± 2.6% for CRH-Tg$^+$, Figure 5). Thus, while CRH-Tg$^+$ mice had less whole body lean tissue mass, they synthesized mixed muscle protein from upper hindlimb skeletal muscle at a similar fractional rate as did their wildtype littermates.

Adipose and liver tissue lipid dynamics

We observed more fat accumulation in subcutaneous and abdominal fat depots in CRH-Tg$^+$ mice relative to their wildtype littermates (Table 1). Accordingly, we measured rates of TG synthesis and DNL in inguinal and epididymal fat depots and in liver.

On average, inguinal fat pads were significantly larger ($P < 0.05$) by 3.2 fold in the CRH-Tg$^+$ mice compared to wildtype mice (Table 1). Fractional TG synthesis rates were similar in the inguinal depot of both genotypes (Table 1). By combining fat pad masses with fractional synthesis, we calculated that total retained triglyceride synthesis was 4.0-fold greater (49.8 ± 9.4 mg/wk for wildtype vs. 202 ± 83.6 mg/wk for CRH-Tg$^+$, $P < 0.01$) in the inguinal depots of CRH-Tg$^+$ mice (Figure 6A).

On average, epididymal fat pads were 3.8-fold larger ($P < 0.01$) in CRH-Tg$^+$ mice compared to wildtype mice (Table 1). Fractional TG synthesis rates were 1.9-fold higher ($P < 0.001$) in the epididymal depot of CRH-Tg$^+$ mice than in their wildtype littermates (Table 1). By combining fat pad masses with fractional synthesis, we calculated that total retained TG synthesis was 7.4-fold greater (61.8 ± 17.8 mg/wk for wildtype vs. 456 ± 204 mg/wk for CRH-Tg$^+$, $P < 0.001$) in the epididymal depots of CRH-Tg$^+$ mice compared to wildtype mice (Figure 6B).

Fractional rates of palmitate DNL in the inguinal depots of CRH-Tg$^+$ mice were 62% lower than wildtype ($P < 0.001$) (Table 1). Adjusting for fat pad mass, absolute retained palmitate DNL was similar in the inguinal depots of CRH-Tg$^+$ and wildtype mice (4.8 ± 0.7 mg/wk for wildtype vs. 6.4 ± 2.4 mg/wk for CRH-Tg$^+$, Figure 6C). Thus, CRH-Tg$^+$ mice have larger inguinal fat pads, but the contribution from newly-synthesized FAs via the DNL pathway was lower, and thus the total retained *de novo* palmitate synthesized in the inguinal depot was similar between the two genotypes.

Fractional rates of palmitate DNL in the epididymal depots of both genotypes were similar (Table 1). Adjusting for fat pad mass, absolute retained palmitate DNL in the epididymal depot was 4.1-fold greater (4.3 ± 1.4 mg/wk for wildtype vs. 17.6 ± 6.1 mg/wk for CRH-Tg$^+$, $P < 0.001$) in CRH-Tg$^+$ mice compared to wildtype (Figure 6D).

Fractional TG synthesis rates in the liver were significantly higher ($P < 0.01$) in CRH-Tg$^+$ mice compared to their wildtype littermates (fraction new was 0.72 ± 0.11 in wildtype and 0.91 ± 0.07 in CRH-Tg$^+$). Liver palmitate fractional DNL was not significantly different between the two groups (fraction new was 0.59 ± 0.06 in wildtype and 0.51 ± 0.10 in CRH-Tg$^+$). However, liver TGs, including TG-glycerol and TG-palmitate, were almost fully turned over after one week, making accurate quantitative comparisons of relative fractional rates of liver TG synthesis or liver palmitate DNL impossible.

Because it has been shown that glyceroneogenesis plays a crucial role in TG/FA cycling (Reshef et al., 2003), and that GCs decrease and increase glyceroneogenesis in the adipose tissue and liver, respectively (Hanson and Reshef, 2003), we used mass isotopomer distribution analysis to identify the source of the TG-glyercol in adipose tissue and in liver and expressed this as percent glyceroneogenesis (Chen et al., 2005). Percent glyceroneogenesis indicates what percent of the TG-glycerol came from glyceroneogenic, rather than glycolytic, pathways. Percent

glyceroneogenesis was not significantly different between the two genotypes in either fat depot or in liver (Figure 7). Percent glycerneogenesis was much higher in the liver than either fat pad of both genotypes ($P < 0.001$) (Figure 7). In summary, we observed that TG-glycerol in liver came mostly from glyceroneogenic pathways, while TG-glycerol in white adipose tissue came mostly from glycolytic pathways. Furthermore, chronic exposure to corticosterone did not significantly change the source of TG-glycerol in either tissue.

Discussion

In this study, we used the CRH-Tg$^+$ mouse to characterize the effects of chronic GC exposure on multiple metabolic pathways concurrently. Because these mice have a phenotype that is derived from central HPA axis overstimulation, they are directly comparable to humans with Cushing's disease in that they have centrally-derived GC excess (Shinahara et al., 2009; Stenzel-Poore et al., 1992; Stenzel-Poore et al., 1996). These mice simultaneously exhibit multiple pathologies caused by chronically-elevated GC exposure, so relevant hormonal axes and signaling pathways that crosstalk with the HPA axis are likely intact and involved. Therefore, this model enables us to observe not just cell autonomous effects of GCs, but also integrated, organismal responses to chronic GC excess. To characterize these mice we used a stable isotope method combined with mass spectrometry to measure fluxes through key regulatory pathways (Busch et al., 2006; Gardner et al., 2007; Roohk et al.; Turner et al., 2007). Pathways were chosen based on their relevance to the mechanistic actions of GCs in different tissues (Buttgereit et al., 2005b; Canalis, 2003; Stanbury and Graham, 1998). To quantify end point accumulation or distribution of bone mass, lean tissue mass, and fat mass, we used DEXA. By applying these analytical techniques to the CRH-Tg$^+$ model, we were able to complete an unusually thorough survey of the many effects of chronic GC excess in an animal model that closely mimics multiple pathologies of GC excess in humans.

The endpoint phenotype of CRH-Tg$^+$ mice closely mimics multiple pathologies observed in human patients with Cushing's disease. Although CRH-Tg$^+$ mice weigh the same as their wildtype littermates (Figure 1A), DEXA scan revealed that CRH-Tg$^+$ mice have less lean tissue, more adipose tissue, and less bone mass, bone area, and bone mineral density than their wildtype littermates (Figure 1B). Like humans with Cushing's disease, CRH-Tg$^+$ mice accumulate fat behind the neck, exhibiting the characteristic buffalo hump, as it is sometimes called in humans. Unlike humans with Cushing's disease, however, CRH-Tg$^+$ mice accumulate rather than lose fat in subcutaneous depots, so instead of redistributing fat from subcutaneous depots to other areas of the body as humans do, CRH-Tg$^+$ mice accumulate fat in subcutaneous and abdominal depots (Table 1). We observed that CRH-Tg$^+$ mice also have thinner skin than their wildtype littermates (Figure 4A), just as patients with Cushing's syndrome have thin skin and increased susceptibility to bruising.

Using the heavy water labeling approach combined with mass spectrometry, we were also able to probe the differences in fluxes between CRH-Tg$^+$ mice and their wildtype littermates through key GC-dependent regulatory pathways, specifically bone and skin collagen synthesis, muscle protein synthesis, and TG synthesis, DNL, and glyceroneogenesis in two fat depots and in liver. Collagen synthesis rates are only slightly lower in the bone of CRH-Tg$^+$ mice and not at all lower in skin (Figure 3D and Figure 4B). Using microCT and DEXA to measure bone mass and other bone parameters (Figure 2 and Figure 3A-C), we observed that bone mass and bone mineral density is lower in CRH-Tg$^+$ mice. Using a micrometer to measure ear skin thickness, we also observed that CRH-Tg$^+$ mice have thinner skin compared to wildtype mice (Figure 4A). Our group and other groups have previously shown that bone and skin collagen synthesis rates are dramatically reduced by relatively acute treatment with GCs in rodents and in humans (Autio et al., 1994; Canalis, 2003; Haapasaari et al., 1996; Roohk et al.). After one week of treatment with 30 mg/kg/d of prednisolone, we previously observed collagen synthesis rates in bone and

skin that were half of those observed in vehicle-treated mice. From these data we draw several conclusions. First, collagen synthesis rates drop dramatically in response to acute, high dose exposure to GCs, resulting in retarded bone growth and thinner skin. Second, after chronic exposure to elevated levels of endogenously-produced GCs, bone mass is lower and skin is thinner in CRH-Tg^{+} mice, likely due to decreased amounts of total collagen synthesized, but fractional rates of collagen synthesis are only slightly lower in bone and similar in skin, when compared to wildtype mice because CRH-Tg^{+} mice have less total collagen in these tissues. Several additional possibilities that are not mutually exclusive exist for the differences observed between this study and the previous study, including exposure to endogenous vs. synthetic GCs, chronic vs. acute exposure, age at time of measurement, and, importantly, unmeasured differences in collagen degradation rates. Because this method directly measures rates of synthesis, and changes in rates of degradation can only be indirectly measured by measuring precise changes in pool size, we cannot know how much of a role changes in rates of degradation play in explaining the differences observed.

Rates of skeletal muscle protein synthesis were the same in CRH-Tg^{+} mice and in their wildtype littermates (Figure 5), despite significant differences in endpoint lean tissue mass as measured by DEXA (Figure 1B). Previously, we reported very modest decreases in rates of muscle protein synthesis in mice treated with 30 mg/kg/d of prednisolone for one week (Roohk et al.). Here we showed that CRH-Tg^{+} mice exposed to chronically elevated corticosterone levels had decreased lean mass compared to wildtype mice, and we report that fractional rates of muscle protein synthesis were the same in both genotypes. Thus, we conclude that long-term decreased lean tissue accumulation in response to GCs is most likely due to increased rates of muscle protein degradation, rather than decreased rates of muscle protein synthesis.

We have previously shown that short term treatment with prednisolone does not substantially affect rates of TG synthesis or DNL in subcutaneous or abdominal adipose tissue of 8-week-old mice (Roohk et al.). In 14-week-old CRH-Tg^{+} mice, we observed significant whole body fat accumulation by DEXA and fat accumulation in both subcutaneous and abdominal depots by weighing dissected fat pads. Accordingly, we measured rates of TG synthesis and DNL in subcutaneous and abdominal adipose tissue depots of CRH-Tg^{+} mice. While fractional rates of TG synthesis were only modestly higher in CRH-Tg^{+} mice relative to wildtype mice in the inguinal depot and about twice as high in the epididymal depot, when we incorporated the larger fat pad masses of CRH-Tg^{+} mice, we calculated that the total amount of retained TG synthesized over the 7 day labeling period was several times higher in CRH-Tg^{+} mice in both depots. Relatively high total, retained synthesis and low or similar fractional synthesis rates compared to controls as measured by this technique has been observed in another obesity model, the ob/ob mouse (Turner et al., 2007). Because CRH-Tg^{+} mice do not accumulate fat at a rate several times faster than wildtype mice, we conclude that both synthesis and lipolysis are several times higher in CRH-Tg^{+} mice, indicating that CRH-Tg^{+} mice have increased TG turnover or mobilization, which could also be described as TG/FA futile cycling. Despite the fact that the total amount of TG synthesized was much greater in both depots in the CRH-Tg^{+} mice, the rate of DNL was lower in the subcutaneous depots and similar in the epididymal depots of CRH-Tg^{+} mice compared to wildtype mice. The amount of total retained palmitate synthesized via the DNL pathway was similar in the inguinal depot and 4-fold higher in the epididymal depot of CRH-Tg^{+} mice relative to wildtype mice. DNL accounted for much less of the total TG synthesized in both

depots in the CRH-Tg$^+$ mice, which supports the conclusion of TG/FA futile cycling, as opposed to net increases in retained TG synthesis, accounting for most of the increased TG synthesis as measured by ^{2}H label incorporation. As is discussed in detail elsewhere, (Turner et al., 2003) futile cycling would only be measured by this method as synthesis when TG molecules are fully broken down to FFAs and glycerol and then reesterified, not when cycling between diacylglycerols or monoacylglycerols and TG. This is because ^{2}H label is only incorporated into the glycerol moiety of a TG molecule when labeled α-glycerol phosphate is esterified with 3 fatty acids, and in the adipose tissue it is very unlikely that a glycerol molecule released during lipolysis would immediately be reesterified into a TG molecule without first passing through the α-glycerol phosphate pool.

Although at first glance TG/FA futile cycling may seem inefficient, we propose that it is in fact beneficial in times of stress when energy demand may increase suddenly. In fact, TG/FA futile cycling is part of a previously-hypothesized model of the integrated role of GCs *in vivo* (Macfarlane et al., 2008). According to this model, GCs increase TG/FA futile cycling, thus increasing the potential flux of energy in the form of FFA between adipocytes and the blood. The hormone milieu greatly influences the direction of that flux. In times of fasting and acute stress the hormone milieu, which includes catecholamines and growth hormone, favors lipolysis. During recovery from acute stress and refeeding the hormone milieu, which is dominated by elevated insulin levels, favors TG storage. CRH-Tg$^+$ mice have previously been shown to be hyperinsulinemic (Shinahara et al., 2009), and in the absence of acute environmental stressors, such as frequent handling, injections, temperature variations, or food scarcity, the observation of increased adiposity of CRH-Tg$^+$ mice is in line with the previously-stated hypothesis that the effects of Cushing's syndrome mirror those observed during recovery from acute stress (Macfarlane et al., 2008). Furthermore, we observed accumulation in both subcutaneous and abdominal fat depots, but observed the highest amount of TG synthesis and DNL in the abdominal depot, supporting previous hypotheses and findings that abdominal adipose tissue is more sensitive to GC-induced changes in fat metabolism (Seckl et al., 2004). One limitation of this technique is that we cannot determine with certainty in which tissue DNL is occuring, such that the increased rate of appearance of FAs synthesized via the DNL pathway could be due to increased DNL in adipose tissue or increased hepatic DNL with subsequent VLDL export to adipose tissue. However, we can conclude that in the CRH-Tg$^+$ mice significantly more fat made via the DNL pathway ended up in the abdominal depot compared to the subcutaneous depot, but in wildtype mice DNL contributed an approximately equal amount of fatty acids to TG molecules in each depot, regardless of where the DNL actually occurred.

We were able to quantify glyceroneogenesis as a source for TG-glycerol in the liver, as well as in the inguinal and epididymal fat depots. It has previously been reported that GCs increase glyceroneogenesis in the liver, and decrease glyceroneogenesis in the adipose tissue via differential regulation of PEP-CK (Hanson and Reshef, 2003). We report here that although the major source of TG-glycerol is indeed glyceroneogenesis in the liver and glycolysis in the adipose tissue, as previously reported, no significant differences in percent contribution from glyceroneogenesis were observed between CRH-Tg$^+$ mice and wildtype mice in either tissue. We weren't able to accurately quantify TG synthesis and DNL in the liver due to the relatively long labeling period.

In summary, we performed here a thorough evaluation of key metabolic pathways affected by chronic GC exposure in CRH-Tg^{+} mice, a mouse model that closely mimics the etiology and symptoms of Cushing's syndrome in humans. When we compared these results to previously-published studies involving acute administration of prednisolone to young mice, we were able to draw conclusions on how GCs affect different tissues over time. In bone and skin fractional collagen synthesis rates are dramatically inhibited by acute administration of prednisolone in young mice, but after being exposed to chronically high levels of endogenous GCs, fractional collagen synthesis rates are only modestly lower in bone and are similar in skin, despite having measurably lower bone mass and thinner skin compared to controls. In muscle, fractional synthesis of total muscle protein is not dramatically inhibited by either acute or chronic exposure to GCs, but because mice exposed to chronically high levels of endogenous GCs have measurably less muscle mass relative to controls, we conclude that degradation, rather than synthesis, pathways are mostly responsible for GC-induced decreases in muscle mass. In previous studies in adipose tissue we observed no remarkable changes in TG dynamics in young mice given an acute dose of prednisolone, but in this study, involving mice exposed to chronically high levels of endogenous GCs, we observed more TG synthesis in subcutaneous and abdominal fat depots, more DNL in the abdominal depot only, and no difference in glyceroneogenesis in response to GCs in either depot. Furthermore, we demonstrated that increased TG/FA futile cycling occurs in both abdominal and subcutaneous fat depots in CRH-Tg^{+} mice, and in these mice TG storage is favored over lipolysis.

Tables

		Inguinal depot			Epididymal depot		
Group	n	Fat pad mass (mg)	Fraction new TG/week (f)	Fraction new palmitate/wk (f)	Fat pad mass (mg)	Fraction new TG/week (f)	Fraction new palmitate /wk (f)
WT	6	182 ± 105	0.35 ± 0.09	0.18 ± 0.07	355 ± 116	0.20 ± 0.04	0.07 ± 0.02
CRH-Tg^{+}	8	581 ± 301*	0.41 ± 0.06	0.07 ± 0.02***	1,370 ± 691**	0.38 ± 0.04***	0.08 ± 0.02

Table 1: Fat pad mass and fractional synthesis in wildype (WT) and CRH-Tg^{+} mice. Data are shown as mean ± S.D. *, $P < 0.05$; **, $P < 0.01$; ***, $P < 0.001$ compared to wildtype by t test.

Figures

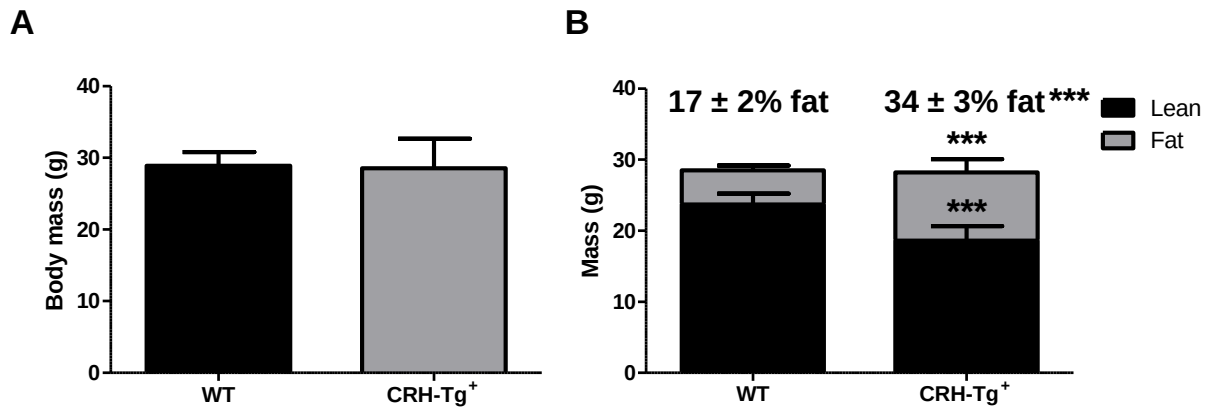

Figure 1. Body mass and body composition in wildype (WT) and CRH-Tg^{+} mice. A. Average group body mass. B. Body composition by DEXA, including lean mass, fat mass, and percent fat. N = 6 for WT group and n = 8 for CRH-Tg^{+} group. ***, $P < 0.001$ compared to wildtype by t test.

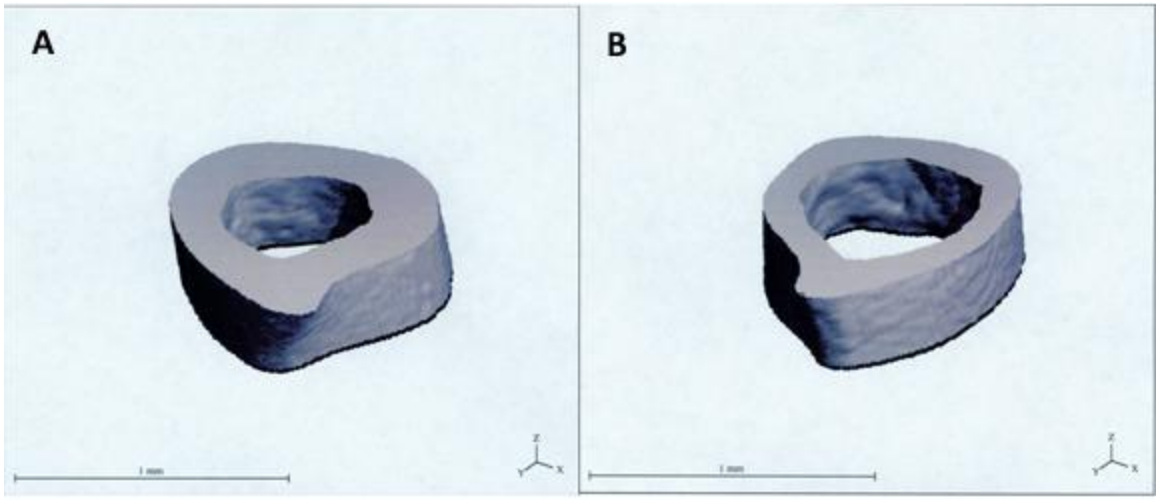

Figure 2. MicroCT scans of femurs in wildtype and CRH-Tg^{+} mice. A. Wildtype femur. B. CRH-Tg^{+} femur.

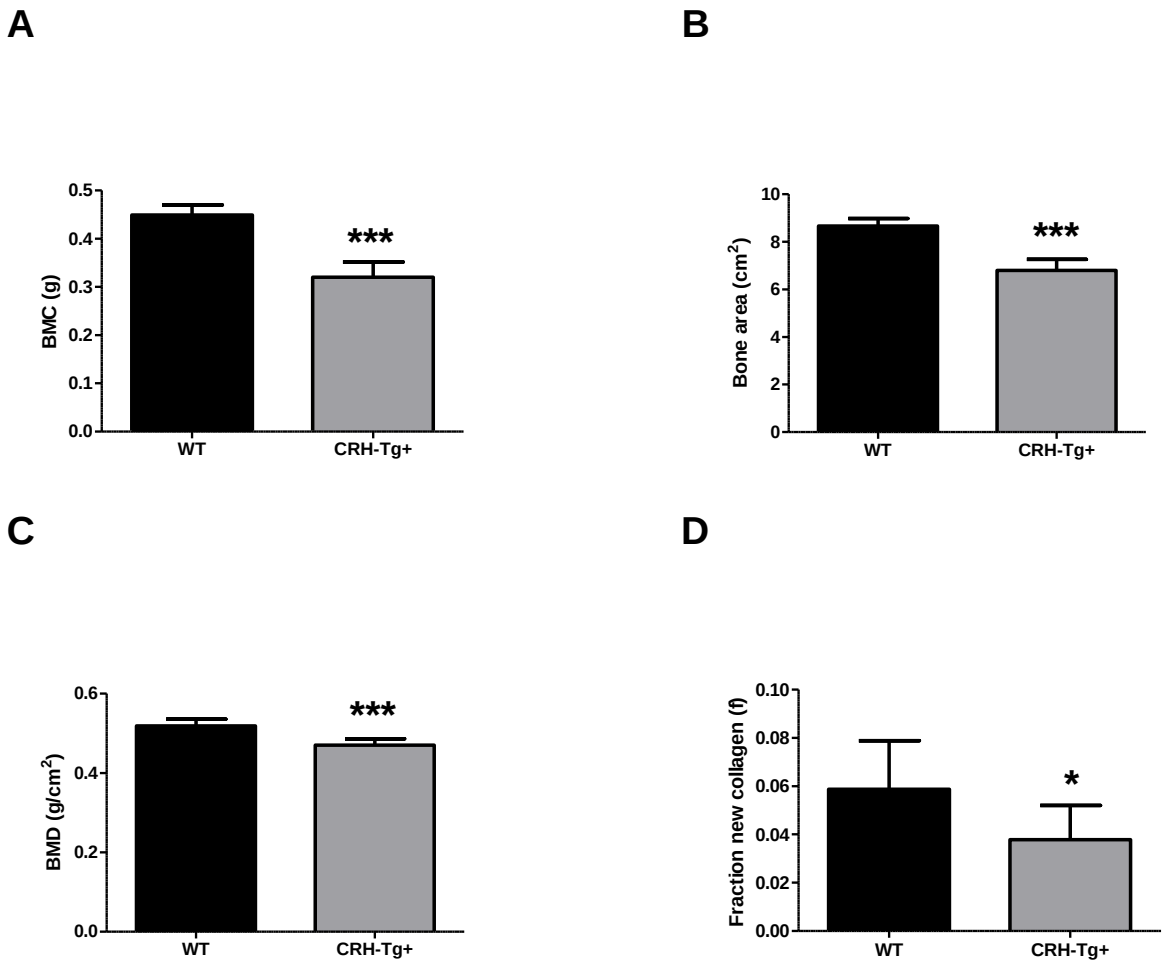

Figure 3. Bone parameters in wildtype (WT) and CRH-Tg^{+} mice. A. Bone mineral content (BMC) in grams. B. Bone area in cm^2. C. Bone mineral density (BMD) in grams per cm^2. D. Fraction new collagen (f) in bone. N = 6 for wildtype and n = 8 for CRH-Tg^{+}. *, $P < 0.05$; *** $P < 0.001$ compared to wildtype by t test.

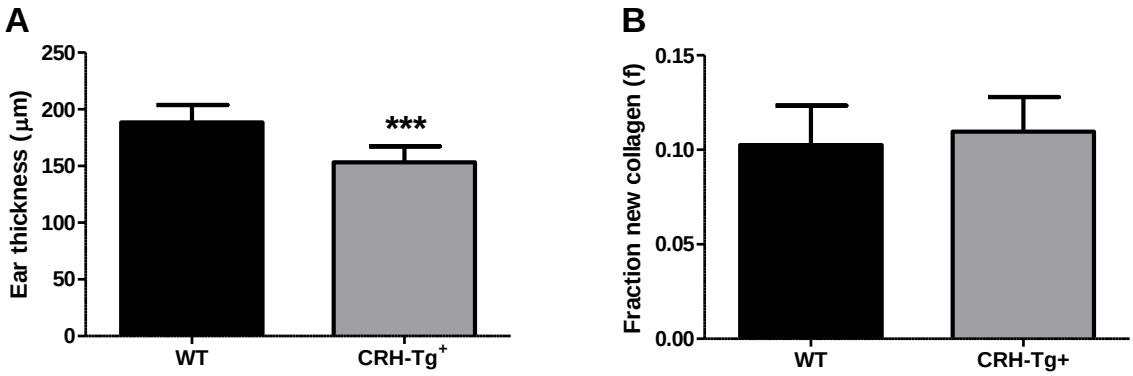

Figure 4. Skin parameters in wildtype (WT) and CRH-Tg$^+$ mice, n = 10 for wildtype and n = 11 for CRH-Tg$^+$. A. Ear skin thickness in micrometers. B. Fraction new collagen in skin, N = 6 for wildtype and n = 8 for CRH-Tg$^+$. *** $P < 0.001$ compared to wildtype by t test.

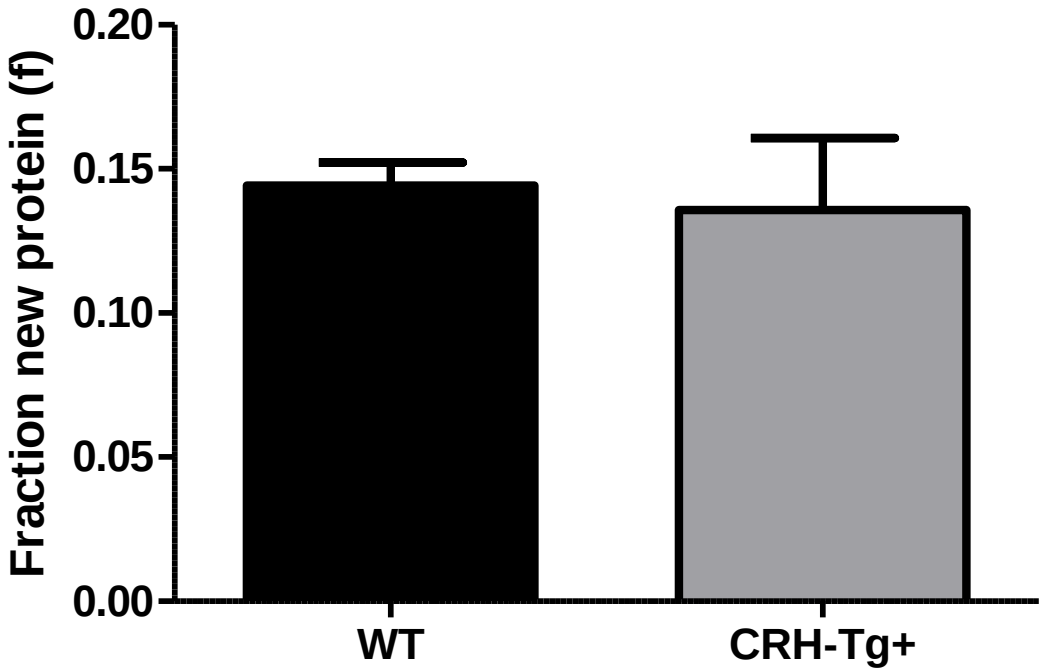

Figure 5. Fraction new protein (alanine) in quadriceps skeletal muscle. N = 6 for wildtype and n = 8 for CRH-Tg^{+}.

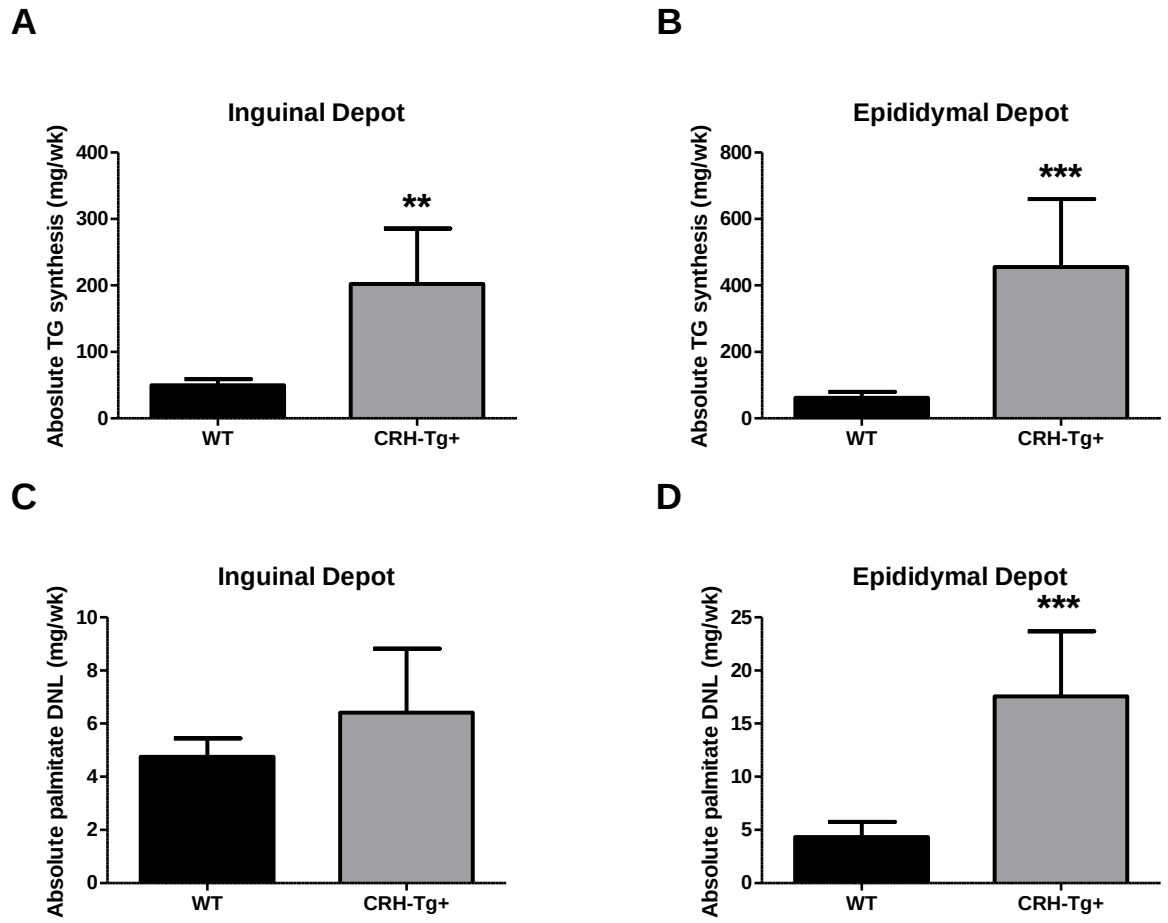

Figure 6. Absolute, retained triglyceride (TG) synthesis and de novo lipogenesis (DNL) over the week-long labeling period in inguinal and epididymal fat pads in wildtype (WT) and CRH-Tg^{+} mice. A. Absolute TG synthesis in the inguinal depot. B. Absolute TG synthesis in the epididymal depot. C. Absolute DNL in the inguinal depot. D. Absolute DNL in the epididymal depot. N = 6 for wildtype and n = 8 for CRH-Tg^{+}. **, $P < 0.01$; ***, $P < 0.001$ compared to wildtype by t test.

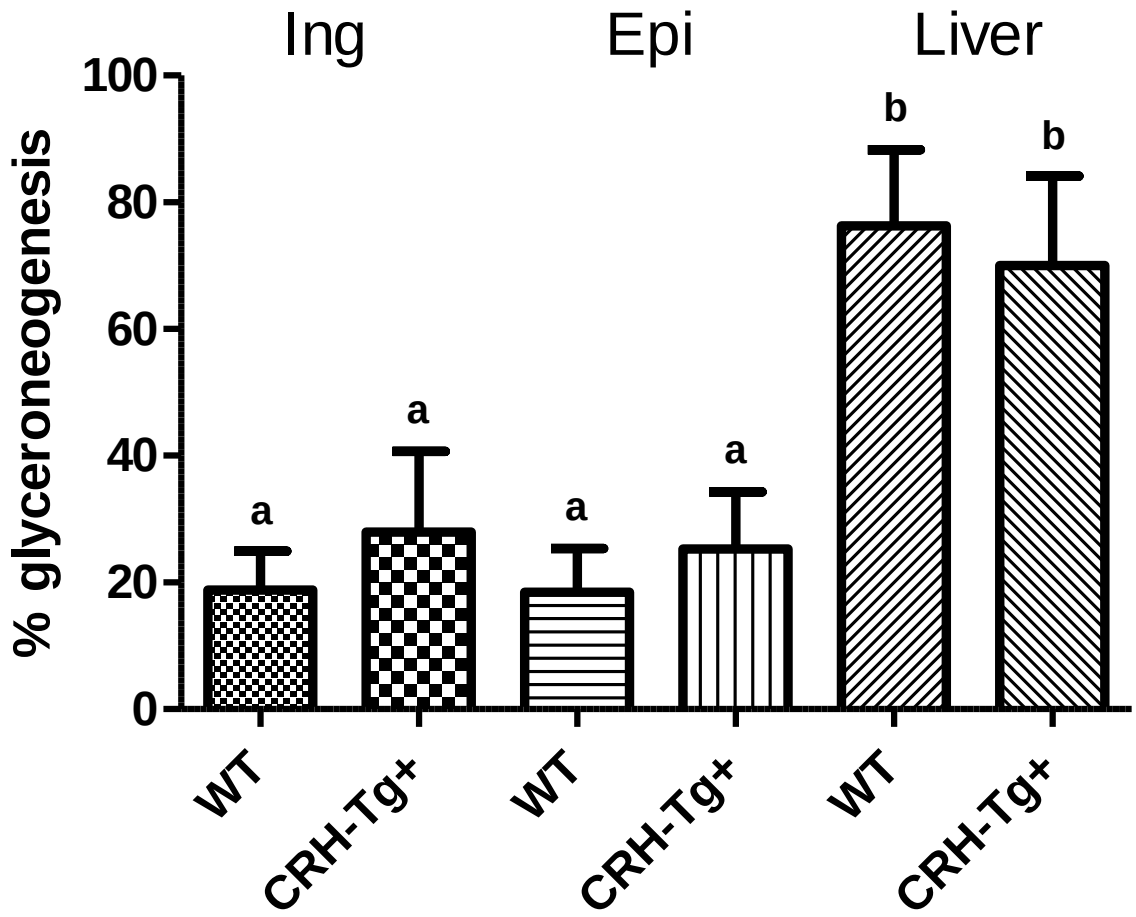

Figure 7. Percent glyceroneogenesis in inguinal and epididymal fat depots and liver in wildtype (WT) and CRH-Tg^{+} mice. Percent glyceroneogenesis indicates what percent of the TG-glycerol came from glyceroneogenic, rather than glycolytic, pathways (i.e. 100% glyceroneogenesis means 100% of TG-glycerol came from glyceroneogenic pathways, and 0% came from glycolytic pathways). N = 6 for wildtype and n = 8 for CRH-Tg^{+}.Groups labeled with the same letter (a or b) are not significantly different and groups labeleld with a different letter are significantly different ($P < 0.001$) by one-way ANOVA followed by Tukey's posttests.

Chapter 5: Summary

Abbreviations

Selective glucocorticoid receptor modulator: SGRM; glucocorticoid receptor: GR; glucocorticoid: GC; triglyceride: TG; dual energy X-ray absorptiometry: DEXA; deuterated glucose disposal test: ^{2}H-GDT; selective nuclear hormone receptors: SNRMs; corticotropin-releasing hormone: CRH; hypothalamic-pituitary-adrenal: HPA; *de novo* lipogenesis: DNL; fatty acid: FA; phosphoenolpyruvate-carboxykinase: PEP-CK;

General summary of studies performed

In these three studies, we systematically characterized in vivo the pleiotropic effects of a putative selective glucocorticoid receptor modulator (SGRM) and prednisolone in wildtype mice, elevated levels of endogenously-produced corticosterone in mice overexpressing corticotropin-releasing hormone (CRH) and wildtype mice, and dexamethasone in mice with a mutation in the glucocorticoid receptor (GR) and wildtype mice. The actions of these glucocorticoids (GCs) were measured by a heavy water labeling strategy that allows measurement of fluxes through multiple target metabolic pathways concurrently. Pathways included collagen synthesis in bone and skin, protein synthesis in skeletal muscle, triglyceride (TG) dynamics in adipose tissue and liver, and splenic and hippocampal neuronal precursor cell proliferation (Busch et al., 2006; Busch et al., 2007; Chen et al., 2007; Gardner et al., 2007; Kim et al., 2005; Neese et al., 2002; Shankaran et al., 2006; Turner et al., 2007). Target pathways were selected based on their believed relevance to the pathophysiology of major adverse effects of GCs in different tissues, such as osteoporosis, loss of muscle mass, redistribution of body fat and obesity, skin thinning and increased susceptibility to bruising, insulin resistance or diabetes mellitus, and neuropsychiatric disturbances, including depression, cognitive dysfunction and mood lability (Buttgereit et al., 2005b; Stanbury and Graham, 1998). To quantify accumulation or distribution of bone mass, lean tissue mass, and fat mass, we used dual energy X-ray absorptiometry (DEXA) and microCT. To quantify changes in glucose homeostasis, we used the deuterated glucose disposal test (^{2}H-GDT), a modified oral glucose tolerance test that also includes glucose absorption and metabolism by peripheral tissues in addition to the usual measurements of glucose and insulin concentrations. By combining these stable isotope methods with non-invasive metrics for body composition, we were able to make sophisticated conclusions about the kinetics of several GC-relevant metabolic pathways in a diverse set of animal models.

Conclusions specific to L5 treatment (SGRM therapeutics)

In this study we quantitatively assessed and compared the effects of a putative SGRM, an arylpyrazole compound called L5, and prednisolone, a potent pan agonist of the GR. This class of arylpyrazole-based compounds, including L5 specifically, had previously been shown to demonstrate selectivity in cell-based assays, but studies testing arylpyrazoles in animals had not been published. Our results provide further evidence that *in vivo* phenotypic selectivity on disease-modifying target pathways can be achieved for GR ligands. Arylpyrazoles can now be added to other classes of SGRMs (De Bosscher; Schacke et al., 2007) that have previously demonstrated selectivity *in vivo*. Although L5 may not represent an attractive drug candidate, L5 is clearly a GR agonist, and these results indicate that further *in vivo* study on arylpyrazoles is warranted. In addition, we have demonstrated the utility of this in vivo approach which can be optimized and incorporated into existing preclinical and clinical screening strategies for other

SGRMs and selective nuclear hormone receptors (SNRMs), in general. Although we failed to establish relative therapeutic indices to compare L5 to prednisolone because of a lack of measured therapeutically favorable actions of L5, we did establish that L5 and prednisolone had different potencies in mediating the different pathways measured. In many pathways, such as bone and skin collagen synthesis and lymphocyte proliferation and death, predisolone was more potent than L5. Prednisolone and L5 were equally potent in inducing peripheral insulin resistance, as measured by elevated insulin levels. Finally, L5 was more potent than prednisolone in suppressing neural progenitor stem cell proliferation in the hippocampus. While we didn't measure relative distribution or metabolism of the two drugs in each tissue, based on the observed GC-like effects on insulin resistance and hippocampal neurogenesis, we know that L5 was absorbed and got to at least some target tissues, and so pharmacokinetic differences likely do not explain the observed difference in potencies in each tissue. Thus, these results point to the need for measuring several GC target pathways in different tissues to establish accurate therapeutic indices in future studies. To establish therapeutic index, effects on inflammation should be evaluated (Buttgereit et al., 2005a; Rosen and Miner, 2005; Schacke et al., 2007), thus this method should be applied to models of inflammation or autoimmune disease, rather than healthy animals if quantitatively assessing therapeutic index is the primary goal. This method can be used to assess and inform selection of upstream cell-based assays used to screen putative SGRMs. While cell-based assays are undeniably useful for assessing cell-autonomous effects of compounds, we found that they do not reliably predict the systemic effects. By correlating the outcomes of cell-based assays with the tissue-specific outcomes of this *in vivo* method for several compounds, predictability of each assay for a specific *in vivo* outcome can be quantitatively assessed, allowing for more informed upstream assay selection. Lastly, this method utilized only a small amount of L5 (< 50 mg) and a relatively small number of mice (42 total, 30 for the heavy water labeling portion, and 12 for the ^{2}H-GDT), demonstrating that this method is both efficient and informative. In summary, it has been demonstrated that the heavy water labeling method for characterizing multiple target pathways concurrently represents an efficient and powerful approach for interrogating the phenotypic selectivity of ligands that bind nuclear transcription factors.

Conclusions specific to $GR^{dim/dim}$ mice

A model has emerged in which the desirable actions of GCs are associated with repression of target genes by GR, and the undesirable actions are associated with transactivation. The $GR^{dim/dim}$ mutation provides an opportunity to test this model, attempting to dissociate repression from transactivation at the level of GR by disrupting the ability of GR to homodimerize. As a corollary, the $GR^{dim/dim}$ mutation is also a tool for characterizing GC-dependent physiological effects mechanistically as being GR homodimerization-dependent or independent. In this study, we directly tested the hypotheses that $GR^{dim/dim}$ mice, which carry a mutation in GR that abrogates GR-GR homodimerization, will experience fewer undesirable effects of and will be less sensitive to dexamethasone than wildtype mice. We also characterized multiple GC-dependent phenotypic outcomes as being GR dimerization dependent or independent. We report that $GR^{dim/dim}$ mice and wildtype mice experience many of the same undesirable, and thus theoretically GR dimerization-independent, effects of dexamethasone, including reductions in bone and skin collagen synthesis rates, reductions in muscle protein synthesis rates, and increases in insulin levels. Furthermore, we report that the sensitivity of $GR^{dim/dim}$ mice to

dexamethasone, relative to wildtype mice, is highly dependent upon the metabolic pathway and tissue examined, and in fact, $GR^{dim/dim}$ mice are more sensitive to the lipogenic effects of dexamethasone in adipose tissue. In summary, we demonstrated for the first time that the $GR^{dim/dim}$ mutation, which up to this point has been described as a loss of function mutation from a molecular standpoint, actually results in mixed gain and loss of GR function, resulting in more or less severely modulated phenotypic outcomes, depending on the pathways measured. We conclude that SGRMs based on dissociating GR transactivation from repression should be evaluated carefully.

Conclusions specific to CRH-Tg^+ mice

CRH-Tg^+ mice carry a stable CRH-containing transgene that causes them to chronically overexpress corticotropin-releasing hormone (CRH), resulting in chronic hyper-activation of the hypothalamic-pituitary-adrenal (HPA) axis, leading to high levels of endogenously-produced corticosterone, the active circulating endogenous GC (analogous to cortisol in humans) in rodents. The phenotype of CRH-Tg^+ mice closely mimics multiple pathologies observed in human patients with Cushing's disease. Our other studies have focused on the acute effects of synthetic GCs, that is, effects that manifest throughout the first week of exposure to high levels of exogenous GCs. In this study we examined the effects of chronically high levels of endogenously-produced corticosterone after GC-induced changes were evident by visual inspection.

To assess differences in lean tissue mass, adipose tissue mass, and bone parameters between CRH-Tg^+ and wildtype mice we used DEXA and microCT. We combined these metrics of body composition with our heavy water labeling approach combined with mass spectrometry to probe the differences in fluxes between CRH-Tg^+ mice and their wildtype littermates through key GC-dependent regulatory pathways, including bone and skin collagen synthesis, muscle protein synthesis, and TG dynamics in adipose tissue and in liver, throughout the 14^{th} week of life. We were then able to compare the results of this study to those of our previous studies to characterize acute (within one week) vs. chronic (after several weeks) effects of GC exposure. CRH-Tg^+ mice weigh the same as wildtype mice, but DEXA revealed that CRH-Tg^+ mice have less lean mass and more fat mass. DEXA and microCT revealed that CRH-Tg^+ mice have less bone mass and less bone mineral density than wildtype mice. CRH-Tg^+ mice also have visibly thinner skin than wildtype mice.

Using our method to study kinetics in these tissues, we found that CRH-Tg^+ mice have lower rates of fractional bone collagen synthesis, similar rates of fractional skin collagen synthesis, similar absolute *de novo* lipogenesis (DNL) in the inguinal depot, higher absolute DNL in the epididymal depot, and higher absolute TG synthesis in both the inguinal and epididymal depot compared to wildtype mice. By combining these methods we found that CRH-Tg^+ mice have less bone mass and slightly lower turnover of bone collagen, thinner skin and similar turnover of skin collagen, less lean mass and similar turnover of muscle protein, and more fat mass and higher turnover of TG in both subcutaneous and abdominal fat depots, with higher rates of DNL in the abdominal fat depot only. We also found that glyceroneogenesis was similar between the two genotypes in fat and liver, and that adipose tissue derives most of its TG-glycerol from glycolytic pathways while liver derives most of its TG-glycerol from glyceroneogenic pathways.

We conclude that GC-induced changes in bone collagen synthesis persist after bone mass has decreased substantially, and changes in skin collagen synthesis do not, although the thin skin phenotype is maintained. Differences in muscle protein synthesis are modest or not apparent after acute or chronic GC exposure, although lean tissue mass dramatically decreases in response to GC exposure, leading us to believe that the primary mechanisms responsible for GC-induced loss of lean tissue cause increases in muscle protein degradation. Finally, GC-induced changes in adipose TG dynamics occur after longer exposure to elevated levels of GC, and they persist after adipose TG mass has increased substantially. We also conclude that chronic GC exposure leads to increases in futile cycling between TG and fatty acids (FA), meaning that both TG synthesis and lipolysis is increased. In the case of CRH-Tg^{+} mice, TG accumulation is favored in both subcutaneous and abdominal depots, but that may not be the case in all models of chronic GC exposure. Virtues of using this mouse model instead of wildtype mice administered exogenous GCs over long periods of time are that CRH-Tg^{+} mice are not exposed to the stresses associated with exogenous administration of GCs, and they do not lose weight, appear sick, or die from infection as mice administered dexamethasone in the drinking water for long periods of time sometimes did in our hands. The drawbacks in using and comparing CRH-Tg^{+} mice to mice administered exogenous GCs include a lack of certainty in the precise dose of GC received, the type of GC used (synthetic prednisolone and dexamethasone vs. corticosterone), exogenous administration vs. endogenous production, and other HPA axis parameters such as feedback inhibition of the HPA axis that occurs with administration of exogenous GCs vs. overstimulation of the HPA axis in CRH-Tg^{+} mice. Regarding the use of CRH-Tg^{+} mice as a model for GC excess, we conclude that they are an excellent preclinical model for testing therapies that may counteract the negative metabolic effects of GC therapy, and that CRH-Tg^{+} mice are a good model for exposure to chronically elevated levels of GCs in the context of low environmental stress.

Glucocorticoid-dependent pathways discussed in detail with regard to time of onset

Bone collagen synthesis

Fractional bone collagen synthesis rates were highest in 8-week-old mice. Baseline (untreated) bone collagen synthesis rates decrease as the mice get older. In the 4-month-old mice of the $GR^{dim/dim}$ study, we were unable to detect significant dexamethasone-dependent decreases in bone collagen synthesis rates, likely because one week of treatment and labeling was not sufficient to observe dexamethasone-dependent reductions in bone collagen synthesis. We conclude that when measuring GC-dependent changes in bone collagen synthesis rates using this heavy water labeling technique, it is advisable to use younger mice (approximately 2 months old) or to label with heavy water for longer than 7 days.

Skin collagen synthesis

Fractional skin collagen synthesis rates were highest in 8-week-old mice, and they were only slightly lower in 4 or 5-month-old mice. Fractional skin collagen synthesis rates are greatly inhibited by acute administration of GCs in 8-week-old and in 4-month-old mice, but are not at all different in mice exposed to chronically high levels of GCs (CRH-Tg^{+} mice). We know in CRH-Tg^{+} mice that the skin is much thinner than in wildtype mice, and we don't believe that CRH-Tg^{+} mice had thinner skin than wildype mice at birth. We therefore propose a model in

which fractional rates of skin collagen synthesis decrease dramatically at the start of elevated GC exposure, regardless of age, resulting in a decrease in the thickness. As GC-exposed and control mice grow, the skin thickness of the two groups diverges, and as the skin in GC-treated mice gets thinner, fractional rates of skin collagen synthesis increase while absolute rates of skin collagen synthesis remain the same. Eventually, the skin in GC-treated mice is so much thinner than in controls that fractional skin collagen synthesis rates are the same in both GC-treated and control mice, the differences in absolute collagen synthesis rates and similarities in fractional collagen synthesis rates between the two genotypes being explained by differences in collagen pool sizes. This model does not take into account changes in degradation rates that occur over time, which may also explain, at least in part, the similar fractional collagen synthesis rates and dissimilarities in skin thickness observed in CRH-Tg^{+} mice compared to wildtype controls. Furthermore, we conclude that GC-induced changes in fractional skin collagen synthesis rates are readily measurable in mice from 8 weeks to 4 months of age and that 7 days of heavy water labeling is optimal for measuring GC-induced changes in fractional skin collagen synthesis rates at this range of ages.

Muscle protein synthesis

In all three studies, muscle protein synthesis rates were always similar, regardless of changes in lean tissue mass and regardless of age. We conclude that muscle protein synthesis rates are relatively consistent throughout the first 4 months of life, and although GC treatment resulted in statistically significant decreases in fractional muscle protein synthesis, we do not believe that this fully explains the difference in lean tissue mass observed in CRH-Tg^{+} mice compared to wildtype. Although we did not directly measure muscle protein degradation in any of these studies, we conclude, by process of elimination and based on studies published by other groups (May et al., 1986; Price et al., 2001; Schacke et al., 2007; Schäcke et al., 2002; Tiao et al., 1996; Wing and Goldberg, 1993), that degradation of muscle proteins is likely the primary mechanism by which GCs cause lean tissue wasting. We conclude that GC-induced changes in muscle protein synthesis rates are readily measurable in mice from 8 weeks to 4 months of age and that 7 days of heavy water labeling is optimal for this age range, however when measuring GC-induced muscle wasting a method optimized for measuring muscle protein degradation would likely be much more useful.

Adipose tissue triglyceride parameters

In wildtype mice we observed very few changes in adipose tissue TG dynamics. We observed a slight, but significant increase in absolute TG synthesis in both depots of 4-month-old wildtype mice in the $GR^{dim/dim}$ study, but no significant GC-dependent changes in DNL in 4-month-old wildtype mice, and no significant GC-dependent changes in TG synthesis or DNL in 8-week-old mice. We saw dramatic GC-dependent increases in TG synthesis in CRH-Tg^{+} mice and in $GR^{dim/dim}$ mice. While CRH-Tg^{+} mice had significant and dramatic GC-dependent increases in DNL in the abdominal fat depot only, $GR^{dim/dim}$ mice had increases in both depots. In CRH-Tg^{+} mice absolute TG synthesis was not proportional to fat accumulation, but in $GR^{dim/dim}$ mice TG synthesis was roughly proportional to fat accumulation. In addition, we did not see large GC-dependent increases in lipolysis in $GR^{dim/dim}$ adipose tissue explants. Interestingly, we saw no GC-dependent increases in TG synthesis or DNL in 8-week-old $GR^{dim/dim}$ mice. We draw several

conclusions regarding GC-dependent changes in adipose tissue TG dynamics from these results. First, these changes are age dependent, only manifesting in 3 or 4 month old mice, but not in 8 week old mice. Second, in wildtype mice the most dramatic changes occur after chronic exposure to GCs. Third, in wildtype mice exposed to chronically high levels of GCs (CRH-Tg^{+} mice) increases in TG synthesis appear to be accompanied by increases in lipolysis, thus chronic exposure to GCs causes increased TG/FA futile cycling which, in this model, leads to gradual accumulation of fat. Fourth, in $GR^{dim/dim}$ mice exposed to acutely elevated GCs increases in DNL and TG synthesis are not accompanied by increases in lipolysis, leading to rapid accumulation of fat. Based on these results, we hypothesize that acute changes in TG synthesis and DNL are GR-GR homodimerization independent, and these pathways are likely activated by GR monomers; however, this hypothesis would need to be tested by incorporating chromatin immunoprecipitation experiments. Furthermore, we conclude that this heavy water labeling method is very well suited to measuring GC-dependent changes in adipose tissue TG dynamics, in part because changes in pool size can be measured non-invasively and by dissecting and weighing fat pads, using 7 days of heavy water labeling in mice between the ages of 8 weeks and 4 months.

Liver TG dynamics

Although Liver TGs were almost fully turned over after 7 days of heavy water labeling, making accurate quantifiable comparisons between groups problematic, CRH-Tg^{+} mice did have significantly higher fractional TG synthesis compared to their wildtype littermates. What is not clear is whether this is indicative of a higher rate of TG synthesis in the livers of CRH-Tg^{+} mice or accumulation of fat in the liver causing TGs to represent a larger proportion of glycerol-containing lipid molecules, the latter instance would result in a higher plateau value of the fully-turned over TG pool. Liver palmitate DNL was not different between the two groups and averaged between 50 and 60% new over the week-long labeling period. We note that both fractional TG synthesis and fractional DNL are much higher in liver than they are in the fat. This makes sense given the relative metabolic activity and size of liver and adipose tissue, and it illustrates the point that because fractional DNL is not uniform across all adipose depots and liver reflects either differential rates of uptake from the circulation of FAs formed by DNL in the liver and depot-autonomous DNL occurring in adipose tissue. We conclude 7 days of heavy water labeling is too long to accurately measure GC-induced changes in liver TG dynamics, and that shorter labeling periods on the order of 1 day would likely be optimal.

GC-dependent changes in glyceroneogenesis

It has previously been reported that glucocorticoids increase glyceroneogenesis in the liver, and decrease glyceroneogenesis in the adipose tissue via differential regulation of phosphoenolpyruvate-carboxykinase (PEP-CK) (Hanson and Reshef, 2003). It has also been hypothesized that glyceroneogenesis increases as TG/FA futile cycling increases in adipose tissue (Reshef et al., 2003). This heavy water labeling method is well suited to measuring the source of TG-glycerol as percent coming from glyceroneogenic vs. glycolytic sources (Chen et al., 2005). Consistent with previously-published results (Hanson and Reshef, 2003; Reshef et al., 2003), we found that the major source of TG-glycerol is glyceroneogenesis in the liver and glycolysis in the adipose tissue, but contrary to previous hypotheses, we did not observe

significant differences in percent contribution from glyceroneogenesis in response to GC exposure or in the adipose tissue of CRH-Tg^{+} mice where we observed marked increases in futile cycling.

Insulin Sensitivity

GC-dependent changes in insulin sensitivity were not fully explored by these models, although our methods included the ^{2}H-GDT, and pancreatic beta cell proliferation. The ^{2}H-GDT is a modified oral glucose tolerance test that measures insulin sensitivity quantitatively by including glucose concentrations, insulin concentrations, and absorption and metabolism by peripheral tissues of glucose to water into one metric. In studies involving acute exposure to GCs, we observed dramatic GC-dependent increases in insulin levels, but no other changes, meaning simply that these results support the large body of literature stating that acute GC administration results in peripheral insulin resistance. The ^{2}H-GDT was not applied to the CRH-Tg^{+} mice, a model of chronic GC exposure, but it was applied to GR$^{dim/dim}$ mice. We observed that plasma insulin levels were slightly higher and blood glucose levels were slightly lower in untreated GR$^{dim/dim}$ mice compared to untreated wildtype mice. It has been previously demonstrated that physiological concentrations of corticosterone inhibit glucose-stimulated insulin secretion in isolated islets from mice (Lambillotte et al., 1997). Based on our observations in GR$^{dim/dim}$ mice, we hypothesize that the pathway responsible for GC-dependent glucose-stimulated insulin secretion is GR-GR homodimerization dependent. To test this hypothesis glucose-stimulated insulin secretion would have to be measured in isolated islets. Because both GR$^{dim/dim}$ mice and wildtype mice are made insulin resistant to a similar extent as measured by the ^{2}H-GDT, we conclude that when high doses of GC are administered peripheral insulin resistance dominates, the pancreas secretes approximately equal amounts of insulin to compensate, and insulin sensitivity, as measured by the ^{2}H-GDT, is similar in both genotypes. We also conclude that when studying GC-dependent decreases in insulin sensitivity and eventual failure of the pancreas to compensate, the ^{2}H-GDT would be best utilized when combined with mouse models that are vulnerable to GC-induced diabetes or in a clinical setting (Beysen et al., 2007).

Conclusions on establishing therapeutic index using these methods, specific to optimal age of animals, potency of drug, and durations of drug administration and label duration for each metric

Whether the desired application of this heavy water labeling method is to quantitatively establish therapeutic index for SGRMs or to elucidate molecular mechanisms by which GCs exert their effects on metabolic pathways by incorporating a mutant mouse model, there are several considerations to take into account. While strain and sex of the mouse are important considerations, the studies presented here all involve male C57Bl/6 mice or mice backcrossed onto a C57Bl/6 background, so we will focus on other considerations. It is evident that different metabolic pathways mediating adverse or beneficial actions exhibit ligand-specific dose response relationships, and age of the animal and duration of treatment and label must be considered for each pathway measured. If the goal is to incorporate as many of the pathways discussed here, a treatment and label duration of 7 days in mice approximately 3 months of age is optimal. Longer treatment durations may need to be used when studying adipose tissue TG dynamics or changes in glucose metabolism or beta cell proliferation. Longer and shorter labeling durations are almost

certainly required when studying hippocampal neural progenitor stem cell proliferation and liver TG dynamics, respectively. To quantitatively and accurately establish therapeutic index, models of inflammation or autoimmune disease should be used, and because different metabolic pathways may have different dose-response relationships for each glucocorticoid pan agonist or SGRM tested, studies must be systematic and include a number of target pathways.

Conclusions regarding kinetics

We have applied a powerful method to quantify the kinetics of several GC-relevent metabolic pathways using heavy water labeling. This method directly measures fractional synthesis of polymers. While fractional synthesis by itself is somewhat informative, absolute synthesis, which incorporates measurement of the final pool size, yields much more information. Ideally, accurate and precise, non-invasive methods for quantifying pool size should be incorporated. If this is impossible or impractical, prior knowledge of expected changes in pool size can assist in the interpretation of measured fractional synthesis rates. This method is well-suited to measuring synthesis rates, but because this method measures products of synthesis rather than degradation, and because pool size measurements are often less precise than fractional synthesis measurements, this method is not well suited to measure degradation rates. Measurement of lymphocyte proliferation and death, as we demonstrated, represents a near-ideal scenario for measuring both absolute synthesis (proliferation) and absolute degradation (cell death) by this method. Lymphocytes can be sorted and counted accurately and precisely, and fractional synthesis can be accurately and precisely measured using the heavy water labeling strategy, meaning that fractional proliferation rates and pool sizes can be combined to yield accurate and precise measurements of absolute cell proliferation and death. If measurement of absolute degradation is desired, but pool sizes cannot be measured with accuracy and precision, direct measurement of a degradation product is recommended, as was conceptually demonstrated in the ^{2}H-GDT where a known amount of ^{2}H-glucose was administered and appearance of $^{2}H_2O$ was measured to quantify degradation of ^{2}H-glucose. In summary, from a kinetic standpoint, this heavy water labeling method is extremely well-suited to measure changes in rates of synthesis, but not changes in rates of degradation.

General advantages of this method

By measuring flux rates through these disease-modifying pathways that may underlie the initiation or progression of undesired outcomes, we were able to characterize GC-dependent changes in a relatively short span of time (i.e. before gross changes are apparent). Because multiple pathway fluxes could be measured concurrently in the same animal and with great sensitivity by the heavy water labeling approach (Busch et al., 2006; Busch et al., 2007; Chen et al., 2007; Gardner et al., 2007; Kim et al., 2005; Neese et al., 2002; Shankaran et al., 2006; Turner et al., 2003; Turner et al., 2007), this systematic characterization was possible with relatively small amounts of GC and small cohort sizes. This is enabled by the sensitivity and reproducibility of mass spectrometric flux measurements after heavy water administration (Hellerstein, 2004; Hellerstein and Murphy, 2004). In addition to demonstrating convincing evidence of side-effect relevant metabolic selectivity for a putative SGRM, we also demonstrated dimerization dependent vs. independent effects and acute vs. chronic effects of GCs by applying this method to transgenic animal models. In addition to small amounts of compound and small

numbers of animals being required, small amounts of tissues are required, and as instruments get more sensitive, even less tissue will be required in the near future, making this method even more amenable to clinical settings. Many of the pathways measured here can also be measured in humans using a similar approach (Beysen et al., 2007; Hellerstein, 2004; Hellerstein and Murphy, 2004). Application of this method can inform upstream assay design and selection in the process of discovery and proof of concept of lead compounds, from clinical studies up to animal studies up to cell-based assays. Finally, application of this method is not limited to studying GCs and their target pathways, and can be adapted to study the metabolic effects of ligands for other nuclear receptors.

General Summary

Several conclusions can be drawn. First, dose response ranges vary depending on the ligand, the pathway measured, and the tissue in which it is measured, so that many pathways need to be measured in different tissues to accurately establish therapeutic index. And while the expectation is that SGRMs will activate only a subset of GR-dependent pathways, it is important to assess the tissue-specific effects of all potential SGRMs on global transcription and GC-dependent metabolic pathways in many different tissues to accurately establish therapeutic indices of compounds. Second, there are several advantages of this method, in particular small amounts of drug, subjects, and tissues are required relative to the large amount of information gained. Finally, this method can be adapted to characterize ligands for GR and other nuclear hormone receptors, and can be applied to disease models and transgenic mice, and can be integrated into preexisting clinical studies.

References

Autio, P., Oikarinen, A., Melkko, J., Risteli, J., and Risteli, L. (1994). Systemic glucocorticoids decrease the synthesis of type I and type III collagen in human skin in vivo, whereas isotretinoin treatment has little effect. British Journal of Dermatology *131*, 660-663.

Besser, G.M., and Edwards, C.R.W. (1972). Cushing's syndrome. Clinics in Endocrinology and Metabolism *1*, 451-490.

Beysen, C., Murphy, E.J., McLaughlin, T., Riiff, T., Lamendola, C., Turner, H.C., Awada, M., Turner, S.M., Reaven, G., and Hellerstein, M.K. (2007). Whole-body glycolysis measured by the deuterated-glucose disposal test correlates highly with insulin resistance in vivo. Diabetes care *30*, 1143-1149.

Bonner-Weir, S., Deery, D., Leahy, J.L., and Weir, G.C. (1989). Compensatory growth of pancreatic beta-cells in adult rats after short-term glucose infusion. Diabetes *38*, 49-53.

Bruning, J.C., Winnay, J., Bonner-Weir, S., Taylor, S.I., Accili, D., and Kahn, C.R. (1997). Development of a novel polygenic model of NIDDM in mice heterozygous for IR and IRS-1 null alleles. Cell *88*, 561-572.

Bruss, M.D., Khambatta, C.F., Ruby, M.A., Aggarwal, I., and Hellerstein, M.K. Calorie restriction increases fatty acid synthesis and whole body fat oxidation rates. American journal of physiology *298*, E108-116.

Busch, R., Kim, Y.K., Neese, R.A., Schade-Serin, V., Collins, M., Awada, M., Gardner, J.L., Beysen, C., Marino, M.E., Misell, L.M*., et al.* (2006). Measurement of protein turnover rates by heavy water labeling of nonessential amino acids. Biochimica et biophysica acta *1760*, 730-744.

Busch, R., Neese, R.A., Awada, M., Hayes, G.M., and Hellerstein, M.K. (2007). Measurement of cell proliferation by heavy water labeling. Nature protocols *2*, 3045-3057.

Buttgereit, F., Burmester, G.R., and Lipworth, B.J. (2005a). Optimised glucocorticoid therapy: the sharpening of an old spear. Lancet *365*, 801-803.

Buttgereit, F., Saag, K.G., Cutolo, M., da Silva, J.A., and Bijlsma, J.W. (2005b). The molecular basis for the effectiveness, toxicity, and resistance to glucocorticoids: focus on the treatment of rheumatoid arthritis. Scandinavian journal of rheumatology *34*, 14-21.

Canalis, E. (2003). Mechanisms of glucocorticoid-induced osteoporosis. Current opinion in rheumatology *15*, 454-457.

Canalis, E. (2005). Mechanisms of glucocorticoid action in bone. Curr Osteoporos Rep *3*, 98-102.

Canalis, E., and Agnusdei, D. (1996). Insulin-like growth factors and their role in osteoporosis. Calcif Tissue Int *58*, 133-134.

Chen, J.L., Peacock, E., Samady, W., Turner, S.M., Neese, R.A., Hellerstein, M.K., and Murphy, E.J. (2005). Physiologic and pharmacologic factors influencing glyceroneogenic contribution to triacylglyceride glycerol measured by mass isotopomer distribution analysis. The Journal of biological chemistry *280*, 25396-25402.

Chen, S., Ogawa, A., Ohneda, M., Unger, R.H., Foster, D.W., and McGarry, J.D. (1994). More direct evidence for a malonyl-CoA-carnitine palmitoyltransferase I interaction as a key event in pancreatic beta-cell signaling. Diabetes *43*, 878-883.

Chen, S., Turner, S., Tsang, E., Stark, J., Turner, H., Mahsut, A., Keifer, K., Goldfinger, M., and Hellerstein, M.K. (2007). Measurement of pancreatic islet cell proliferation by heavy water labeling. American journal of physiology *293*, E1459-1464.

Chen, T.L., Mallory, J.B., and Hintz, R.L. (1991). Dexamethasone and 1,25(OH)2 vitamin D3 modulate the synthesis of insulin-like growth factor-I in osteoblast-like cells. Calcif Tissue Int *48*, 278-282.

Coghlan, M.J., Jacobson, P.B., Lane, B., Nakane, M., Lin, C.W., Elmore, S.W., Kym, P.R., Luly, J.R., Carter, G.W., Turner, R*., et al.* (2003). A novel antiinflammatory maintains glucocorticoid efficacy with reduced side effects. Molecular endocrinology (Baltimore, Md *17*, 860-869.

Collins, M.L., Eng, S., Hoh, R., and Hellerstein, M.K. (2003). Measurement of mitochondrial DNA synthesis in vivo using a stable isotope-mass spectrometric technique. J Appl Physiol *94*, 2203-2211.
De Bosscher, K. Selective Glucocorticoid Receptor modulators. The Journal of Steroid Biochemistry and Molecular Biology *120*, 96-104.
De Bosscher, K., Vanden Berghe, W., Beck, I.M., Van Molle, W., Hennuyer, N., Hapgood, J., Libert, C., Staels, B., Louw, A., and Haegeman, G. (2005). A fully dissociated compound of plant origin for inflammatory gene repression. Proceedings of the National Academy of Sciences of the United States of America *102*, 15827-15832.
Delany, A.M., Gabbitas, B.Y., and Canalis, E. (1995). Cortisol downregulates osteoblast alpha 1 (I) procollagen mRNA by transcriptional and posttranscriptional mechanisms. J Cell Biochem *57*, 488-494.
Dittmar, K.D., Demady, D.R., Stancato, L.F., Krishna, P., and Pratt, W.B. (1997). Folding of the glucocorticoid receptor by the heat shock protein (hsp) 90-based chaperone machinery. The role of p23 is to stabilize receptor.hsp90 heterocomplexes formed by hsp90.p60.hsp70. The Journal of biological chemistry *272*, 21213-21220.
Dutertre, M., and Smith, C.L. (2000). Molecular mechanisms of selective estrogen receptor modulator (SERM) action. The Journal of pharmacology and experimental therapeutics *295*, 431-437.
Epstein, E.H., Jr., and Munderloh, N.H. (1978). Human skin collagen. Presence of type I and type III at all levels of the dermis. The Journal of biological chemistry *253*, 1336-1337.
Frijters, R., Fleuren, W., Toonen, E.J., Tuckermann, J.P., Reichardt, H.M., van der Maaden, H., van Elsas, A., van Lierop, M.J., Dokter, W., de Vlieg, J.*, et al.* Prednisolone-induced differential gene expression in mouse liver carrying wild type or a dimerization-defective glucocorticoid receptor. BMC Genomics *11*, 359.
Gaillard, D., Wabitsch, M., Pipy, B., and Negrel, R. (1991). Control of terminal differentiation of adipose precursor cells by glucocorticoids. J Lipid Res *32*, 569-579.
Gardner, J.L., Turner, S.M., Bautista, A., Lindwall, G., Awada, M., and Hellerstein, M.K. (2007). Measurement of liver collagen synthesis by heavy water labeling: effects of profibrotic toxicants and antifibrotic interventions. Am J Physiol Gastrointest Liver Physiol *292*, G1695-1705.
Giguère, V., Hollenberg, S.M., Rosenfeld, M.G., and Evans, R.M. (1986). Functional domains of the human glucocorticoid receptor. Cell *46*, 645-652.
Haapasaari, K.M., Risteli, J., and Oikarinen, A. (1996). Recovery of human skin collagen synthesis after short-term topical corticosteroid treatment and comparison between young and old subjects. British Journal of Dermatology *135*, 65-69.
Halloran, B.P., Wronski, T.J., VonHerzen, D.C., Chu, V., Xia, X., Pingel, J.E., Williams, A.A., and Smith, B.J. Dietary dried plum increases bone mass in adult and aged male mice. J Nutr *140*, 1781-1787.
Hanson, R.W., and Reshef, L. (2003). Glyceroneogenesis revisited. Biochimie *85*, 1199-1205.
Heck, S., Kullmann, M., Gast, A., Ponta, H., Rahmsdorf, H.J., Herrlich, P., and Cato, A.C. (1994). A distinct modulating domain in glucocorticoid receptor monomers in the repression of activity of the transcription factor AP-1. EMBO J *13*, 4087-4095.
Hellerstein, M.K. (2004). New stable isotope-mass spectrometric techniques for measuring fluxes through intact metabolic pathways in mammalian systems: introduction of moving pictures into functional genomics and biochemical phenotyping. Metabolic engineering *6*, 85-100.
Hellerstein, M.K., Christiansen, M., Kaempfer, S., Kletke, C., Wu, K., Reid, J.S., Mulligan, K., Hellerstein, N.S., and Shackleton, C.H. (1991). Measurement of de novo hepatic lipogenesis in humans using stable isotopes. J Clin Invest *87*, 1841-1852.
Hellerstein, M.K., and Murphy, E. (2004). Stable isotope-mass spectrometric measurements of molecular fluxes in vivo: emerging applications in drug development. Current opinion in molecular therapeutics *6*, 249-264.

Hellerstein, M.K., and Neese, R.A. (1999). Mass isotopomer distribution analysis at eight years: theoretical, analytic, and experimental considerations. The American journal of physiology *276*, E1146-1170.
Hellerstein, M.K., Neese, R.A., and Schwarz, J.M. (1993). Model for measuring absolute rates of hepatic de novo lipogenesis and reesterification of free fatty acids. The American journal of physiology *265*, E814-820.
Hench, P.S., Kendall, E.C., and et al. (1949). The effect of a hormone of the adrenal cortex (17-hydroxy-11-dehydrocorticosterone; compound E) and of pituitary adrenocorticotropic hormone on rheumatoid arthritis. Mayo Clin Proc *24*, 181-197.
Hollenberg, S.M., Weinberger, C., Ong, E.S., Cerelli, G., Oro, A., Lebo, R., Brad Thompson, E., Rosenfeld, M.G., and Evans, R.M. (1985). Primary structure and expression of a functional human glucocorticoid receptor cDNA. Nature *318*, 635-641.
Jung, H.R., Turner, S.M., Neese, R.A., Young, S.G., and Hellerstein, M.K. (1999). Metabolic adaptations to dietary fat malabsorption in chylomicron-deficient mice. The Biochemical journal *343 Pt 2*, 473-478.
Kim, S.J., Turner, S., Killion, S., and Hellerstein, M.K. (2005). In vivo measurement of DNA synthesis rates of colon epithelial cells in carcinogenesis. Biochemical and biophysical research communications *331*, 203-209.
Kleiman, A., and Tuckermann, J.P. (2007). Glucocorticoid receptor action in beneficial and side effects of steroid therapy: lessons from conditional knockout mice. Molecular and cellular endocrinology *275*, 98-108.
Koletzko, B., Sauerwald, T., and Demmelmair, H. (1997). Safety of stable isotope use. European journal of pediatrics *156 Suppl 1*, S12-17.
Lambillotte, C., Gilon, P., and Henquin, J.C. (1997). Direct glucocorticoid inhibition of insulin secretion. An in vitro study of dexamethasone effects in mouse islets. J Clin Invest *99*, 414-423.
LoCascio, V., Bonucci, E., Imbimbo, B., Ballanti, P., Adami, S., Milani, S., Tartarotti, D., and DellaRocca, C. (1990). Bone loss in response to long-term glucocorticoid therapy. Bone and Mineral *8*, 39-51.
Long, W., Wei, L., and Barrett, E.J. (2001). Dexamethasone inhibits the stimulation of muscle protein synthesis and PHAS-I and p70 S6-kinase phosphorylation. American journal of physiology *280*, E570-575.
Louard, R.J., Bhushan, R., Gelfand, R.A., Barrett, E.J., and Sherwin, R.S. (1994). Glucocorticoids antagonize insulin's antiproteolytic action on skeletal muscle in humans. The Journal of clinical endocrinology and metabolism *79*, 278-284.
Lubach, D., Rath, J., and Kietzmann, M. (1995). Skin atrophy induced by initial continuous topical application of clobetasol followed by intermittent application. Dermatology *190*, 51-55.
Macallan, D.C., Fullerton, C.A., Neese, R.A., Haddock, K., Park, S.S., and Hellerstein, M.K. (1998). Measurement of cell proliferation by labeling of DNA with stable isotope-labeled glucose: studies in vitro, in animals, and in humans. Proceedings of the National Academy of Sciences of the United States of America *95*, 708-713.
Macfarlane, D.P., Forbes, S., and Walker, B.R. (2008). Glucocorticoids and fatty acid metabolism in humans: fuelling fat redistribution in the metabolic syndrome. J Endocrinol *197*, 189-204.
Manolagas, S.C., and Weinstein, R.S. (1999). New Developments in the Pathogenesis and Treatment of Steroid-Induced Osteoporosis. Journal of Bone and Mineral Research *14*, 1061-1066.
Martin-Sanz, P., Vance, J.E., and Brindley, D.N. (1990). Stimulation of apolipoprotein secretion in very-low-density and high-density lipoproteins from cultured rat hepatocytes by dexamethasone. The Biochemical journal *271*, 575-583.
May, R.C., Kelly, R.A., and Mitch, W.E. (1986). Metabolic acidosis stimulates protein degradation in rat muscle by a glucocorticoid-dependent mechanism. J Clin Invest *77*, 614-621.

Mayo-Smith, W., Hayes, C.W., Biller, B.M., Klibanski, A., Rosenthal, H., and Rosenthal, D.I. (1989). Body fat distribution measured with CT: correlations in healthy subjects, patients with anorexia nervosa, and patients with Cushing syndrome. Radiology *170*, 515-518.
McCarthy, T.L., Centrella, M., and Canalis, E. (1989). Insulin-like growth factor (IGF) and bone. Connect Tissue Res *20*, 277-282.
Miner, J.N. (2002). Designer glucocorticoids. Biochem Pharmacol *64*, 355-361.
Miner, J.N., and Yamamoto, K.R. (1992). The basic region of AP-1 specifies glucocorticoid receptor activity at a composite response element. Genes & development *6*, 2491-2501.
Neese, R.A., Misell, L.M., Turner, S., Chu, A., Kim, J., Cesar, D., Hoh, R., Antelo, F., Strawford, A., McCune, J.M.*, et al.* (2002). Measurement in vivo of proliferation rates of slow turnover cells by 2H2O labeling of the deoxyribose moiety of DNA. Proceedings of the National Academy of Sciences of the United States of America *99*, 15345-15350.
Neese, R.A., Siler, S.Q., Cesar, D., Antelo, F., Lee, D., Misell, L., Patel, K., Tehrani, S., Shah, P., and Hellerstein, M.K. (2001). Advances in the stable isotope-mass spectrometric measurement of DNA synthesis and cell proliferation. Analytical biochemistry *298*, 189-195.
Nissen, R.M., and Yamamoto, K.R. (2000). The glucocorticoid receptor inhibits NFkappa B by interfering with serine-2 phosphorylation of the RNA polymerase II carboxy-terminal domain. Genes & Dev *14*, 2314-2329.
O'Brien, C.A., Jia, D., Plotkin, L.I., Bellido, T., Powers, C.C., Stewart, S.A., Manolagas, S.C., and Weinstein, R.S. (2004). Glucocorticoids act directly on osteoblasts and osteocytes to induce their apoptosis and reduce bone formation and strength. Endocrinology *145*, 1835-1841.
Ocasio, C.A., Scanlan, T.S. (2005). Clinical prospects for new thyroid hormone analogs. Curr Opin Endocrinol Diabetes *12*, 363—370.
Odedra, B.R., Bates, P.C., and Millward, D.J. (1983). Time course of the effect of catabolic doses of corticosterone on protein turnover in rat skeletal muscle and liver. The Biochemical journal *214*, 617-627.
Paris, M., Bernard-Kargar, C., Berthault, M.F., Bouwens, L., and Ktorza, A. (2003). Specific and combined effects of insulin and glucose on functional pancreatic beta-cell mass in vivo in adult rats. Endocrinology *144*, 2717-2727.
Pourcet, B., Fruchart, J.C., Staels, B., and Glineur, C. (2006). Selective PPAR modulators, dual and pan PPAR agonists: multimodal drugs for the treatment of type 2 diabetes and atherosclerosis. Expert opinion on emerging drugs *11*, 379-401.
Pouteau, E., Turner, S., Aprikian, O., Hellerstein, M., Moser, M., Darimont, C., Fay, L.B., and Mace, K. (2008). Time course and dynamics of adipose tissue development in obese and lean Zucker rat pups. Int J Obes (Lond) *32*, 648-657.
Price, S.R., Du, J., Bailey, J.L., and Mitch, W.E. (2001). Molecular Mechanisms Regulating Protein Turnover in Muscle. American Journal of Kidney Diseases *37*, S112-S114.
Rannels, S.R., and Jefferson, L.S. (1980). Effects of glucocorticoids on muscle protein turnover in perfused rat hemicorpus. The American journal of physiology *238*, E564-572.
Rannels, S.R., Rannels, D.E., Pegg, A.E., and Jefferson, L.S. (1978). Glucocorticoid effects on peptide-chain initiation in skeletal muscle and heart. The American journal of physiology *235*, E134-139.
Rauch, A., Seitz, S., Baschant, U., Schilling, A.F., Illing, A., Stride, B., Kirilov, M., Mandic, V., Takacz, A., Schmidt-Ullrich, R.*, et al.* Glucocorticoids suppress bone formation by attenuating osteoblast differentiation via the monomeric glucocorticoid receptor. Cell Metab *11*, 517-531.
Ray, A., and Prefontaine, K.E. (1994). Physical association and functional antagonism between the p65 subunit of transcription factor NF-kappa B and the glucocorticoid receptor. Proceedings of the National Academy of Sciences of the United States of America *91*, 752-756.

Rebuffe-Scrive, M., Krotkiewski, M., Elfverson, J., and Bjorntorp, P. (1988). Muscle and adipose tissue morphology and metabolism in Cushing's syndrome. The Journal of clinical endocrinology and metabolism *67*, 1122-1128.
Reichardt, H.M., Kaestner, K.H., Tuckermann, J., Kretz, O., Wessely, O., Bock, R., Gass, P., Schmid, W., Herrlich, P., Angel, P.*, et al.* (1998). DNA binding of the glucocorticoid receptor is not essential for survival. Cell *93*, 531-541.
Reichardt, H.M., Tuckermann, J.P., Gottlicher, M., Vujic, M., Weih, F., Angel, P., Herrlich, P., and Schutz, G. (2001). Repression of inflammatory responses in the absence of DNA binding by the glucocorticoid receptor. EMBO J *20*, 7168-7173.
Reshef, L., Olswang, Y., Cassuto, H., Blum, B., Croniger, C.M., Kalhan, S.C., Tilghman, S.M., and Hanson, R.W. (2003). Glyceroneogenesis and the triglyceride/fatty acid cycle. The Journal of biological chemistry *278*, 30413-30416.
Rogatsky, I., Wang, J.C., Derynck, M.K., Nonaka, D.F., Khodabakhsh, D.B., Haqq, C.M., Darimont, B.D., Garabedian, M.J., and Yamamoto, K.R. (2003). Target-specific utilization of transcriptional regulatory surfaces by the glucocorticoid receptor. Proceedings of the National Academy of Sciences of the United States of America *100*, 13845-13850.
Roohk, D.J., Varady, K.A., Turner, S.M., Emson, C.L., Gelling, R.W., Shankaran, M., Lindwall, G., Shipp, L.E., Scanlan, T.S., Wang, J.C.*, et al.* Differential in vivo effects on target pathways of a novel arylpyrazole glucocorticoid receptor modulator compared with prednisolone. The Journal of pharmacology and experimental therapeutics *333*, 281-289.
Rosen, J., and Miner, J.N. (2005). The search for safer glucocorticoid receptor ligands. Endocrine reviews *26*, 452-464.
Rydziel, S., Delany, A.M., and Canalis, E. (2004). AU-rich elements in the collagenase 3 mRNA mediate stabilization of the transcript by cortisol in osteoblasts. The Journal of biological chemistry *279*, 5397-5404.
Samra, J.S., Clark, M.L., Humphreys, S.M., MacDonald, I.A., Bannister, P.A., and Frayn, K.N. (1998). Effects of physiological hypercortisolemia on the regulation of lipolysis in subcutaneous adipose tissue. The Journal of clinical endocrinology and metabolism *83*, 626-631.
Schacke, H., Berger, M., Rehwinkel, H., and Asadullah, K. (2007). Selective glucocorticoid receptor agonists (SEGRAs): novel ligands with an improved therapeutic index. Molecular and cellular endocrinology *275*, 109-117.
Schäcke, H., Döcke, W.-D., and Asadullah, K. (2002). Mechanisms involved in the side effects of glucocorticoids. Pharmacology & Therapeutics *96*, 23-43.
Schacke, H., Schottelius, A., Docke, W.D., Strehlke, P., Jaroch, S., Schmees, N., Rehwinkel, H., Hennekes, H., and Asadullah, K. (2004). Dissociation of transactivation from transrepression by a selective glucocorticoid receptor agonist leads to separation of therapeutic effects from side effects. Proceedings of the National Academy of Sciences of the United States of America *101*, 227-232.
Scheinman, R., Gualberto, A., Jewell, C., Cidlowski, J., and Baldwin, A., Jr (1995). Characterization of mechanisms involved in transrepression of NF-kappa B by activated glucocorticoid receptors. Mol Cell Biol *15*, 943-953.
Schoneveld, O.J.L.M., Gaemers, I.C., and Lamers, W.H. (2004). Mechanisms of glucocorticoid signalling. Biochimica et Biophysica Acta (BBA) - Gene Structure and Expression *1680*, 114-128.
Seckl, J.R., Morton, N.M., Chapman, K.E., and Walker, B.R. (2004). Glucocorticoids and 11beta-hydroxysteroid dehydrogenase in adipose tissue. Recent Prog Horm Res *59*, 359-393.
Seimandi, M., Lemaire, G., Pillon, A., Perrin, A., Carlavan, I., Voegel, J.J., Vignon, F., Nicolas, J.C., and Balaguer, P. (2005). Differential responses of PPARalpha, PPARdelta, and PPARgamma reporter cell lines to selective PPAR synthetic ligands. Analytical biochemistry *344*, 8-15.

Shah, N., and Scanlan, T.S. (2004). Design and evaluation of novel nonsteroidal dissociating glucocorticoid receptor ligands. Bioorganic & medicinal chemistry letters *14*, 5199-5203.
Shah, O.J., Anthony, J.C., Kimball, S.R., and Jefferson, L.S. (2000). Glucocorticoids oppose translational control by leucine in skeletal muscle. American journal of physiology *279*, E1185-1190.
Shankaran, M., King, C., Lee, J., Busch, R., Wolff, M., and Hellerstein, M.K. (2006). Discovery of novel hippocampal neurogenic agents by using an in vivo stable isotope labeling technique. The Journal of pharmacology and experimental therapeutics *319*, 1172-1181.
Shinahara, M., Nishiyama, M., Iwasaki, Y., Nakayama, S., Noguchi, T., Kambayashi, M., Okada, Y., Tsuda, M., Stenzel-Poore, M.P., Hashimoto, K.*, et al.* (2009). Plasma adiponectin levels are increased despite insulin resistance in corticotropin-releasing hormone transgenic mice, an animal model of Cushing syndrome. Endocr J *56*, 879-886.
Slavin, B.G., Ong, J.M., and Kern, P.A. (1994). Hormonal regulation of hormone-sensitive lipase activity and mRNA levels in isolated rat adipocytes. J Lipid Res *35*, 1535-1541.
Stanbury, R.M., and Graham, E.M. (1998). Systemic corticosteroid therapy--side effects and their management. The British journal of ophthalmology *82*, 704-708.
Stenzel-Poore, M.P., Cameron, V.A., Vaughan, J., Sawchenko, P.E., and Vale, W. (1992). Development of Cushing's syndrome in corticotropin-releasing factor transgenic mice. Endocrinology *130*, 3378-3386.
Stenzel-Poore, M.P., Duncan, J.E., Rittenberg, M.B., Bakke, A.C., and Heinrichs, S.C. (1996). CRH overproduction in transgenic mice: behavioral and immune system modulation. Ann N Y Acad Sci *780*, 36-48.
Stenzel-Poore, M.P., Heinrichs, S.C., Rivest, S., Koob, G.F., and Vale, W.W. (1994). Overproduction of corticotropin-releasing factor in transgenic mice: a genetic model of anxiogenic behavior. J Neurosci *14*, 2579-2584.
Sznaidman, M.L., Haffner, C.D., Maloney, P.R., Fivush, A., Chao, E., Goreham, D., Sierra, M.L., LeGrumelec, C., Xu, H.E., Montana, V.G.*, et al.* (2003). Novel selective small molecule agonists for peroxisome proliferator-activated receptor delta (PPARdelta)--synthesis and biological activity. Bioorganic & medicinal chemistry letters *13*, 1517-1521.
Taskinen, M.R., Nikkila, E.A., Pelkonen, R., and Sane, T. (1983). Plasma lipoproteins, lipolytic enzymes, and very low density lipoprotein triglyceride turnover in Cushing's syndrome. The Journal of clinical endocrinology and metabolism *57*, 619-626.
Tiao, G., Fagan, J., Roegner, V., Lieberman, M., Wang, J.J., Fischer, J.E., and Hasselgren, P.O. (1996). Energy-ubiquitin-dependent muscle proteolysis during sepsis in rats is regulated by glucocorticoids. J Clin Invest *97*, 339-348.
Trost, S.U., Swanson, E., Gloss, B., Wang-Iverson, D.B., Zhang, H., Volodarsky, T., Grover, G.J., Baxter, J.D., Chiellini, G., Scanlan, T.S.*, et al.* (2000). The thyroid hormone receptor-beta-selective agonist GC-1 differentially affects plasma lipids and cardiac activity. Endocrinology *141*, 3057-3064.
Turner, S.M., Murphy, E.J., Neese, R.A., Antelo, F., Thomas, T., Agarwal, A., Go, C., and Hellerstein, M.K. (2003). Measurement of TG synthesis and turnover in vivo by 2H2O incorporation into the glycerol moiety and application of MIDA. Am J Physiol Endocrinol Metab *285*, E790-803.
Turner, S.M., Roy, S., Sul, H.S., Neese, R.A., Murphy, E.J., Samandi, W., Roohk, D.J., and Hellerstein, M.K. (2007). Dissociation between adipose tissue fluxes and lipogenic gene expression in ob/ob mice. American journal of physiology *292*, E1101-1109.
van Gaalen, M.M., Stenzel-Poore, M.P., Holsboer, F., and Steckler, T. (2002). Effects of transgenic overproduction of CRH on anxiety-like behaviour. Eur J Neurosci *15*, 2007-2015.
Varady, K.A., Roohk, D.J., and Hellerstein, M.K. (2007a). Dose effects of modified alternate-day fasting regimens on in vivo cell proliferation and plasma insulin-like growth factor-1 in mice. J Appl Physiol *103*, 547-551.

Varady, K.A., Roohk, D.J., Loe, Y.C., McEvoy-Hein, B.K., and Hellerstein, M.K. (2007b). Effects of modified alternate-day fasting regimens on adipocyte size, triglyceride metabolism, and plasma adiponectin levels in mice. J Lipid Res *48*, 2212-2219.
Vayssiere, B.M., Dupont, S., Choquart, A., Petit, F., Garcia, T., Marchandeau, C., Gronemeyer, H., and Resche-Rigon, M. (1997). Synthetic Glucocorticoids That Dissociate Transactivation and AP-1 Transrepression Exhibit Antiinflammatory Activity in Vivo. Molecular endocrinology (Baltimore, Md *11*, 1245-1255.
Waddell, D.S., Baehr, L.M., van den Brandt, J., Johnsen, S.A., Reichardt, H.M., Furlow, J.D., and Bodine, S.C. (2008). The glucocorticoid receptor and FOXO1 synergistically activate the skeletal muscle atrophy-associated MuRF1 gene. American journal of physiology *295*, E785-797.
Walker, B.R. (2006). Cortisol—cause and cure for metabolic syndrome? Diabetic Medicine *23*, 1281-1288.
Wang, J.C., Shah, N., Pantoja, C., Meijsing, S.H., Ho, J.D., Scanlan, T.S., and Yamamoto, K.R. (2006). Novel arylpyrazole compounds selectively modulate glucocorticoid receptor regulatory activity. Genes & development *20*, 689-699.
Webb, P., Nguyen, P., and Kushner, P.J. (2003). Differential SERM effects on corepressor binding dictate ERalpha activity in vivo. The Journal of biological chemistry *278*, 6912-6920.
Weinstein, R.S., Jilka, R.L., Parfitt, A.M., and Manolagas, S.C. (1998). Inhibition of osteoblastogenesis and promotion of apoptosis of osteoblasts and osteocytes by glucocorticoids. Potential mechanisms of their deleterious effects on bone. J Clin Invest *102*, 274-282.
Wing, S.S., and Goldberg, A.L. (1993). Glucocorticoids activate the ATP-ubiquitin-dependent proteolytic system in skeletal muscle during fasting. The American journal of physiology *264*, E668-676.
Yang-Yen, H.-F., Chambard, J.-C., Sun, Y.-L., Smeal, T., Schmidt, T.J., Drouin, J., and Karin, M. (1990). Transcriptional interference between c-Jun and the glucocorticoid receptor: Mutual inhibition of DNA binding due to direct protein-protein interaction. Cell *62*, 1205-1215.
Yu, C.Y., Mayba, O., Lee, J.V., Tran, J., Harris, C., Speed, T.P., and Wang, J.C. Genome-wide analysis of glucocorticoid receptor binding regions in adipocytes reveal gene network involved in triglyceride homeostasis. PLoS One *5*, e15188.